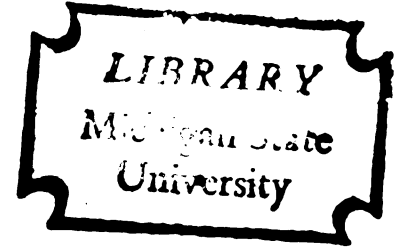




3 1293 10462 0848



This is to certify that the

thesis entitled

ENERGY CONSERVATION IN GRAIN DRYERS
USING HEAT PIPE EXCHANGERS

presented by

Shahab Sokhansanj

has been accepted towards fulfillment
of the requirements for

Ph.D. degree in Agricultural Engineering

Major professor

Date 11-1-77

RUBEN-1970

~~1970-1971~~

1970-1971

MD

JUN 18

JUL 4 1970

PVS 1A

**ENERGY CONSERVATION IN GRAIN DRYERS
USING HEAT PIPE EXCHANGERS**

By

Shahab Sokhansanj

A DISSERTATION

**Submitted to
Michigan State Universtiy
in partial fulfillment of the requirements
for the degree of**

DOCTOR OF PHILOSOPHY

Agricultural Engineering Department

1977

PLEASE NOTE:

Dissertation contains computer print-outs that have broken and indistinct print. Filmed best way possible.

UNIVERSITY MICROFILMS

ABSTRACT

ENERGY CONSERVATION IN GRAIN DRYERS USING HEAT PIPE EXCHANGERS

By

Shahab Sokhansanj

Grain drying is a major energy consumer in the processing of agricultural products. A heat exchanger used to recover the waste heat from exhaust air is one way to increase the energy efficiency of the process. However, gas to gas heat recovery is a low efficiency heat transfer process and, consequently, a large and expensive heat exchanger is required to transfer a certain amount of heat. The newly developed heat pipe exchangers are more efficient than the conventional types. Transportation of heat by evaporation and condensation of a liquid in an enclosed pipe is the principle of heat pipe operation.

In this investigation the heat pipe characteristics important in a grain dryer application are considered. The performance of a compact heat pipe exchanger is analyzed when both sensible and latent heat are present. A nonlinear optimization technique is used for an optimal design. Also the possibility of using a linear optimization scheme is investigated.

The profitability of heat pipe exchanger as influenced by the annual fuel escalation, inflation, interest, and tax rates is investigated. A 5-year and a 10-year service life and 750 hours of operation per year are the assumptions used in the economic analysis.

Experimental results show that up to 18 percent of the energy can be saved in a concurrent-flow dryer by the use of a heat pipe exchanger.

Fouling in a heat pipe exchanger results in increased pressure drop rather than in decreased heat transfer. To prevent the heat exchanger blockage, particles larger than .6 mm must be filtered out of the grain dryer exhaust air prior to entry into the heat exchanger. At least twice a year cleaning is recommended for the heat exchanger surface area.

Heat recovery with and without a heat pipe exchanger was investigated by simulation. Results show that direct recirculation in concurrent-counter-flow dryers yields comparable savings to those obtained when recycling is performed through a heat pipe exchanger. A combination of direct recycling of the cooler exhaust and, indirect recycling of the dryer exhaust through a heat pipe exchanger, reduces the energy consumption to about 2964 kj per kg of water removed, as compared to 3488 kj for a concurrent-flow dryer without recirculation and use of a heat pipe exchanger. Simulation results also show that the heat pipe exchanger in crossflow dryers is less profitable than in concurrent-flow dryers.

The annual fuel escalation, inflation rate, interest rate and the rate of taxation have significant effects on the profitability and the net present value of a heat pipe exchanger.

Approved *F. W. Bell*
Major Professor
11-1-77

Approved *D. R. Feldman*
Department Chairman

ACKNOWLEDGEMENTS

The author expresses his deep appreciation to his academic advisor Dr. F. W. Bakker-Arkema. Professor Bakker-Arkema's friendship and generous advice made the graduate study a joyful experience, and the present work possible.

Sincere appreciation is extended to Dr. L. J. Segerlind, Agricultural Engineering Department, Dr. M. C. Smith, Mechanical Engineering, Dr. J. R. Black, Agricultural Economics Department, and Dr. J. V. Beck of the Mechanical Engineering Department for their valuable advice during the author's academic program and this research.

The author appreciates the opportunity of being associated with the very special people of the Agricultural Engineering Department and particularly benefited from the processing group: Mitch Roth, Lloyd Lerew, Roger Brook, Edison Rugumayo, Larry Walker, Steve Kalchik, Dennis Kline, and Ralph Gygax.

Thankful acknowledgement is extended to the people of Iran who supported and inspired the author through the ministry of higher education to continue a profession in food production.

The financial support of the Andersons, Maumee, Ohio, is deeply appreciated.

To Gity

TABLE OF CONTENTS

	Page
ACKNOWLEDGEMENTS	ii
LIST OF TABLES	vi
LIST OF FIGURES	viii
LIST OF SYMBOLS	x
INTRODUCTION	1
OBJECTIVES	3
1. REVIEW OF LITERATURE	4
1.1 Grain drying	4
1.2 Heat pipe	9
1.3 Heat pipe exchangers	10
2. REVIEW OF HEAT PIPE PRINCIPLES	12
2.1 Introduction	12
2.2 Heat pipe construction	13
2.2.1 Pipe	14
2.2.2 Wick	14
2.2.3 Fluid	15
2.3 Heat pipe thermal transport capability.	16
3. HEAT PIPE EXCHANGER ANALYSIS.	24
3.1 Introduction	24
3.2 Heat pipe exchanger effectiveness.	27
3.2.1 Finite differences	31
3.2.2 Finite elements	38
3.3 Heat transfer coefficient and friction factor	50
3.4 Fouling factor	59
3.5 Profitability model	63
3.6 Simulation	66

	Page
4. EXPERIMENTAL.	69
4.1 Introduction.	69
4.2 Heat pipe exchanger	69
4.3 Grain dryer	71
5. HEAT PIPE EXCHANGER OPTIMIZATION.	78
5.1 Introduction.	78
5.2 Linear optimization	79
5.3 Nonlinear optimization.	88
5.3.1 Application to heat pipe exchanger	89
5.3.2 Results	91
6. RESULTS AND DISCUSSIONS	101
6.1 Introduction.	101
6.2 Laboratory test results	101
6.3 Simulation results	105
6.4 Economics of heat pipe exchanger.	112
6.4.1 Heat pipe exchanger and concurrentflow dryer	114
6.4.2 Heat pipe exchanger and commercial crossflow dryers	119
6.4.3 Heat pipe exchanger and batch type dryers	126
6.4.4 The effects of fouling on heat pipe exchanger economics	127
7. CONCLUSIONS	132
8. SUGGESTIONS FOR FUTURE WORK.	134
9. LIST OF REFERENCES	136
APPENDIX A	143
APPENDIX B	172

LIST OF TABLES

Table		Page
1-1	Energy requirements of different types of dryers to evaporate one kilogram of water from wet grain. . . .	5
2-1	Operating temperature range, melting and boiling points of some commercial heat pipe fluids	17
2-2	Physical and thermal properties of some of the commercial heat pipe fluids.	18
2-3	Typical resistances against the heat flow in a water-operated heat pipe	22
3-1	Comparison of high temperature heat recovery units . . .	26
3-2	Correlations for predicting the heat transfer coefficient and the pressure drop in a heat pipe exchanger. . . .	52
3-3	Dimensional specifications of finned tube heat exchangers, utilized in the comparison of heat transfer coefficient and pressure drop correlations	54
4-1	Performance characteristics and the construction of the experimental heat pipe exchanger, ISO-FIN, as specified by the manufacturer	70
4-2	Settings for the concurrent-counterflow dryer utilized in the soft wheat drying experiment	75
4-3	Settings for the concurrent-counterflow dryer utilized in the corn drying experiment	77
5-1	Tabulation of the sample linear programming problem. . .	87
5-2	The output of the linear programming optimization using the inputs of Table 5-1	87
5-3	A comparison between an optimal design of heat pipe exchanger with ISO-FIN unit	92
5-4	The Westelaken grain dryer specifications.	95
5-5	The inputs for optimal design of heat pipe exchangers for various models of Westelaken grain dryers	96
5-6	Comparison of different values of the convergence criterion for the optimal designed heat pipe exchanger	97

Table	Page
5-7 The optimal designed heat pipe exchangers for various models of Westelaken grain dryers.	99
5-8 The effect of fouling resistance on the optimal designed heat pipe exchanger for the Westelaken grain dryer Model 810-A	100
6-1 Heat pipe exchanger performance test results	102
6-2 Test results of wheat drying in a concurrent-counterflow dryer equipped with heat pipe exchanger	106
6-3 Test results of corn drying in a concurrent-counterflow dryer	107
6-4 Settings for simulation of the concurrent-counterflow grain dryer. Model 810-A	109
6-5 Simulated test results, using a heat pipe exchanger in the concurrent-counterflow dryer, the Westelaken Model 810-A	110
6-6 Simulated test results, using direct recycling, in the concurrent-counterflow dryer, the Westelaken Model 810-A	111
6-7 The effect of drying temperature on the savings, as a result of simulating the use of a heat pipe exchanger in the concurrent-counterflow dryer Model 810-A	113
6-8 Present (first year) costs and savings data for use in the profitability analysis of heat pipe exchangers, used in different models of the Westelaken grain dryers	115
6-9 Cashflow and net present value analysis of different sizes of heat pipe exchangers, used in the Westelaken grain dryers	116
6-10 Some typical dimensions and process values of a commercial crossflow dryer manufactured by Ferrel-Ross Co., Saginaw, Michigan	123
6-11 Input for the optimal design and output specifying the optimal designed heat pipe exchanger for use in the Ferrel-Ross crossflow dryer	124
6-12 Annual cashflow and net present value analysis of the optimal heat pipe exchanger, used in the Ferrel-Ross crossflow dryer	125
6-13 Particle size and the weight percentage in a typical exhaust air from a crossflow dryer	130

LIST OF FIGURES

Figure		Page
2-1	The principle of heat pipe operation	13a
2-2	A tubular heat pipe construction and operation	13a
2-3	A thermosyphon construction and operation	13a
2-4	Heat path through a heat pipe and its analogy to an electrical resistance network	21
3-1	A bundle of heat pipes in a housing	25
3-2	A cross section of heat pipe exchanger parallel to the airflow.	32
3-3	Specific humidity of the air-vapor mixture in the element and on the fin surface in a heat pipe exchanger	33
3-4	The psychrometrics of the air-vapor mixture in a heat pipe exchanger	33
3-5	A section of the heat pipe (or a solid bar) for which equation 3-41 is written	40
3-6	Division of a heat pipe exchanger into square grids	42
3-7	A typical element with the specified nodes	42
3-8	Heat transfer coefficient predicted by different correlations for various surface configurations	55
3-9	Pressure drop predicted by different correlations for various surface configurations	56
3-10	Heat transfer coefficient versus airflow for surface G (Table 3-3), predicted by different correlations	57
3-11	Pressure drop versus airflow for surface G (Table 3-3) predicted by different correlations	58
3-12	Fouling resistance versus time for systems in which the deposition rate predominates (Curve A) and in which the removal rate increases with the fouling thickness (Curve B)	61

Figure	Page
3-13	A flow chart of the subroutine "PROCESS". 67
4-1	Experimental set up for the performance tests of the heat pipe exchanger 72
4-2	Schematic of the concurrent-counterflow dryer used in the wheat drying experiments 74
4-3	Schematic of the concurrent-counterflow dryer used in the corn drying experiments 76
5-1	Box (COMPLEX ALGORITHM) logic diagram 90
5-2	Westelaken grain dryer 94
6-1	Deviations of the predicted energy savings from the experimental values; (0 line) 104
6-2	Net present value as a function of fuel escalation and tax rate, for a heat pipe exchanger life of 5 and 10 years of service; and 750 hours of operation per year 118
6-3	Net present value as a function of fuel escalation and inflation rate for a heat pipe exchanger life of 5 and 10 years of service; and 750 hours of operation per year 120
6-4	Net present value as a function of fuel escalation and discounted cashflow rate of return (DCFR), for a heat pipe exchanger life of 5 and 10 years of service; and 750 hours of operation per year. 121
6-5	Ferrel-Ross recirculating crossflow dryer 122
6-6	The effect of fouling thickness on the total annual costs and savings of a heat pipe exchanger specified for the Westelaken grain dryer Model 810-A 128
6-7	Time required for the fouling thickness to reach to the critical thickness for various values of removal rate (K_2); see equation 3-108 129

LIST OF SYMBOLS

A	Heat transfer area	m ²
A _C	Minimum free flow area	m ²
A _f	Finned area	m ²
AO	Annual operating cost	\$
AS	Annual fuel savings	\$
A _w	Wick cross sectional area	m ²
A _y	Pipe or a solid bar cross sectional area	m ²
C	Specific heat	kJ/kg-°C
C _d	Duct concentration	kg/kg
CF _k	Cashflow at year k	\$
CI _k	Cash income at year k	\$
D	Pipe diameter	m
D	Diffusion coefficient	m ² /s
D	Depreciation	\$
DCF _k	Discounted cashflow at year k	\$
DCFR _k	Discounted cashflow rate of return	\$
D _h	Hydraulic diameter	m
e	Enthalpy	kJ/kg
EUC	Electricity unit cost	\$
f	Friction factor	-
f	Annual fuel escalation	decimal
FC	First costs	\$
FP	Friction power	kWhr

FUC	Fuel unit cost	\$/million kg
G	Mass velocity	kg/hr - m ²
G _{max}	Maximum mass velocity based on the minimum free flow area	kg/hr - m ²
g	Gravity acceleration	9.8 m/s ²
h	Convective heat transfer coefficient	W/m ² - °C
h _{fg}	Heat of vaporization	kJ/kg
H	Fin height	m
Hr	Operating hours per year	hr
i	True interest rate	decimal
j	Energy	joule
j	Rate of inflation	decimal
K	Thermal conductivity	W/m - °C
K ₁	Constant	
K ₂	Constant	
kw	Wick permeability	m ²
KWH	Kilowatt hours	kWhr
L	Pipe length	m
ℓ	Heat exchanger depth	m
m	Flow rate	kg/hr
n	Number of years of service life	years
N _f	Number of fins per cm	decimal
NPV	Net present value	\$
N _r	Number of rows	-
O	Operating costs at year, k	\$
p	Perimeter	m ²
P	Pressure	N/m ² , P _a (Pascal)
P ₁ , P ₂ , P ₃	Constants	

Q	Heat transfer rate	kJ/hr
R	Resistance against heat flow	°C/W
R	Exhaust ratios	decimal
r_c	Wick pore radius	m
s	Seconds	s
s	Distance between fins	m
s_l	Longitudinal pitch	m
s_t	Transverse pitch	m
S	Slope of the condensation line	
S_k	Fuel savings at year, k	\$
T	Temperature	°C
t	Time	hr
t	Fin thickness	m
t	Tax rate	decimal
U	Overall heat transfer coefficient	W/m ² - °C
U_m	Convective mass transfer coefficient	Kg/m ² - s
V	Volume	m ³
V_c	Free volume	m ³
v	Velocity	m/s
W	Humidity ratio	decimal
WB	Wet basis	
x_f	Fouling thickness	m

Subscripts

a	air side
b	bare pipe (without fin)
c	cold side
ci	cold side inlet
co	cold side outlet

d	dust
f	fin, fluid, fouling
eff	effective
g	air-vapor mixture
h	hot side
hi	hot side inlet
ho	hot side outlet
i	inlet, inside
j	year j
k	year k
l	liquid
m	metal, mixture
o	outlet, outside
r	radial
s	saturation
t	pipe, tube
uf	unfinned
v	vapor
w	wick, wall

Greek symbols

Δ	Difference	
ϵ	Heat exchanger performance effectiveness	
η	Heat exchanger surface effectiveness	
θ	Wetting angle	degrees
μ	Viscosity	kg/m - hr
ρ	Density	kg/m ³
σ	Liquid surface tension	N/m

τ	Shear stress	P_a
ϕ	Heat pipe tilt angle	degrees
ϕ_d	Rate of deposition	m/hr
ϕ_r	Rate of removal	m/hr
<u>Dimensionless numbers</u>		
Eu	Euler number	$g_c \frac{\Delta p}{\rho v^2}$
Nu	Nusselt number	$\frac{hD_o}{K}$
Pr	Prandtl number	$\frac{C_p \mu}{K}$
Re	Reynolds	$\frac{\rho v D_o}{\mu}$
Sc	Schmidt number	$\frac{\mu}{\rho D}$

INTRODUCTION

The grain drying process consumes more than 65 percent of the total energy used for on-farm corn production. To dry 100 kg of corn from 25 percent to 15 percent moisture content (WB), an energy expenditure of 3500 to 8000 kj is required in a conventional dryer. The United States produced more than 1.58×10^8 tons of corn in 1976. Assuming that 75 percent was artificially dried for safe storage, it can be estimated that 7.15×10^7 m³ of LP gas was consumed for the drying process. As the fuel availability decreases and its price escalates, the proportion of drying to the overall production cost will increase. To preserve the grain quality, to keep the costs down, and to match up with a high capacity harvesting operation, improved or new drying methods must be devised.

Considerable research and development are carried out to improve the energy utilization of grain dryers. The advent of the new, continuous flow concurrent grain dryers is the result of such endeavors. Preliminary investigations have shown that concurrent flow dryers are more efficient in energy utilization than the conventional dryers. The efficiency may further be improved by using a proper heat recovery unit to capture the exhausted heat.

Applications of heat exchangers in grain dryers have always been of interest. The low efficiency of air to air heat transfer results in large surface areas and high initial costs which are the two main obstacles

in the heat exchanger application. Heat pipes capable of transporting a large amount of heat are promising devices for the heat recovery applications in grain dryers.

A heat pipe is a closed pipe into which a small amount of fluid has been introduced. When heat is applied to one end of the pipe the fluid evaporates and the vapor travels to the other end of the pipe where it condenses. The condensate flows back to the evaporator by either gravitational forces or capillary pumping or both. Because vaporization and condensation take place at a constant temperature, the rate of heat transfer along the pipe will be high. As a result, the heat pipe becomes an excellent thermal conductor. A bundle of these pipes equipped with fins in a housing forms a compact heat exchanger that is referred to here as "heat pipe exchanger". The heat pipe exchanger is able to exchange heat between the supply and exhaust air streams in a grain dryer.

OBJECTIVES

The objectives of this study are to evaluate the technical and economic aspects of the heat pipe and to investigate the future potential of this device in grain drying operations. The following steps are to be followed in the analysis:

- a) the heat transfer coefficient, pressure drop and fouling in a heat pipe exchanger along with the performance of the individual heat pipes will be analyzed and the proper mathematical relationships will be developed;
- b) a profitability analysis of the heat pipe exchanger will be performed in conjunction with commercial concurrent flow grain dryers, and the analysis will include the effects of interest rate, inflation rate, and fuel escalation on the project profitability;
- c) an optimization procedure for design and analysis of an optimum heat pipe exchanger will be developed and utilized;
- d) a set of experiments will be performed to validate the computer programs.

1. REVIEW OF LITERATURE

1.1 Grain drying

Artificial grain drying in the United States was first practiced in 1947 using World War II bomber engine heaters (Foster et al., 1976). Since then commercial grain dryers have been manufactured to dry large quantities of wet grain harvested with high capacity combines. These dryers dry large volumes of grain by using a high temperature and a high airflow rate. Grain exposed to high temperatures is susceptible to breakage in subsequent handlings, and may not be suitable for some end uses (Brooker et al., 1975). Serious quality problems have prompted researchers to look for new ways of grain drying which not only ensure a high capacity, but also result in a better quality grain. The high rate of energy consumption in grain dryers becomes a serious problem as energy prices increase. Theoretically 2258 kj is required for one kg of water at 100°C to evaporate at atmospheric pressure. To the above energy, an additional amount has to be added in the grain drying process for sensible heating of the grain, and moving the grain and the air. Depending on the design, commercial dryers consume from about 3500 to about 8000 kj of heat energy to extract 1 kg of water from the grain. Table 1-1 shows energy requirements of different types of dryers.

One type of dryer that shows promising features is of the concurrent type. In this dryer the grain and drying air flow in the same direction.

Table 1-1. Energy requirements of different types of dryers to evaporate one kilogram of water from wet grain.

<u>Type of Dryer</u>	<u>kJ/kg</u>	<u>Specific Conditions</u>	<u>Source</u>
Layer drying 15 cm deep (wheat)	4290 - 8350	Inlet air 32°C Inlet humidity Ratio .0085 kg/kg	Woodforde and Lawton (1965)
Batch drying 61 cm deep (wheat)	2845 - 5194	Inlet air 15°C	Clark and Lamond (1968)
Modified cross-flow	3700	Air partially recycled	Converse (1972)
Modified cross-flow	3000	Corn dried from 22 to 15.5%	Lerew et al. (1972)
Concurrent flow with counterflow cooler	3387	Corn dried from 21.7 to 16.4% (Anderson design)	Anderson (1972)
Crossflow (conventional)	5803	5-point removal optimized conditions	Morey and Lueschen (1974)
Fixed-bed	2456	Heat pipe and heat pump	Lai et al. (1975)
Concurrent flow with counterflow cooler	4062	5-point removal (Westelaken design)	Westelaken (1977)

The air and grain reach an equilibrium temperature well below the inlet air temperature within a few centimeters from the top. Therefore, high temperature air with high flow rates can be used without damaging the grain due to excessive heat. This dryer not only preserves the quality of the grain, but also proves to be efficient in energy consumption (Graham, 1967). Becker and Isaacson (1971) simulated a concurrent-flow dryer in a wheat drying experiment and reported favorable results in energy consumption and in grain quality. Carano et al. (1971) built a laboratory size concurrent grain dryer with a counterflow cooler; the dryer was tested for quality and drying performance. Anderson (1972) reported the experimental results of a commercially sized concurrent dryer and confirmed the favorable energy and quality characteristics. Bakker-Arkema et al. (1972) after an evaluation of different grain dryer types stated that "the concurrent flow dryer should be considered more seriously in future designs because of its favorable quality characteristics".

The majority of the commercial continuous dryers are of crossflow type. In these dryers a moving layer of grain about 30-45 cm thick is exposed to the drying air. Uneven drying and short residence time for the air in the bed makes the crossflow dryers the least efficient dryer as far as energy and grain quality are concerned.

A number of modifications have been done to improve crossflow grain dryers. Converse (1972) conducted a series of tests with a recirculating crossflow dryer (the Hart-Carter Model), and reported a 50 percent decrease in energy consumption. However, the resulting quality of the dried grain was not investigated. Lerew et al. (1972) reported a value of 3084 kJ per kg of water removed when a modified crossflow was

simulated. In these analyses the recirculating air is a mixture of the exhaust air from the middle and the bottom sections of a three-stage crossflow column. New commercially available recirculating crossflow dryers such as the ones manufactured by Ferrel-Ross (Anon, 1977) and Beard Industries (Noyes, 1977) have been claimed to improve the energy efficiency and to preserve the grain quality.

Much of the on-farm grain drying takes place in a fixed-bed type grain dryer. In these operations a stationary layer of grain with a depth from .3 to several meters is dried using heated or natural air. There have been many changes and improvements both in fixed-bed drying equipment (circulating grain, stirring, fluidized, etc.) and the drying process (dryeration, low temperature drying, etc.) to make the operation economical in terms of energy consumption and quality grain. Brooker et al. (1975) presented a comprehensive review of these innovations and listed the advantages and disadvantages of each system.

Definition of a dryer's efficiency is expressed differently by various researchers. In order to standardize this definition, Bakker-Arkema et al. (1973) proposed a new dryer performance evaluation index (DPEI). The index is a measure of the total energy required by a dryer to remove one kg of water from grain dried under a set of specified conditions. Later Bakker-Arkema et al. (1974) introduced a variety of computer programs to evaluate the design parameters affecting the "DPEI" values.

Although the concurrent dryers are more efficient than the other types, the exhausted air temperatures are high enough to motivate further investigations to recycle the waste heat back into the system. Roth et al. (1973) simulated a heat exchanger in conjunction with a closed

loop recirculating counterflow heater and counterflow cooler. They showed that the theoretical DPEI can be reduced to almost zero under ideal conditions. Roth and DeBoer (1973) optimized a concurrent-counterflow grain dryer with and without the use of a heat exchanger. They found that utilizing a heat exchanger reduces the DPEI by more than 20 percent. Additional work on the same type of dryer by Bakker-Arkema et al. (1974) and Sokhansanj (1974) showed that fluids other than air in the heater section improve the efficiency of the heat exchanger.

Although heat exchangers proved to be effective in improving the energy efficiency of grain dryers, the problems of size and initial costs remained a question. Lai and Foster (1975) conducted preliminary investigations on the use of heat pipes in a batch type grain dryer. The dryer consisted of a cylindrical bin of .75 m diameter and a height of 1.2 m. The heat pipe exchanger was of a 6-row plate-finned type with a face area of .30x 38 m on each side. The heat pump consisted of a 3/4 hp compressor and a 3/4-ton refrigerator. The dryer exhaust was directed to the heat exchanger and then over the heat pump evaporator coil. The simulation results showed that with 21°C ambient air temperature and 49°C drying temperature energy savings of up to 30 percent with heat pipe only, and up to 55 percent with both heat pipe and heat pump can be obtained. However, the reported savings as a result of experiments were in order of 10 and 40 percent for heat pipe and for heat pipe and heat pump, respectively. Part of the discrepancy between the experimental and simulated results may be due to the inaccuracy of the simulation models.

Bakker-Arkema et al. (1975) optimized a system of heat pipes and concurrentflow dryer based on minimizing a cost objective function. An energy saving of 21 percent was obtained for a set of optimized conditions

(45 m³/min/m² airflow, 230°C drying air temperature, and 5 percent moisture removal); the present study is a follow-up to this study.

1.2 Heat pipe

According to NASA (1975) the first technical paper on the heat pipe was published by Grover et al. (1964). Since then a large number of references have appeared in the literature on all aspects of this device.

Feldman and Whiting (1968) reviewed the commercial applications of the device. Excellent reviews on the technology of the heat pipe were published by Winters and Barsch (1971). Asselman and Green (1973) gave details on the heat pipe theory and the principles of operation.

Rohani (1974) reported the limits of heat pipe operation when noncondensable gases are present in the pipe. The most recent publication on the heat pipe are books by Dunn and Reay (1976) and Chi (1976). In both books the design relationships, limitations, and manufacturing aspects of the heat pipes are discussed.

Parallel to the development of heat pipes, thermosyphon technology was investigated. A thermosyphon is a simple version of the heat pipe where condensate flows by gravity forces to the evaporator. Therefore, the wick is eliminated and as a result the construction of the pipe is simpler. The review by Japikse (1973) on the advances in thermosyphon technology is of practical interest. Streltsov (1975) presented simplified equations for calculating the heat transfer and the amount of working fluid in a thermosyphon.

1.3 Heat pipe exchangers

In spite of the commercial availability of heat pipe exchangers, not much research has been published in the open literature. Amode and Feldman (1975) reported the results of a test and an analysis of a heat pipe exchanger made from arterial¹ type heat pipes. Aronson (1976) and Ruch (1976) reported the application of heat pipes as heat recovery units, but did not give any specific data or relationships. Their report contains a detailed description of a heat pipe exchanger operation. At present the only available data is that published in the sales literature on some specific heat pipe exchangers.

One of the major problems in a heat pipe exchanger operation is fouling. There is not much reported research on the subject of fouling. The investigations usually are carried out by the manufacturing and process industries. However, in recent years some investigators have classified different modes of fouling and have proposed mathematical models. Among these investigations those by Friedlander and Johnston (1957), Kern and Seaton (1959), Beal (1970), and the excellent reviews by Taborek et al. (1972a, 1972b) are of practical interest. Most of these studies are on industrial fouling where the process fluids are of a liquid type. The proposed models are of a specific nature and cannot be applied to general cases.

The characteristics of dust particles emitted from grain dryers have not been investigated extensively. Converse (1971), expressed the need for removing dust particles from the grain dryer exhaust to comply to the state and federal regulations. Johnson (1976) recommended specially designed dust collectors for grain dryers. Meiering and Hoefkes (1976)

¹Heat pipes with a grooved inside wall.

investigated the type and size of the dust particles emitted from a number of crossflow grain dryers. Avant (1976) reported analysis and performance test results of a sorghum dust collection system.

2. REVIEW OF HEAT PIPE PRINCIPLES

2.1 Introduction

One way of transferring a large amount of heat with a small temperature difference is through a phase change process. Energy that is used for the evaporation of a liquid is transported through a duct by the vapors, and is released upon condensation. In order to perform the operation continuously the condensate must be returned to the evaporator. A completely closed container in which this process takes place is called a heat pipe or thermosyphon, depending on the way the condensate returns from the condenser to the evaporator.

The principle of heat pipe operation is shown in Figure 2.1. In the steady state, the temperature of the liquid in the condenser and the evaporator approximate the temperature of the heat sink (cold side), and the heat source (hot side), respectively. The difference in temperature results in difference in vapor pressure; consequently the vapor travels from the evaporator to the condenser. The depletion of the liquid by evaporation causes the vapor/liquid interface in the evaporator to retreat inward. The pressure of the liquid in the condenser is slightly higher than that in the evaporator. This pressure difference causes the liquid to travel from the condenser to the evaporator through the capillary structure of the wick. Since the temperature remains constant during the phase change, theoretically a considerable amount of heat can be transported with no or a very small temperature difference between the condenser

and evaporator. As a result the heat pipe has a high thermal conductivity.

Figure 2.2 shows a tubular heat pipe construction and operation. The heat pipe is equipped with circular fins to extend the heat transfer area. The pipe's external area is divided into a supply side (heat sink), and an exhaust side (heat source). The average pressure inside the pipe is the saturation pressure of the working fluid at the operating temperature. The performance of a heat pipe is often expressed in terms of equivalent thermal conductivity. A tubular heat pipe of the type illustrated in Figure 2.2, using water as a working fluid and operating at 150°C has a thermal conductivity several hundred times more than copper (Asselman and Green, 1973).

The thermosyphon is a simple version of the heat pipe in which the wick has been eliminated. Thermosyphons are used in a vertical position where the gravity facilitates the return of the condensate to the evaporator (Figure 2.3). To wet the wall evenly the inside wall of a thermosyphon is usually grooved. Except for capillary pumping, other features of the thermosyphon are identical to those of the heat pipe.

2.2 Heat pipe construction

There are three main components in a heat pipe: (1) the pipe, (2) the wick, and (3) the fluid.

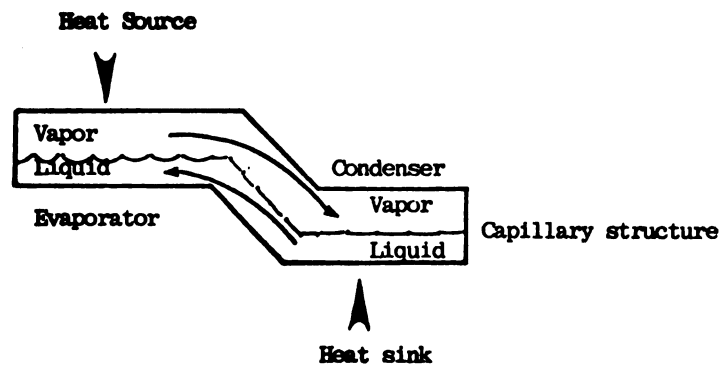


Figure 2-1. The principle of heat pipe operation

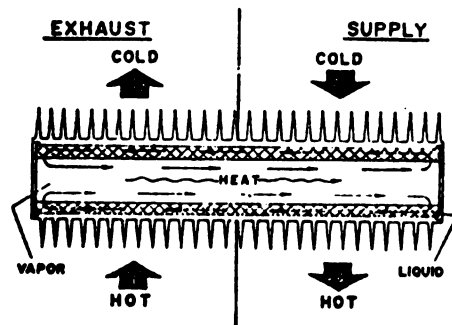


Figure 2-2. A tubular heat pipe construction and operation.

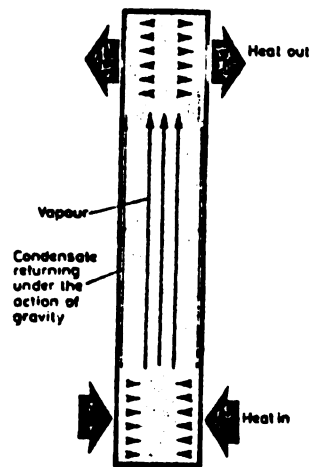


Figure 2-3. A thermosyphon construction and operation.

2.2.1 Pipe

The pipe separates the working fluid from the surrounding environment. The pipe is usually equipped with circular or plate fins on the outside to increase the heat transfer area. The pipe material must be compatible with the wick and fluid. Generation of non-condensable gases and subsequent corrosion of the pipe is a result of the incompatibility of the pipe material and the fluid. Non-condensable gases in the pipe also block the transfer of the fluid and vapor along the complete length of the pipe and sharply reduce thermal conductivity and the effective length of the pipe. Copper, aluminum and stainless steel are the most common materials used in heat pipe construction. The pipe diameter is usually in the range of 15 to 25 mm. The pipe wall thickness is about 1.25 mm. The length of the heat pipes used in thermal recovery devices ranges from 30 cm to 125 cm. The circular or plate fins on the external surface of the pipes range from 2 to 6 fins per cm. The height and thickness of the fins is 30-50 mm and .3-.5mm, respectively.

2.2.2 Wick

The wick is a porous layer that forms the capillary structure of the pipe. The prime function of a wick is to generate a capillary pressure sufficient to transport the working fluid from the condenser to the evaporator. The wick also provides a means of spreading the working fluid evenly throughout the pipe.

The wick performance greatly depends on the construction material and the geometry of the pipe. Usually, the most expensive and hard to

manufacture part of a heat pipe is the wick. Materials such as monel beads, nickel powder, and fiberglass have been developed for heat pipes. A layer of this material is bonded to the inside surface of the pipe wall. The selection of the wick depends on the type of operation and performance expected from the heat pipe. Wicks with a large pore size are suitable for gravity assisted flows, while wicks with small pores have inherently high capillary pumping capability.

The wick thickness depends on the type of wick. A typical value for a wick made from wire mesh is .058 cm for a 1 cm pipe diameter. Sometimes, the inside wall is grooved for the condensate return (arterial wicks). By this method the amount of wick material is either reduced or totally eliminated. A combination of arteries and porous materials usually improves the performance of the heat pipe.

The overall cost of a heat pipe depends largely on the structure, materials, and manufacturing practices of the pipe and its wick. It is important not to choose pipes with expensive wicks for applications where gravity may be used. A simple and cheap arterial structure probably will serve the purpose.

2.2.3 Fluid

The fluid is the medium through which the energy is transferred from one end of the pipe to the other end. A proper fluid must have a high latent heat, high surface tension, and high thermal stability. Chemical compatibility between the fluid, the wick and the pipe material, is the prime requirement. To prevent fluid degradation a high thermal stability is needed. Often it is necessary to keep the operating temperature of a heat pipe below a specified value to prevent fluid breakdown.

A high surface tension is required in order to enable the heat pipe to work against gravity, and as a result the fluid can flow uphill from the condenser to the evaporator. It is necessary for the fluid to wet the wick and the pipe in order to generate a high heat transfer coefficient and to spread heat evenly throughout the pipe surface. A high latent heat of vaporization is desirable to transfer large amounts of heat with a minimum amount of liquid in the pipe. Thermal conductivity of the fluid should be high to reduce the radial temperature gradient and the possibility of nucleate boiling at the interface of the wall or the wick and the fluid.

The amount of fluid in the pipe should be sufficient to wet the wick plus a small amount to flow freely for safe and efficient operation. The pipe is vacuumed thoroughly prior to the filling. Tables 2-1 and 2-2 list some of the characteristics of some commercial working fluids used in heat pipes.

2.3 Heat pipe thermal transport capability

The maximum heat that a heat pipe is able to transport depends on the rate of fluid flow inside the pipe:

$$Q = m h_{fg} \quad (2-1)$$

Where m is a function of the working fluid properties such as density, viscosity, and surface tension, and of the wick properties such as pore radius, permeability, and thickness.

The expression for m can be developed from a pressure balance in the pipe. The result is given by Dunn and Reay (1976):

Table 2-1. Operating temperature range, melting and boiling points of some commercial heat pipe fluids.¹

	Melting Point °C	Boiling Point °C	Useful Operating Range °C		
	<hr/>	<hr/>	<hr/>	<hr/>	<hr/>
Ammonia	-18	-33	-60	to	100
Freon 113	-35	48	-10	to	100
Methanol	-98	64	10	to	130
Water	0	100	30	to	200

Source: Dunn and Reay (1976)

¹For complete properties of the fluids, see Table 2-2

Table 2-2. Physical and thermal properties of some of the commercial heat pipe fluids.

Temp.	Latent heat	Liquid density	Vapor density	Liquid thermal cond.	Liquid viscos.	Vapor viscos.	Vapor spec. heat	Liquid surface tension	Vapor pressure
°C	h_{fg} kJ/kg	ρ_l kg/m ³	ρ_v kg/m ³	k_l W/m°C	μ_l Ns/m ²	μ_v Ns/m ²	C_v kg/kg°C	σ N/m	P_v pa x 10 ⁵
Ammonia	1101	580	12.0	.272	.020	.116	2.16	1.833	15.34
Freon - 113	536	768	1.05	.175	.0269	.086	2.22	2.12	.6
Methanol	1085	746	1.47	.201	.0314	.111	1.61	1.85	1.31
Water	2258	958	.60	.680	.028	.127	1.88	5.89	1.01

Source: Dunn and Reay (1976)

$$m = \frac{\rho_l \text{ kw } A_w}{\mu_l L_{\text{eff}}} \left(\frac{2 \sigma_l}{r_c} \cos\theta - \rho_l g L_{\text{eff}} \sin\theta \right) \quad (2-2)$$

For a typical water heat pipe of 2 cm bore size and 30 cm long, operating at 100°C, the values of m and Q will be calculated for horizontal heat transport under the following conditions:

- (1) The wick is made of a 4-layer, 100-mesh wire with a diameter of .0045 cm; the thickness of the 4-layer is .036 cm,
- (2) The pore radius of this wire mesh, r_c is .002 cm and the permeability kw, is $1.52 \times 10^{-10} \text{ m}^2$
- (3) Using the water properties at 100°C with $h_{fg} = 2.256 \times 10^6$ kJ/kg and the assumption of perfect wetting, equation (2-2) becomes:

$$m = \frac{958 \times 1.52 \times 10^{-10} \times .226 \times 10^{-4}}{.283 \times 10^{-3} \times .3} \left(\frac{2 \times .0589}{.02 \times 10^{-3}} \right)$$

$$= 2.28 \times 10^{-4} \text{ kg/s}$$

and $Q = 2.28 \times 10^{-4} \times 2.256 \times 10^6$

$$= 51.2 \text{ j/s or W}$$

The heat transport capability of a thermosyphon reported by Streltsov (1975) is:

$$Q = \frac{4}{3} \pi D_o \left[\frac{h_{fg} \rho_l g K_l^3 (\Delta T)^3 L_h^3 L_c^3}{4 \mu_f (L_h + L_c)^3} \right]^{1/4} \quad (2-3)$$

where ΔT is the temperature difference between the condenser and the evaporator.

As it is indicated in Figure 2-4, heat transfer through a heat pipe is analogous to an electrical resistance network. In Table 2-3 typical values of the resistances are shown for a water heat pipe. The resistances to the heat flow in the vapor duct, vapor/liquid, and liquid/vapor interface are small compared to those between the outside surface and the air stream flowing over the pipes. The axial heat conduction through the pipe wall can be neglected, because its resistance value is large compared with the resistance of the vapor in the duct. Radial conduction strongly depends on the dimensions and the material properties of the wick and the pipe. The radial resistance can be found from the following relationship:

$$R_{wr} = \frac{\ln\left(\frac{D_o}{D_i}\right)}{2 \pi K_t L} \quad (2-4)$$

The value of the radial resistance in a copper heat pipe of 30 cm length, 2.5 cm diameter and a wall thickness of .25 cm is about $1.89 \times 10^{-4} \text{ }^\circ\text{C/W}$.

The operating temperature of a pipe depends on the ratio of the heat transfer coefficients of hot and the cold sides of the heat exchanger. To find the operating temperature, an energy balance over the pipe is written:

$$C (T_{th} - T_{tc}) = h_h L_h (T_h - T_{th}) + h_c L_c (T_c - T_{tc}) \quad (2-5)$$

Assuming equal lengths on the hot and cold sides of the heat exchanger and isothermal operation of the pipe:

$$T_{th} = T_{tc} = T_t$$

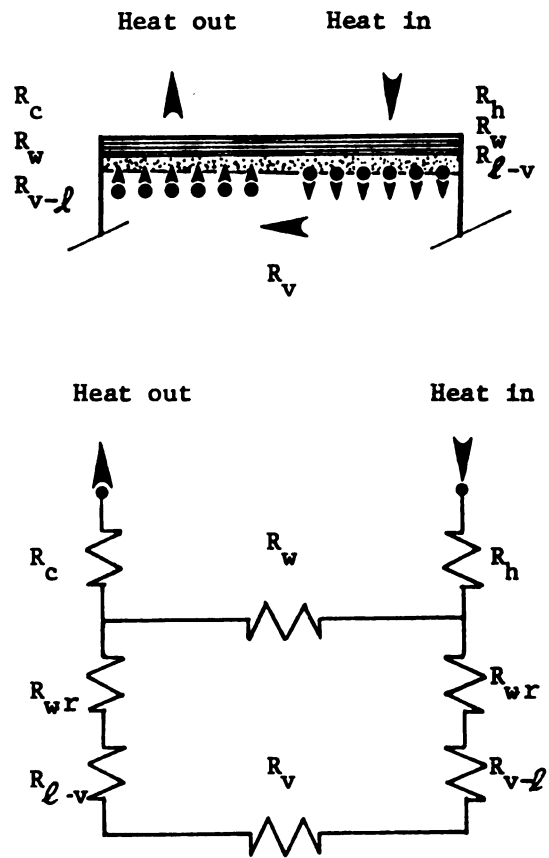


Fig. 2-4. Heat path through a heat pipe and its analogy to an electrical resistance network.

Table 2-3. Typical resistances against the heat flow in a water-operated heat pipe.

<u>Resistance*</u>	<u>°C/W</u>
R_c , R_h	$10^3 - 10$
R_w	$10 - 1$
$R_{\ell - v}$	10^{-5}
R_v	10^{-8}
$R_{v - \ell}$	10^{-5}

Source: Asselman and Green (1972)

*See Figure 2-4 for the nomenclature.

$$\text{and} \quad L_h = L_c \quad (2-6)$$

solving equation (2-5) for the heat pipe temperature gives:

$$T_t = \frac{T_h + H T_c}{(H + 1)} \quad (2-7)$$

$$\text{where:} \quad H = \frac{h_c}{h_h}$$

Equation (2-7) indicates that the average temperature of the pipe and so the vapor, in the duct approaches the temperature of the hot side if $h_h > h_c$, and to that of the cold side if $h_c > h_h$.

3. HEAT PIPE EXCHANGER ANALYSIS

3.1 Introduction

The heat pipe exchanger consists of a bundle of finned heat pipes placed in a housing (Figure 3-1) and separated into two sections by a partition. The hot air flows through the exhaust side while the cold air passes through the supply side. The evaporator section of the heat pipes is located in the exhaust side and the condenser in the supply side.

The pipes are either individually equipped with circular fins, or they are bundled in a series of plate fins. The arrangement of the pipes is usually staggered forming several rows. The typical distance between two pipes in a row is about 6.4 cm, center to center, and the longitudinal distance between two rows is about 4.4 cm. The commercially available heat pipe exchangers usually have 4 to 8 rows and the face surface area ranges from 2800 cm² to 30,000 cm².

A heat pipe exchanger is similar in construction to circular and plate type compact heat exchangers. In the operation, a heat pipe exchanger is similar to a liquid-coupled heat exchanger. The cooling system of an automobile engine is an example of a liquid-coupled heat exchanger. A comparison between different types of heat exchangers including the heat pipe is given in Table 3-1. Heat pipes are more efficient than other types of heat recovery units, because of low pressure drops and high overall heat transfer coefficients, as is indicated in

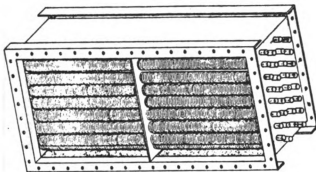


Figure 3-1. A bundle of heat pipes in a housing

Source: Isothermics (1976)

Table 3-1. Comparison of high temperature heat recovery units.

Unit Type	Pressure Drop	Heat Transfer Film Coefficient	Cost	Auxiliary Power	Cross Contamination	Transfer Area Per Volume
Regenerators	Mod	High	High	Yes	Yes	High
Shell & Tube	High	High	Mod	No	No	Low
Plate-Fin	Low	Mod	High	No	No	Very High
Secondary Fluid	Low	Low	High	Yes	No	Mod
Heat Pipe	Low	High	Mod	No	No	High

*Source: Hughes Electron Dynamic Division (1975)

Table 3-1. The partition separates the supply side and the exhaust side to prevent cross contamination.

In the following sections the parameters and relationships which govern the performance of a heat pipe exchanger are identified. The performance relationships will be coded in FORTRAN and the predicted results will be compared with experimental data.

3.2 Heat pipe exchanger effectiveness

The effectiveness of a heat exchanger is measured by determining its ability to transfer heat from the hot side to the cold side. The maximum heat available to be transferred in a counterflow arrangement can be written:

$$Q_{\max} = m_{\min} (e_{hi} - e_{ci}) \quad (3-1)$$

where m_{\min} is the minimum flow rate, the smaller value of m_h and m_c .

The ratio of the heat gain by the cold side or the heat loss by the hot side to Q_{\max} (whichever has the minimum value of m) is called the effectiveness:

$$\epsilon = Q_h / Q_{\max} \quad \text{if} \quad m_{\min} = m_h \quad (3-2)$$

$$\epsilon = Q_c / Q_{\max} \quad \text{if} \quad m_{\min} = m_c \quad (3-3)$$

$$\text{where: } Q_c = m_c (e_{co} - e_{ci}) \quad (3-4)$$

$$Q = m_h (e_{hi} - e_{ho}) \quad (3-5)$$

and the enthalpy (e) is:

$$e = 419 W + C T \quad (3-6)$$

$$\text{where } C = C_a + C_v W \quad (3-7)$$

The heat exchanger effectiveness (ϵ), has been related to the ratio of $UA/(mc)_{\min}$ by Kays and London (1964). The ratio is called the number of transfer units (NTU). The ϵ - NTU relationships for a counterflow heat exchanger is:

$$\epsilon = \frac{1 - \exp[-NTU(1 - (mc)_{\min}/(mc)_{\max})]}{1 - (mc)_{\min}/(mc)_{\max} \exp[-NTU(1 - (mc)_{\min}/(mc)_{\max})]} \quad (3-8)$$

For the case of $(mc)_{\min}/(mc)_{\max} = 1$, equation (3-8) reduces to:

$$\epsilon = \frac{NTU}{1 + NTU} \quad (3-9)$$

To obtain the rate of heat transfer, Q can be written as:

$$Q = U A \Delta T_{\ln} \quad (3-10)$$

Where ΔT_{\ln} , the log mean temperature difference, is obtained from:

$$\Delta T_{\ln} = \frac{(T_{ho} - T_{ci}) - (T_{hi} - T_{co})}{\ln[(T_{ho} - T_{ci})/(T_{hi} - T_{co})]} \quad (3-11)$$

Equations (3-1) through (3-5) are written based on the overall enthalpy difference rather than the temperature difference. The reason for the choice is that the exhaust air from the dryer usually contains large quantities of water vapor that will condense on the exchanger upon cooling. However, the enthalpy difference reduces to the temperature difference if there is no condensation.

For the evaluation of U_m , ASHRAE (1974) and McQuiston (1975) suggested to use:

$$U_m = \frac{U_h}{C_h} \times 10^{-3} \quad (3-12)$$

for the situations where the diffusion rates of the water vapor to the wall is low. When the rate of diffusion is high due to excessive amounts of vapor in the air stream, Mizushina (1974) suggested modification of equation (3-12) to:

$$U_m = \frac{U_h}{aC_h} \times 10^{-3} \quad (3-13)$$

where:

$$a = \frac{P_a - P_g}{P_a - P_{st}} \left(\frac{Sc}{Pr} \right)^{1/2} \quad (3-14)$$

ASHRAE (1974) gave a value of .845 for Sc/Pr ratio in case of air-water vapor mixtures. P_{st} , the saturation vapor pressure is evaluated at the pipe temperature. The pipe temperature is obtained using equation (2-7), for each element. C_h , can be evaluated by using equation (3-7).

The overall heat transfer coefficient (U) is defined as:

$$\frac{1}{U} = \frac{1}{h_c \eta_c} + \frac{1}{h_h \eta_h} + R_f + R_m \quad (3-15)$$

The fin surface effectivenesses, η_h and η_c , are developed based on the effectiveness of the individual fins. The effective surface area of a finned tube heat exchanger is:

$$A_{\text{eff}} = A_{\text{uf}} + A_f \eta_f \quad (3-16)$$

Equation (3-16) can be used to define the extended surface area effectiveness:

$$\frac{A_{\text{eff}}}{A} = \frac{A_{\text{uf}}}{A} + \frac{A_f}{A} \eta_f \quad (3-17)$$

also,

$$\eta = 1 - \frac{A_f}{A} (1 - \eta_f) \quad (3-18)$$

Where η_f , the individual fin effectiveness is the ratio of the actual heat transferred from a fin to the heat that would be transferred if the entire fin area was at the base temperature. For a long square fin of uniform thickness, the fin effectiveness is:

$$\eta_f = \frac{\tanh(bh)}{bh} \quad (3-19)$$

where

$$b = \left(\frac{2h}{K_f t} \right)^{1/2} \quad (3-20)$$

Equation (3-19) can be used for circular fins with less than 8 percent error (Holman, 1976).

The effectiveness of a wet surface is affected by the condensate film. McQuiston (1975) added the latent heat to the heat balance over a fin and consequently modified equation (3-20) to:

$$b = \left[\frac{2h}{K_f t} \left(1 + \frac{S}{aC} h_{fg} \right) \right]^{1/2} \quad (3-21)$$

The slope of condensation line (S) will be discussed in the next section. Equation (3-21) reduces to (3-20) when there is no condensation (S = 0).

The value of η_f for a wet fin is 2 to 3 percent lower than that of a dry surface. Rich (1973) expressed the metal resistance R_m by:

$$R_m = \left(\frac{1 - \eta}{\eta} \right) R_a + R_{wr} \quad (3-22)$$

Equation (3-8) will be used to calculate the effectiveness of the heat exchanger when the humidity ratio of the exhaust air is low (this will be discussed in Chapter 6). Knowing the effectiveness, the heat transfer rate is calculated from equations (3-2) and (3-3), and the outlet conditions from equations (3-4) and (3-5).

Although the foregoing procedure is fast and simple, it fails to predict the effectiveness and the outlet conditions correctly since the exhaust air humidity is sufficiently high (more than .05 kg/kg) to release large amounts of latent heat upon condensation. For such cases the heat exchanger must be divided in smaller segments for the analysis. In the following sections two such analysis methods are developed.

3.2.1 Finite differences

A cross section parallel to the airflow in a 6-row heat pipe exchanger is shown in Figure 3-2. The heat exchanger is divided into 6 elements each containing one row of heat pipes. Assuming a constant flow rate in the

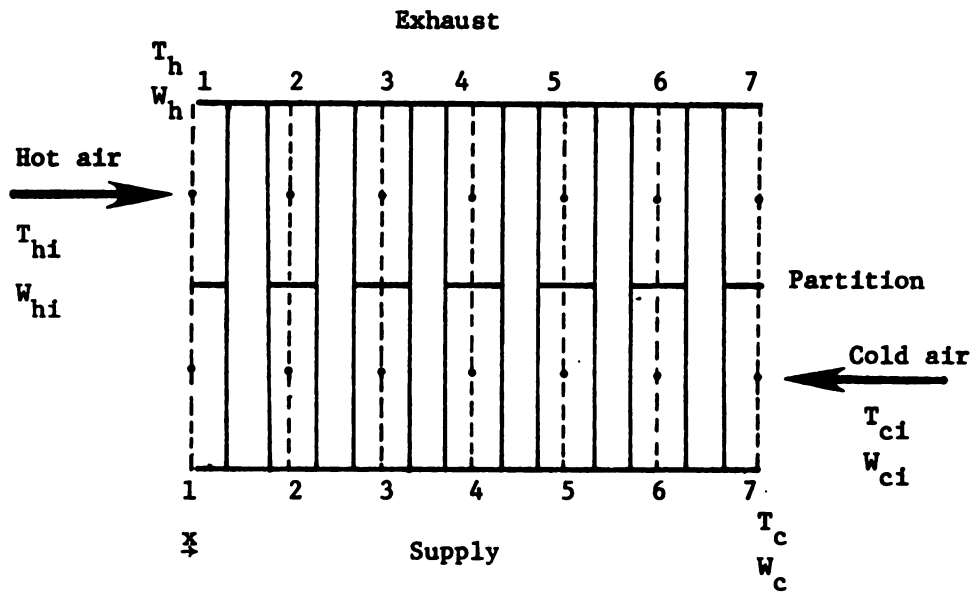


Figure 3-2. A cross section of heat pipe exchanger parallel to the airflow.

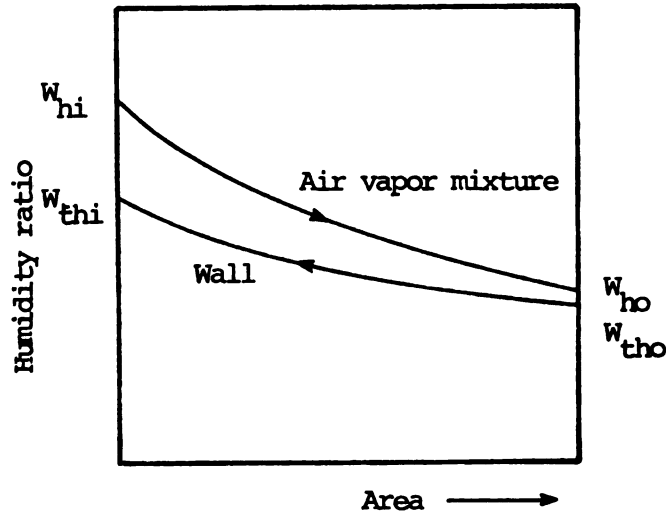


Fig. 3-3. Specific humidity of the air-vapor mixture in the element and on the fin surface in a heat pipe exchanger.

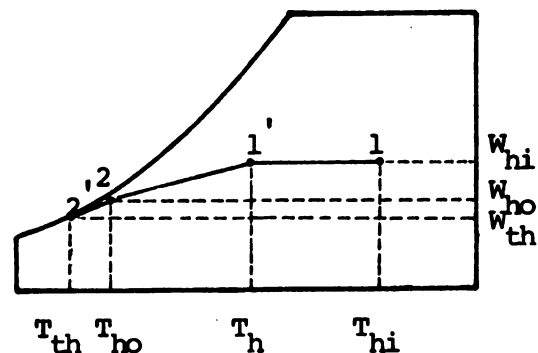


Fig. 3-4. The psychrometrics of the air-vapor mixture in a heat pipe exchanger. Point 1 depicts the inlet air, and point 1' represents the air at a point where the wall temperature is below the air dew point temperature; point 2 approximates the outlet air condition; and point 2' represents the condition of the air close to the wall at the exit.

heat exchanger the energy balance on each of the elements can be written:

for the hot side:

$$\begin{aligned} dQ &= m_h C_h dT_h + m_h dw h_{fg} & (3-23) \\ &= U_m dA (W_h - W_{th}) h_{fg} + U_h dA (T_h - T_{th}) \end{aligned}$$

and for the cold side:

$$\begin{aligned} dQ &= m_c C_c dT_c & (3-24) \\ &= U_c dA (T_{tc} - T_c) \end{aligned}$$

Equation (3-23) for the hot side is based on the total enthalpy since the possibility of condensation exists. In equation (3-24) the terms associated with the heat of condensation are absent because the air at the cold side is gaining sensible heat.

dA is the average surface area of the row of heat pipes (and fins) in each element. dw is the amount of water condensed from the hot air in an element.

In a counterflow arrangement the inlet temperatures, T_{hi} and T_{ci} and humidity ratios W_{hi} and W_{ci} are the known values (Figure 3-2).

In order to find the temperatures and humidities, equations (3-23) and (3-24) must be written for every element of the exchanger and then solved simultaneously. Before writing these equations, proper relationships are required for expressing humidities in terms of temperatures. The humidity ratio of the air and the humidity ratio at the wall in an element are shown in Figure 3-3. As the figure shows the humidity ratio of the air decreases continuously and approaches a value close to that of the wall. In Figure 3-4 the state of the air is shown on a psychrometric chart, as the air proceeds through an element. Point 1 depicts

the temperature and humidity ratio of the air at the entrance point of an element. The air cools down as it reaches a point where the wall surface temperature is below the air dew-point temperature (Point 1'). Point 2 approximates the state of the leaving air at the exit point of the element. The condition at the wall surface corresponding to the outlet air is depicted by Point 2'.

Mizushina (1974) and McQuiston (1975) showed experimentally that the broken line 1-1'-2-2' can be approximated by a straight line, or:

$$S = \frac{W_h - W_{th}}{T_h - T_{th}} \quad (3-25)$$

or:

$$W_h - W_{th} = S (T_h - T_{th})$$

Also:

$$W_{hi} - W_{ho} = S (T_{hi} - T_{ho})$$

or:

$$dW_h = S dT_h \quad (3-26)$$

Substituting equations (3-25) and (3-26) in (3-23) and (3-24) gives:

$$dQ = (m_h C_h + m_h Sh_{fg}) dT_h \quad (3-27)$$

$$dQ = (U_m Sh_{fg} + U_h) (T_h - T_{th}) dA \quad (3-28)$$

Rearranging equations (3-27) and (3-24) gives:

$$dT_h = dQ \left(\frac{1}{m_h C_h + m_h Sh_{fg}} \right) \quad (3-29)$$

$$dT_c = dQ \left(\frac{1}{m_c C_c} \right) \quad (3-30)$$

Combining equation (3-29) and (3-30) results in:

$$dT_h - dT_c = \left[\frac{1}{m_h (C_h + Sh_{fg})} - \frac{1}{m_c C_c} \right] dQ \quad (3-31)$$

Equation (3-28) and the second part of equation (3-24) are combined to give the temperature differences:

$$T_h - T_{th} = \frac{dQ}{(U_m S h_{fg} + U_h) dA} \quad (3-32)$$

$$T_{tc} - T_c = \frac{dQ}{U_c dA} \quad (3-33)$$

Assuming the heat pipe is isothermal, addition of equation (3-32) to equation (3-33) and solving for (dQ) gives:

$$dQ = U dA (T_h - T_c) \quad (3-34a)$$

where:

$$\frac{1}{U} = \frac{1}{U_m S h_{fg} + U_h} + \frac{1}{U_c} \quad (3-34b)$$

Substituting (dQ) from equation (3-34) into equation (3-31) yields:

$$d(T_h - T_c) = U dA c (T_h - T_c) \quad (3-35)$$

where:

$$c = \frac{1}{m_h (C_h + Sh_{fg})} + \frac{1}{m_c C_c}$$

An overall energy balance also holds on the two air streams in the element.

Equating equations (3-24) and (3-27) yields:

$$dT_h = R dT_c \quad (3-36)$$

where:

$$R = \frac{m_c C_c}{m_h (C_h + S h_{fg})}$$

Equations (3-35) and (3-36) are the two main relationships to be written for the elements. The quantities U_c , U_h , h_{fg} , m_c , m_h , and C_c are assumed to be constant throughout the heat exchanger. U_m , the convective mass transfer coefficient, C_h the heat capacity of the mixture of air-vapor, and S the slope of condensation line have to be evaluated in each element.

Equations (3-35) and (3-36) will be solved by finite difference techniques:

$$(T_h - T_c)_x - (T_h - T_c)_{x + \Delta x} = dA U_c (T_h - T_c)_{x + 1/2 \Delta x} \quad (3-37)$$

and

$$T_{hx} - T_{hx + \Delta x} = R (T_{cx} - T_{cx + \Delta x}) \quad (3-38)$$

where:

$$(T_h - T_c)_{x + 1/2 \Delta x} \quad \text{can be approximated by:}$$

$$\frac{(T_h - T_c)_x + (T_h - T_c)_{x + \Delta x}}{2}$$

Equations (3-37) and (3-38) can be simplified and rearranged:

$$T_{hx} (1 - b) + T_{cx} (-1 + b) + T_{hx + \Delta x} (-1 + b) + T_{cx + \Delta x} (1 + b) = 0 \quad (3-39)$$

$$T_{hx} (+1) + T_{cx} (-R) + T_{hx + \Delta x} (-1) + T_{cx + \Delta x} (R) = 0 \quad (3-40)$$

where

$$b = \frac{dA U}{2} \left[\frac{1}{m_h (C_h + S h_{fg})} + \frac{1}{m_c C_c} \right]$$

Equations (3-39) and (3-40) are written for all elements and after substituting for the known temperatures T_{h1} and T_{c7} (Figure 3-2) the resulting matrix can be solved for the rest of temperatures. An iteration scheme is utilized to calculate the constants in case of condensation and to reconstruct and evaluate the matrix.

3.2.2 Finite elements

In the foregoing discussion the assumption was made that the pipes are isothermal and thus the temperature stays constant along the pipe. This temperature can be calculated from equation (2-7). For the cases where an effective thermal conductivity can be defined for the heat pipe or where some other means of heat transport such as a solid copper bar replaces the heat pipe, the assumption of isothermality is not valid. For a solid bar which gains or loses heat in a stream of air, the temperature profile in the axial direction is found from the following

differential equation:

$$K A_y \frac{d^2 T_t}{dy^2} = U p (T - T_t) \quad (3-41)$$

Equation (3-41) is derived by writing a heat balance on an element of the pipe shown in Figure (3-5). When there is condensation on the pipe an additional term, which represents the heat released by the condensed vapor, is added to the equation (3-41):

$$K A_y \frac{d^2 T_t}{dy^2} = U p (T - T_t) + U_m p (W - W_t) \quad (3-42)$$

Simplifying equation (3-42) by using equations (3-13) and (3-26) and rearranging results in:

$$\frac{d^2 T_t}{dy^2} = \frac{U p}{K A_y} (T - T_t) \left(1 + \frac{S}{a C} h_{fg} \right) \quad (3-43)$$

A theorem from the calculus of variations states that the points that satisfy equation (3-43) will also minimize the following integral:

$$X = \int_v \frac{1}{2} K \left(\frac{dT_t}{dy} \right)^2 dv + \int_s \frac{1}{2} U (T_t - T)^2 ds \quad (3-44)$$

For the case of equation (3-44) where (U) contains more than one term:

$$X = \int_v \frac{1}{2} K \left(\frac{dT_t}{dy} \right)^2 dv + \frac{1}{2} U \left(1 + \frac{S}{a C} h_{fg} \right) \int_s (T_t - T)^2 ds \quad (3-45)$$

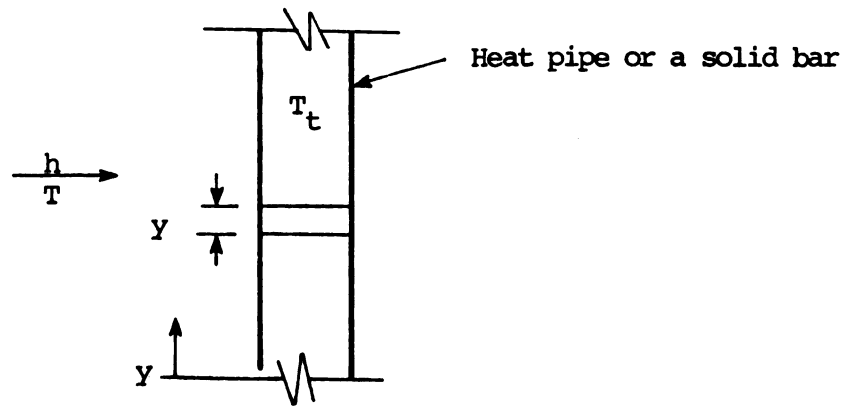


Fig. 3-5. A section of the heat pipe (or a solid bar) for which equation 3-41 is written.

The exchanger is divided into square elements (Figure 3-6). Each element contains a small segment of the pipe in the middle. The nodal points are located in the middle of each side. Equation (3-45) must be written and evaluated for each element.

Nodes 1 and 3 in Figure 3-7 are on the pipe and nodes 2 and 4 represent the state of the process stream at the inlet and outlet locations. The section of the tube in the element depicts a one-dimensional element. It will be assumed that temperature changes linearly over the length of the pipe in this element (Seegerlind, 1976):

$$T = C_1 + C_2 Y \quad (3-46)$$

with the following boundaries:

$$T(Y_1) = T_1 \quad (3-47)$$

$$T(Y_3) = T_3 \quad (3-48)$$

Applying the boundary conditions, solving for C_1 and C_2 , and substituting back in equation (3-46) will give:

$$T = N_1 T_1 + N_3 T_3 \quad (3-49)$$

where

$$N_1 = \frac{Y_3 - Y}{L} \quad (3-50)$$

$$N_3 = \frac{Y - Y_1}{L} \quad (3-51)$$

N_1 and N_3 are called shape functions.

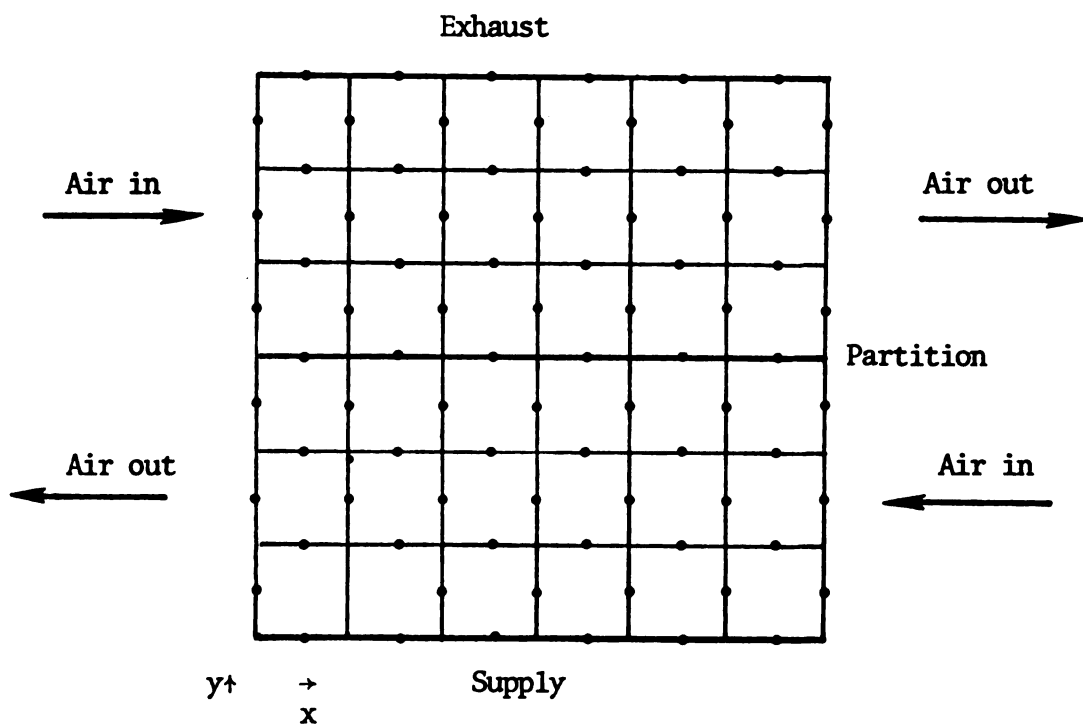


Fig. 3-6. Division of a heat pipe exchanger into square grids.

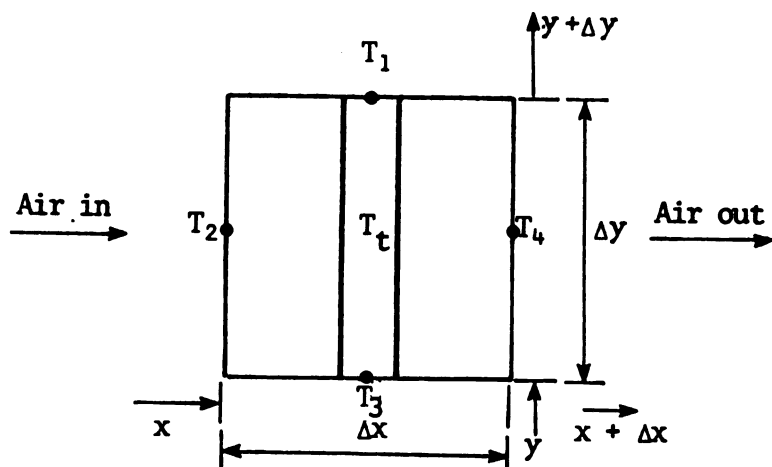


Fig. 3-7. A typical element with the specified nodes.

The temperature profile in the element can be written in terms of the four nodes:

$$T = N_1 T_1 + N_2 T_2 + N_3 T_3 + N_4 T_4 \quad (3-52)$$

The shape functions associated with nodes 2 and 4 do not enter into the coordinate system, so their values are zero:

$$T = N_1 T_1 + 0 T_2 + N_3 T_3 + 0 T_4 \quad (3-53)$$

In matrix notation, (3-53) becomes :

$$T = [N] \{T\} \quad (3-54)$$

where $[N]$ is a row matrix:

$$[N] = [N_1 \ 0 \ N_3 \ 0] \quad (3-55)$$

and $\{T\}$ is a column matrix:

$$\{T\} = \begin{Bmatrix} T_1 \\ T_2 \\ T_3 \\ T_4 \end{Bmatrix} \quad (3-56)$$

Differentiating T with respect to Y in (3-54) yields:

$$\frac{dT}{dY} = \frac{dN}{dY} \{T\} \quad (3-57)$$

Let

$$[g] = \left[\frac{dT}{dY} \right] \quad (3-58)$$

and

$$[B] = \left[\frac{dN}{dY} \right] = \left[\frac{dN_1}{dY} \ 0 \ \frac{dN_3}{dY} \ 0 \right] \quad (3-59)$$

Then (3-57) can be written:

$$[g] = [B] \{T\} \quad (3-60)$$

and its transpose

$$[g]^T = \{T\}^T [B]^T \quad (3-61)$$

Substituting (3-54), (3-57), (3-60) and (3-61) in (3-45) will give:

$$\begin{aligned} X = & \int_V \frac{1}{2} K [g]^T [g] dv + \frac{1}{2} U \left(1 + \frac{S}{C} h_{fg} \right) \int_S \{ [T - T_2]^T [T - T_2] \\ & + [T - T_4]^T [T - T_4] \} ds \end{aligned} \quad (3-62)$$

where

$$\begin{aligned} [T - T_2] &= [N_1 T_1 + 0 T_2 + N_3 T_3 + 0 T_4 - T_2] \\ &= [N_1 T_1 - T_2 + N_3 T_3 + 0 T_4] \end{aligned}$$

or

$$[T - T_2] = [N_1 \quad -1 \quad N_3 \quad 0] \begin{pmatrix} T_1 \\ T_2 \\ T_3 \\ T_4 \end{pmatrix}$$

Let

$$[\phi] = [N_1 \quad -1 \quad N_3 \quad 0]$$

then

$$[T - T_2] = [\phi] \{T\} \quad (3-63)$$

and

$$[T - T_2]^T = \{T\}^T [\phi]^T \quad (3-64)$$

Similarly it can be written for $[T - T_4]$:

let

$$[\psi] = [N_1 \quad 0 \quad N_3 \quad -1] \quad (3-65)$$

then

$$[T - T_k] = [\psi] \{T\} \quad (3-66)$$

and

$$[T - T_k]^T = \{T\}^T [\psi]^T \quad (3-67)$$

Substituting equations (3-63), (3-64), (3-66) and (3-67) in equation (3-60) and expanding, gives:

$$X = \int_V \frac{1}{2} K \{T\}^T [B]^T [B] \{T\} dv + \frac{1}{2} U \left(1 + \frac{S}{C} h_{fg}\right) \left\{ \int_{S_2} \{T\}^T [\phi]^T [\phi] \{T\} ds_2 + \int_{S_4} \{T\}^T [\psi]^T [\psi] \{T\} ds_4 \right\} \quad (3-68)$$

s_2 and s_4 refer to each half side of the pipe surface area exposed to the nodes 2 and 4, respectively.

Equation (3-68) is the one to be minimized with respect to the temperatures in order to find stationary points where the differential equation (3-43) will be satisfied.

Differentiation of X in equation (3-68) with respect to $\{T\}$ and equating the result to zero will give:

$$\frac{\partial X}{\partial \{T\}} = K \int_V [B]^T [B] \{T\} dv + U \left(1 + \frac{h_{fg}}{C_p} S\right) \left\{ \int_{S_2} [\phi]^T [\phi] \{T\} ds_2 + \int_{S_4} [\psi]^T [\psi] \{T\} ds_4 \right\} = 0 \quad (3-69)$$

Each integral in equation (3-67) can be evaluated separately as follows:

a. Evaluation of: $K \int_V [B]^T [B] \{T\} dv \quad (3-70)$

Substituting equation (3-59) in expression (3-70) yields:

$$K \int_V \begin{Bmatrix} \frac{dN_1}{dY} \\ 0 \\ \frac{dN_2}{dY} \\ 0 \end{Bmatrix} \begin{bmatrix} \frac{dN_1}{dY} & 0 & \frac{dN_2}{dY} & 0 \end{bmatrix} \begin{Bmatrix} T_1 \\ T_2 \\ T_3 \\ T_4 \end{Bmatrix} dv \quad (3-71)$$

Differentiating the shape functions with respect to Y and substituting in expression (3-71) gives:

$$K \int_V \begin{Bmatrix} -1/L \\ 0 \\ 1/L \\ 0 \end{Bmatrix} \begin{bmatrix} -\frac{1}{L} & 0 & \frac{1}{L} & 0 \end{bmatrix} \begin{Bmatrix} T_1 \\ T_2 \\ T_3 \\ T_4 \end{Bmatrix} dv \quad (3-72)$$

and after multiplication:

$$K \int_V \begin{bmatrix} 1/L^2 & 0 & -1/L^2 & 0 \\ 0 & 0 & 0 & 0 \\ 1/L^2 & 0 & 1/L^2 & 0 \\ 0 & 0 & 0 & 0 \end{bmatrix} \begin{Bmatrix} T_1 \\ T_2 \\ T_3 \\ T_4 \end{Bmatrix} dv \quad (3-73)$$

The cross section of the pipe is constant therefore we can write:

$$dv = A dL \quad (3-74)$$

Integration of expression (3-73) between 0 and L, after substituting equation (3-74) for (dv) gives:

$$\frac{KA}{L} \begin{bmatrix} 1 & 0 & -1 & 0 \\ 0 & 0 & 0 & 0 \\ -1 & 0 & 1 & 0 \\ 0 & 0 & 0 & 0 \end{bmatrix} \begin{Bmatrix} T_1 \\ T_2 \\ T_3 \\ T_4 \end{Bmatrix} \quad (3-75)$$

The ratio $\frac{KA}{L}$ can be replaced by $1/R$ where R is the heat pipe thermal resistance

$$b. \text{ Evaluation of: } \int_{S_2} [\phi]^T [\phi] \{T\} ds_2 \quad (3-76)$$

When $[\phi]$ is replaced by its defining elements and the matrix multiplication is carried out, the elements of the resulting square matrix will contain terms of second order in Y . Integration of this matrix is rather difficult. In order to avoid the complexity, the shape functions will be replaced by the area coordinates. Area coordinates, ratio of areas, have been originally developed for a triangular element (Seegerlind, 1976). The area coordinate for a one-dimensional element is a local coordinate having the origin at one of the nodes. L_1 and L_3 , the area coordinates replacing the shape functions N_1 and N_3 have the same properties as the shape functions. Integration equations for the area coordinates over length, area and volume are tabulated, and can be applied to the square matrix resulting from expression (3-76).

Substituting L_1 for N_1 and L_3 for N_3 in (3-63) gives:

$$\phi = [L_1 - 1 \quad L_3 \quad 0] \quad (3-77)$$

expression (3-76) can be written:

$$\int_{S_2} \begin{Bmatrix} L_1 \\ -1 \\ L_3 \\ 0 \end{Bmatrix} \begin{bmatrix} L_1 & -1 & L_3 & 0 \end{bmatrix} \begin{Bmatrix} T_1 \\ T_2 \\ T_3 \\ T_4 \end{Bmatrix} ds_2 \quad (3-78)$$

or

$$\Pi \frac{D}{2} \int_1 \begin{bmatrix} L_1^2 & -L_1 & L_1 L_3 & 0 \\ -L_1 & 1 & -L_3 & 0 \\ L_1 L_3 & -L_3 & L_3^2 & 0 \\ 0 & 0 & 0 & 0 \end{bmatrix} \begin{Bmatrix} T_1 \\ T_2 \\ T_3 \\ T_4 \end{Bmatrix} dL \quad (3-79)$$

In expression (3-79) ds_2 has been replaced by half of the pipe surface area:

$$ds_2 = \pi \frac{D}{2} dL \quad (3-80)$$

Using the tabulated integration formulas for area coordinates (Seegerlind, 1976), we get:

$$\int L_1^2 dL = \frac{L}{3} \quad (3-81)$$

$$\int L_1 L_3 dL = \frac{L}{6} \quad (3-82)$$

$$\int L_1 dL = \frac{L}{2} \quad (3-83)$$

Substituting equations (3-81) through (3-83) in expression (3-79) will yield:

$$\frac{\pi DL}{12} \begin{bmatrix} 2 & -3 & 1 & 0 \\ -3 & 6 & -3 & 0 \\ 1 & -3 & 2 & 0 \\ 0 & 0 & 0 & 0 \end{bmatrix} \begin{Bmatrix} T_1 \\ T_2 \\ T_3 \\ T_4 \end{Bmatrix} \quad (3-84)$$

Similarly it can be written

$$\int_{s_4} [\psi]^T [\psi] \{T\} ds_4 = \frac{\pi DL}{12} \begin{bmatrix} 2 & 0 & 1 & -3 \\ 0 & 0 & 0 & 0 \\ 1 & 0 & 2 & -3 \\ -3 & 0 & -3 & 6 \end{bmatrix} \begin{Bmatrix} T_1 \\ T_2 \\ T_3 \\ T_4 \end{Bmatrix} \quad (3-85)$$

Substituting equations (3-75), (3-84), and (3-85) in equation (3-69) results in:

$$\frac{KA}{L} \begin{bmatrix} 1 & 0 & -1 & 0 \\ 0 & 0 & 0 & 0 \\ -1 & 0 & 1 & 0 \\ 0 & 0 & 0 & 0 \end{bmatrix} \begin{Bmatrix} T_1 \\ T_2 \\ T_3 \\ T_4 \end{Bmatrix} + U \left(1 + \frac{h_{fg}}{C_p} \right) \frac{IDL}{12} \begin{bmatrix} 4 & -3 & 2 & -3 \\ -3 & 6 & -3 & 0 \\ 2 & -3 & 4 & -3 \\ -3 & 0 & -3 & 6 \end{bmatrix} \begin{Bmatrix} T_1 \\ T_2 \\ T_3 \\ T_4 \end{Bmatrix} = 0 \quad (3-86)$$

$$\text{Let } C_1 = \frac{KA}{L}$$

$$\text{and } C_2 = \frac{IDL}{12} U \left(1 + \frac{h_{fg}}{C} S \right)$$

Then (3-86) can be written

$$\begin{bmatrix} C_1 + 4C_2 & -3C_2 & -C_1 + 2C_2 & -3C_2 \\ -3C_2 & 6C_2 & -3C_2 & 0 \\ -C_1 + 2C_2 & -3C_2 & C_1 + 4C_2 & -3C_2 \\ -3C_2 & 0 & -3C_2 & 6C_2 \end{bmatrix} \begin{Bmatrix} T_1 \\ T_2 \\ T_3 \\ T_4 \end{Bmatrix} = \begin{Bmatrix} 0 \\ 0 \\ 0 \\ 0 \end{Bmatrix} \quad (3-87)$$

$$\text{or } \quad [k] \quad \{T\} = \{f\} \quad (3-88)$$

The matrix $[k]$ and $\{f\}$ are called the element stiffness matrix and the element force vector respectively. The vector $\{T\}$ contains the unknown temperature. Similar equations are written and then evaluated for every element. All elemental equations have to be assembled into a global matrix. The method of "direct stiffness" as explained by Segerlind (1976) is efficient method of performing the assembling process. The force matrix initially has zero terms, but when the boundary conditions are applied, the global system will be modified to incorporate the known temperatures. As a result of this modification some of the zero terms in the force matrix

are replaced by non zero values, and the system of equations becomes non-homogenous.

3.3 Heat transfer coefficient and friction factor

The performance of a heat pipe exchanger greatly depends on the heat transfer coefficient and friction factor. These values in turn depend on the Reynolds number and other process variables such as temperature and humidity of the process streams. Kays and London (1964) reported their extensive investigations on the performance of compact heat exchangers for some specific surface configurations. Further investigations by McQuiston and Tree (1972), Guillory and McQuiston (1973) and Rich (1973 and 1975) analysed the effect of design variables on the performance of the compact heat exchangers.

It is customary to approximate a heat exchanger surface by models for which the performance data is available. There are no mathematical models to cover the wide range of variables and to calculate the heat transfer coefficient and friction factor for different values of the Reynolds number. The empirical models are usually limited to a specific type of heat exchanger and the predicted values by the empirical relationship are often within ± 20 percent of the actual values (Rohsenow and Hartnet, 1973).

Shephard (1956) showed that for air at low velocities of about 1 m/s the heat transfer coefficient is about 28 to 34 $W/m^2-^{\circ}C$, and a pressure drop of 3 mm of water. The manufacturers (Hughes, 1975; Isothermics, 1975; Q-Dot, 1976) of the heat pipe exchangers usually require a face velocity of about 2.54 m/s for an efficient design

resulting in an h value of about $60 \text{ W/m}^2\text{-}^\circ\text{C}$. The pressure drop resulting from the specified velocity is about 5 mm of water. Table 3-2 contains some of the equations found in the literature that have been applied to the design and analysis of finned tube heat exchangers.

In order to choose the proper correlations for heat transfer and pressure drop, eight different sizes of circular finned tubes were chosen from Kays and London (1964). Table 3-3 contains the dimensions of the selected heat exchangers along with a given alphabetical designation. The pressure was calculated by using the following equation:

$$\Delta P = f \frac{\rho V^2}{2g} \frac{l}{D_h} \quad (3-89)$$

A program that was written for the WANG 2200 Computer facilitated the generation of data for different surfaces by different correlations. The results are presented in graphical form in Figures 3-8, 3-9, 3-10, and 3-11. An airflow of $53 \text{ m}^3/\text{min-m}^2$ was used for Figures 3-9 and 3-10. For Figures 3-11 and 3-12, airflows of 23, 53, 230 and $530 \text{ m}^3/\text{min-m}^2$ were chosen.

Figure 3-8 shows the heat transfer coefficients as predicted by different correlations for different heat exchanger sizes. The predictions follow a similar pattern indicating that each variable has similar effects on the correlation. The heat transfer coefficient varies from 17 ± 6 to $80 \pm 12 \text{ W/m}^2\text{-}^\circ\text{C}$. Commercial heat pipe exchangers have specifications similar to the groups D and G in Table 3-3. For these groups the heat transfer coefficient is between 15 and $30 \text{ W/m}^2\text{-}^\circ\text{C}$. The data from Kays and London (1964) fall somewhere in between; Mirkovich's correlation predicts the lowest and McQuiston's the highest. Perry's

Table 3-2. Correlations for predicting the heat transfer coefficient and the pressure drop in a heat pipe exchanger.

McQuiston (1972) and Schmidt (1949) :

$$Nu = h_b [1 - .217 (H/s)^{.469}] \left(\frac{D_h}{K_f} \right) \quad (3-90)$$

and

$$f = .33 [1 - .467 (H/s)^{.298}] Re^{-.2} \quad (3-91)$$

where (h_b), the heat transfer coefficient on the bare tubes :

$$h_b = .8 v_{\max}^{.6} / D_0^{.4} \quad (\text{Perry, 1974}) \quad (3-92)$$

Mirkovich (1974) :

$$Nu = .244 (s'-1)^{.1} (r'-1)^{-.15} \left(\frac{1 - N_f t}{N_f H} \right)^{-.25} Re_h^{.67} Pr^{.33} \quad (3-93)$$

$$Eu = 3.96 (s'-1)^{.14} (r'-1)^{-.18} \left(\frac{1 - N_f t}{N_f H} \right)^{-.2} Re_f^{-.31} \quad (3-94)$$

where

$$s' = s_t / D_0, \quad r' = s_l / D_0 \quad (3-95)$$

$$Re_h = d_t G / \mu \quad \text{where} \quad d_t = \frac{2 A}{P_{fII}} \quad (3-96)$$

$$\text{and} \quad Re_f = d_h G / \mu \quad \text{where} \quad d_h = \frac{4 Vc}{V} \quad (3-97)$$

Perry (1974) :

$$Nu = .45 Re^{.625} R_f^{-.375} Pr^{1/3} \quad (3-98)$$

where

$$R_f = \frac{A_f}{A}$$

Jameson (1945) :

$$4P = 3.99 \times 10^{-9} D_e^{-.25} N_r G^{1.75} \quad (3-99)$$

(Table 3-2 continued)

where

$$D_e = \frac{d_t}{\left[\left(\frac{H}{2s} \right)^4 \left(\frac{1}{2\sqrt{s'-1}} + \frac{1}{2\sqrt{r'-1}} \right) \right]^4} \quad (3-100)$$

Rohsenow and Hartnet (1973) :

$$Nu = .135 \left(\frac{D_0 G_{max}}{\mu} \right)^{.681} Pr^{1/3} \left(\frac{s}{H} \right)^{.2} \left(\frac{s}{t} \right)^{.113} \quad (3-101)$$

$$f = 18.93 \left(\frac{D_0 G_{max}}{\mu} \right)^{-.316} (s')^{-.927} \left(\frac{s_t}{s_l} \right)^{.515}$$

$$\Delta P = 61 f N_r G_{max}^2 / (g\rho) \quad (3-102)$$

Table 3-3. Dimensional specifications of finned tube heat exchangers, utilized in the comparison of heat transfer coefficient and pressure drop correlations.

Model designation	Tube diam cm	Fin diam cm	Fin thick cm	Trans pitch cm	Long pitch cm	Fins ¹ per cm	Max No. of pipes in a row	No. of rows
A	.96	2.34	.046	2.48	2.03	2.89	4	6
B	1.64	2.85	.065	3.13	3.43	2.76	4	6
C	1.97	4.17	.031	3.96	4.45	3.56	4	6
D	2.60	4.41	.031	4.98	5.24	3.46	4	6
E	1.97	3.72	.031	6.92	4.45	3.56	4	6
F	1.97	3.72	.031	6.92	4.45	3.56	10	6
G	2.60	4.41	.031	7.82	5.24	3.46	4	6
H	1.97	3.72	.031	6.92	4.45	3.56	4	10

Source : Kays and London (1964)

¹Number of fins of a pipe divided by the length of the pipe.

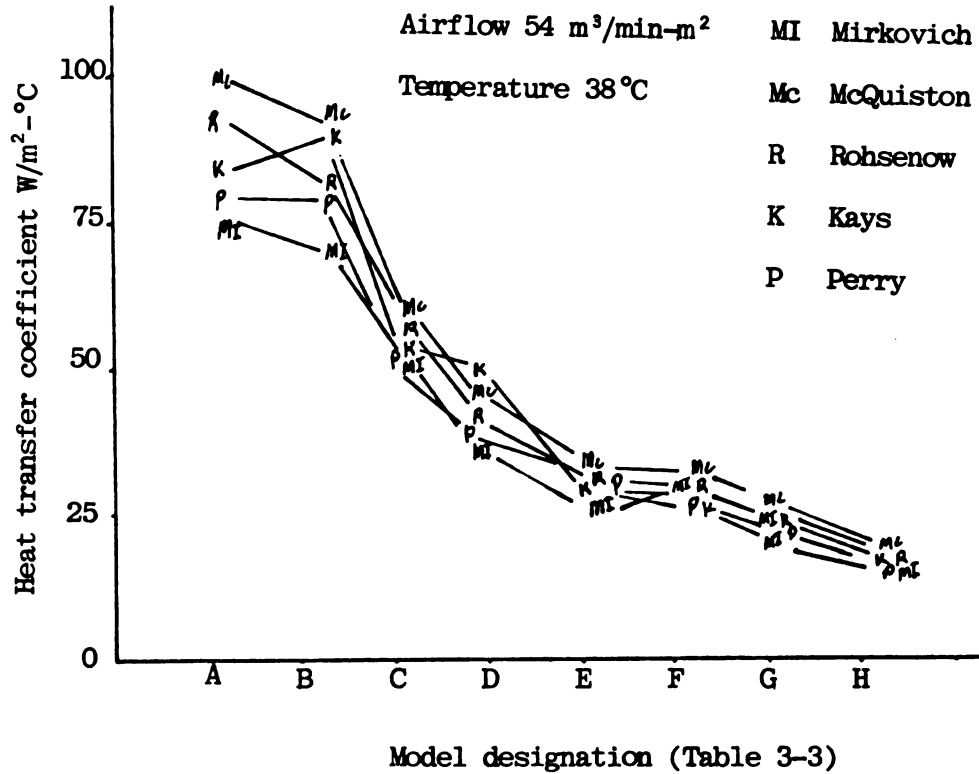


Figure 3-8. Heat transfer coefficient predicted by different correlations for various surface configurations.

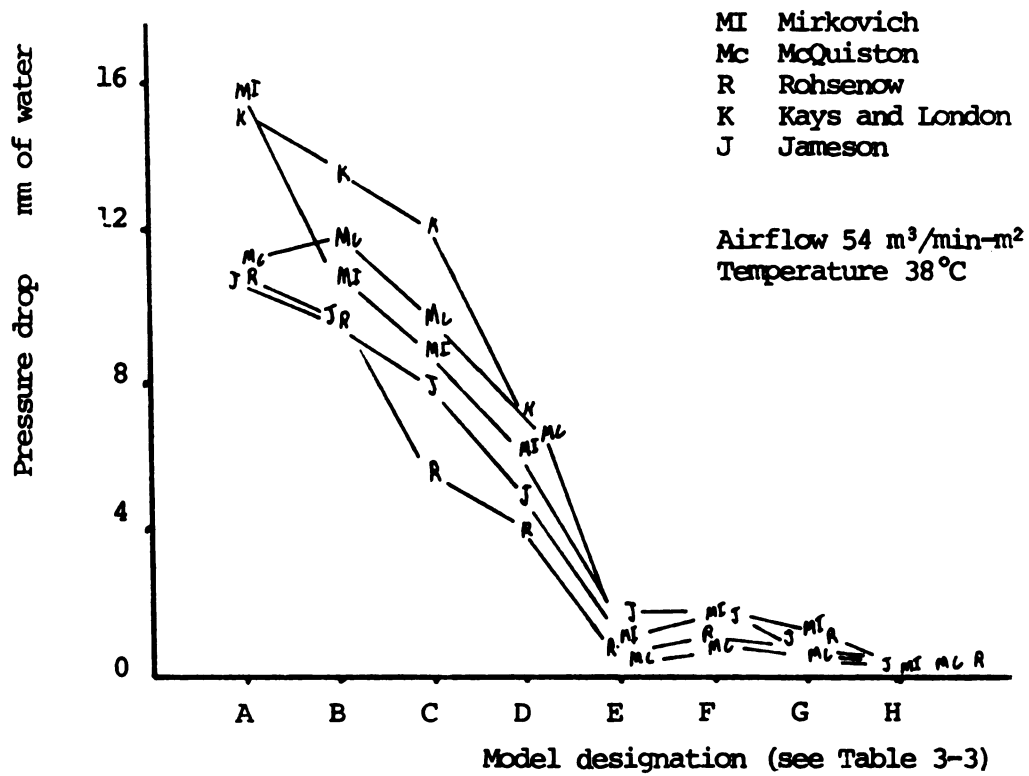


Fig. 3-9. Pressure drop predicted by different correlations for various surface configurations.

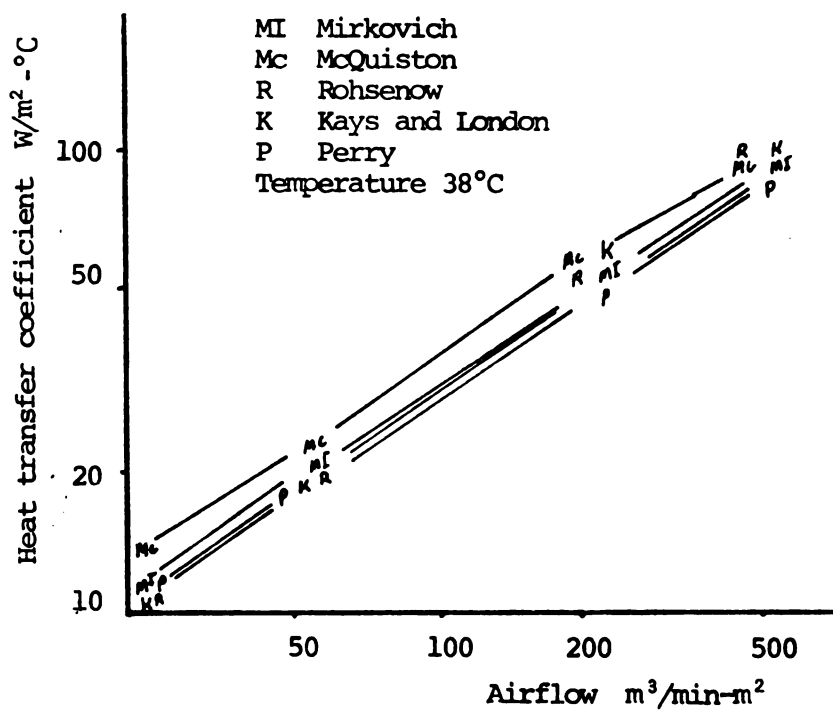


Fig. 3-10. Heat transfer coefficient versus airflow for surface G (Table 3-3) , predicted by different correlations.

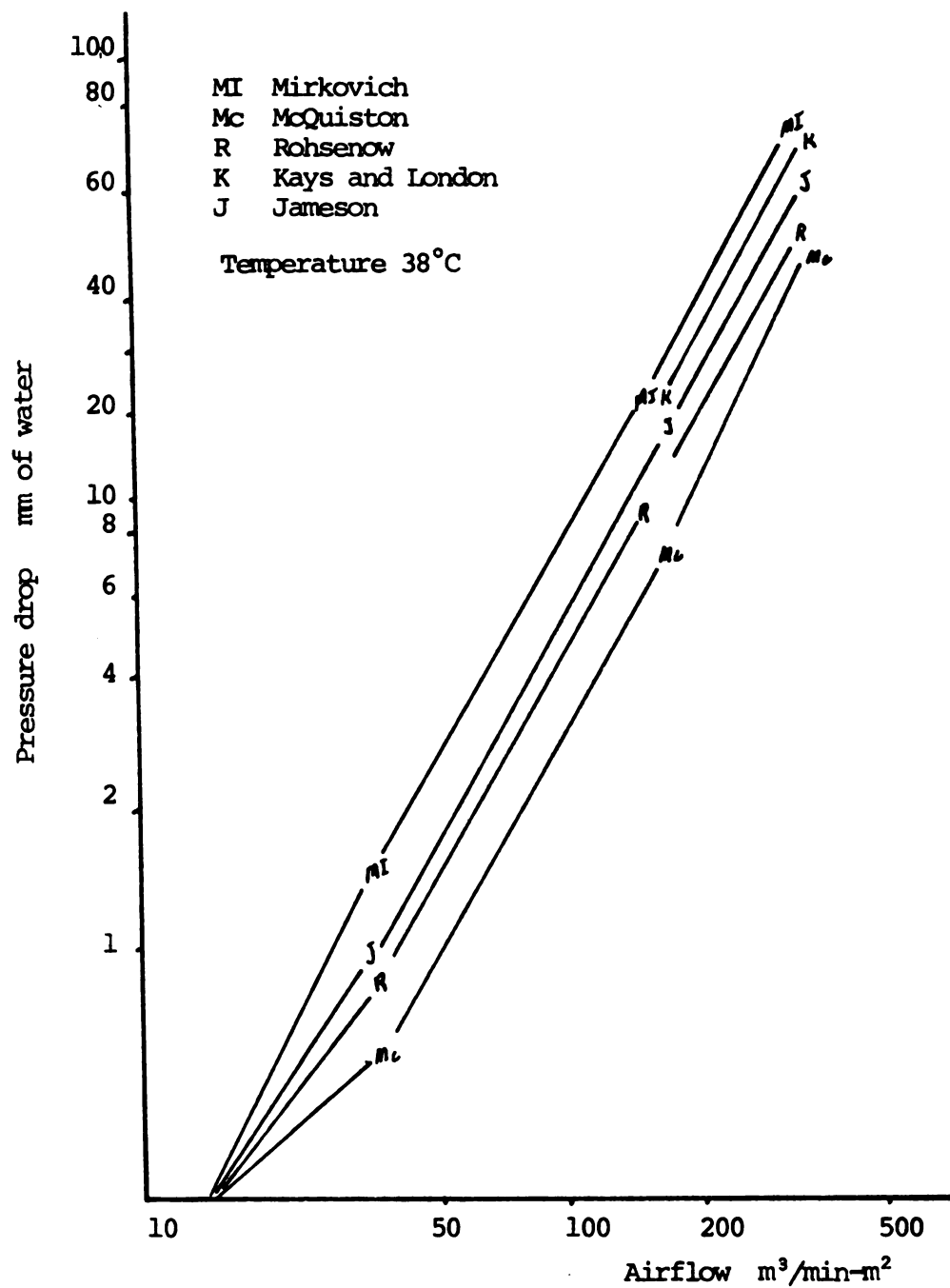


Fig. 3-11. Pressure drop versus airflow for surface G (Table 3-3) predicted by different correlations.

and Rohsenow's values are consistently in the mid-range. Although both Perry's and Rohsenow's correlations are valid in a wide range of heat exchanger dimensions, Rohsenow's correlation contains most of the variables explicitly.

Figure 3-9 shows the pressure drop as predicted by the correlations of Table 3-2 for the different models listed in Table 3-3. Although a large variation between the predicted values is indicated, the overall pressure drop in a heat pipe exchanger is small. The difference between the McQuiston's and Rohsenow's relationships for a D surface is about 2.54 mm of water and for the G-surface is even smaller. Jameson's correlation also seems to be valid over the range of surfaces.

Figures 3-10 and 3-11 show the effect of airflow rate on the heat transfer and pressure drop. Both figures indicate that for various airflows the correlations follow each other rather closely. The variation in heat transfer values as indicated before is less than that for pressure drop. Figure 3-11 shows that for normal flow rates between 20 and 50 m³/min-m² the pressure drop is very small. The correlations given by Rohsenow and Hartnet (1974) are chosen for the performance evaluation of the heat pipe exchanger, because the resulting heat transfer and pressure drop values are in the mid-range of other correlations' predicted values.

3.4 Fouling factor

The process by which dust particles are deposited on the heat exchanger surface area is called fouling. Fouling increases the resistance against the transmission of the heat from the pipes to the process

stream. Fouling also increases the pressure drop when there are enough deposits to narrow air passages and to block the airflow.

The constants h_c , h_h , η_c , η_h , and R_m of the overall heat transfer coefficient (equation 3-15) have been considered in previous sections. The resistance to heat flow R_f , due to the fouling is the subject of this section.

The exhaust air from a dryer contains a full spectrum of particle sizes and densities. Grain dust, clay dust, trash, broken kernels, stone particles, and light materials such as bees wings can be expected in the dryer exhaust air. Each of these materials foul differently and have their own specific fouling characteristics. A crust on the individual heat pipes resulting from the caking of grain dust when the air is moist and hot can be expected. Also, temporary clogging due to loose, light, and larger particles is inevitable. Bacterial growth in the heat exchanger is also another source of fouling (Anderson, 1977).

Two modes of fouling may happen in a heat exchanger as shown in Figure 3-12. One is when the deposition rate predominates the removal rate and there is a constant increase in the deposit thickness (Curve A). As a consequence of this mode there will be a build-up of sediment on the heat exchanger surface area. In the other mode, as the deposit thickness grows the rate of removal will increase to a point where the rates of deposition and removal will be equal. Curve B of Figure 3-12 shows this second mode of fouling.

Based on the foregoing discussion the change of deposit thickness with time can be written as:

$$\frac{dx_f}{dt} = \phi_d - \phi_r \quad (3-103)$$

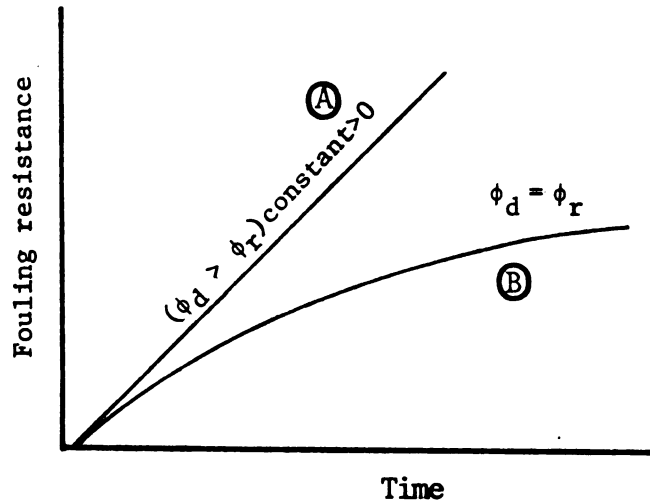


Fig. 3-12. Fouling resistance versus time for systems in which the deposition rate predominates (Curve A) and in which the removal rate increases with the fouling thickness (Curve B).

Source: Taborek et al. (1972)

Depending on the type of fouling process, (ϕ_d) and (ϕ_r) can be formulated in a number of different ways.

Kern and Seaton (1959) suggested the following definitions for (ϕ_d) and (ϕ_r) :

$$\phi_d = K_1 C_d m \quad (3-104)$$

$$\phi_r = K_2 \tau x_f(t) \quad (3-105)$$

where (τ) , the shear stress of the air on the surface is equal to:

$$\tau = f \frac{v^2 \rho}{2g} \quad (3-106)$$

Substituting equations (3-104), (3-105), and (3-106) in (3-103) yields:

$$\frac{dx_f}{dt} = K_1 C_d m - K_2 f \frac{v^2 \rho}{2g} x_f(t) \quad (3-107)$$

Equation (3-107) can be solved for time necessary for the deposits to reach a value of x_f^*

$$t = \int_0^{x_f^*} \frac{dx_f}{K_1 C_d m - K_2 f \frac{v^2 \rho}{2g} x_f(t)} \quad (3-108)$$

v , the maximum air velocity is a function of time, because as the deposit thickness increases with time the air velocity also increases. After the values of K_1 and K_2 were defined for a particular heat exchanger, equation (3-108) can be integrated numerically.

K_1 depends on the properties of the particles and the type of fouling. K_1 can be defined as a sticking probability and expressed as a fraction of particles sticking on impact. K_1 must be found experimentally, using equation (3-104). Kern and Seaton (1959), for a fouling depicted by Curve B in Figure 3-12, proposed the following simplified relationship:

$$R_f = R_f^* (1 - e^{-Bt}) \quad (3-109)$$

Where R_f^* is the value of fouling resistance (R_f), at the asymptote. The coefficient B is a removal rate expression, related to the shear stress as:

$$B = K_2 \tau \quad (3-110)$$

The value of B is the slope of $\log (1 - \frac{R_f}{R_f^*})$ plotted experimentally versus time.

3.5 Profitability model

Savings or costs resulting from an investment in the future have a different value at the present. Factors such as the rise in energy cost, the rate of inflation, the tax rate, and the service life influence the profitability of a heat recovery system.

If the annual fuel escalation is at a rate of (f), the fuel savings (S_k), at any year (k), can be written as:

$$S_k = AS (1 + f)^k \quad k = 0, 1, 2, \dots, n \quad (3-111)$$

where (AS) is the present fuel price, (savings)

Similarly, the annual operating costs (Q_k), with an annual inflation rate of (j) can be written as:

$$Q_k = AO (1 + j)^k \quad (3-112)$$

where (AO) is the present annual operating costs.

Subtracting (Q_k) from (S_k) yields the cash income (CI):

$$CI_k = S_k - Q_k \quad (3-113)$$

Assuming a straight line depreciation and a zero value for the heat exchanger after n years of service, the annual depreciation (D_k) can be written as:

$$D_k = \frac{FC_0}{n} \quad (3-114)$$

where (FC_0) is the total first costs.

The annual tax (TAX_k) is calculated based on cash income minus depreciation, or:

$$TAX_k = (CI_k - D_k) t \quad (3-115)$$

The net cashflow (CF_k) results from subtracting taxes from the cashflow:

$$CF_k = CI_k - TAX_k - FC_0 \quad (3-116)$$

In order to calculate the present value, the net cashflow must be

discounted at the true interest rate $(i)^1$. In addition, the purchase power of a sum of money will decrease at the rate of j percent inflation.

Therefore the net cashflow must be discounted at the rate of (i) and (j) as suggested by Holland and Watson (1977a and 1977b):

$$DCF_k = \frac{CF_k}{(1+i)^k (1+j)^k} \quad (3-117)$$

The net present value (NPV) of the discounted cashflow can be written as:

$$NPV = \sum_0^n \frac{CF_k}{(1+i)^k (1+j)^k} \quad (3-118)$$

Equation (3-118) is the model used in the economic analysis of the heat pipe exchanger. Equation (3-118) can be rearranged to give,

$$dC = \sum_1^n \frac{CF_k}{(1+i)^k (1+j)^k} \quad (3-119)$$

where

$$dC = NPV - FC_0$$

Whenever (dC) is equal to zero, the project is at the break-even point. The values of (dC) greater than zero represent a profit, and the values less than zero indicate a loss. Setting (dC) equal to zero and solving for (i) in equation (3-119) for any particular value of (n) will give the discounted cashflow rate of return (DCFR).

¹A true interest rate does not include the inflation rate.

3.6 Simulation

The performance relationships developed in the foregoing sections were coded in FORTRAN; and the routine was called "SUBROUTINE PROCESS". Evaluation of the overall heat transfer coefficient and pressure drop is performed using Rohsenow's equations (3-101), (3-102) and (3-102-1). In the case of the finite element and finite difference analyses the temperature and corresponding humidities in each element are checked for condensation. When the overall effectiveness method (equation 3-8) is used, condensation is checked at the exit points of the heat exchanger. In case of condensation the overall heat transfer coefficient must be re-evaluated using equation (3-34b). A flowchart of the subroutine PROCESS is shown in Figure 3-13.

Equations (3-39) and (3-40) were solved using a package called "SIMQ", which obtains the solution of a set of simultaneous linear equations by the elimination method (Lukey, 1975). A set of subroutines developed by Segerlind (1976) for solving a one-dimensional heat transfer problem is utilized in the solution of equation (3-88).

The following subroutines are used:

- a) ASMBLY ----- constructs the global and stiffness matrices
- b) BDY ----- applies the boundary conditions to the system of equations and modifies the stiffness matrix.
- c) DCMPBD ----- decomposes the global stiffness matrix into an upper triangular matrix
- d) SLVED ----- solves the system of equations by the backward substitution method.

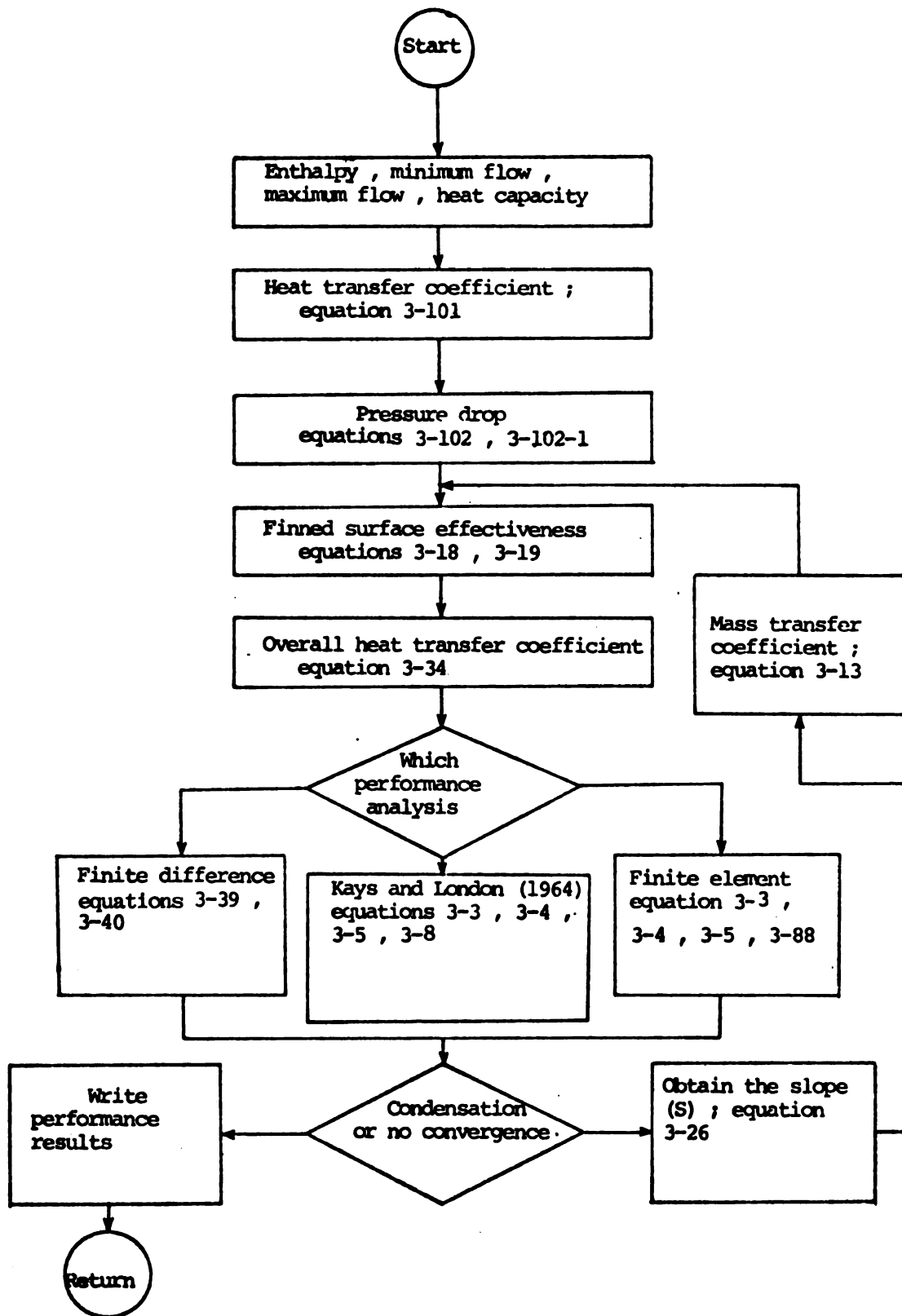


Figure 3-13. A flow chart of the subroutine PROCESS.

Additional subroutines for grid generation (FINITEEL), reconstruction of matrices in case of condensation (CONDENS) supplement the package. A listing of the programs and samples of inputs and outputs can be found in the Appendices A and B.

Parts of the analyses such as the heat transfer coefficient, pressure drop, fouling factor and economic analysis were performed on a WANG computer which utilizes BASIC. A listing of these programs can be found in Appendix A.

For the purpose of drying simulation, the programs already available (Bakker-Arkema et al., 1974) were utilized. In order to couple the heat exchanger to the drying simulation programs a subroutine was written to calculate the properties of the air recycled to the heat exchanger and the grain dryer.

The subroutine receives the temperatures, the humidity ratios and the flow rates of the n-number of air streams to be mixed. The enthalpy of the mixture is calculated using equations (3-6) and (3-7).

Specifying the ratio of each stream (R), the final mixture properties can be written:

$$e_m = \frac{\sum_{i=1}^n G_i R_i e_i}{\sum_{i=1}^n G_i R_i} \quad (3-120)$$

$$W_m = \frac{\sum_{i=1}^n G_i R_i W_i}{\sum_{i=1}^n G_i R_i} \quad (3-121)$$

$$G_m = \sum_{i=1}^n G_i R_i \quad (3-122)$$

Equations (3-120) through (3-122) are contained in the subroutine called "INPUTMIX". A listing of "INPUTMIX" can be found in Appendix A.

4. EXPERIMENTAL

4.1 Introduction

The experimental tests were carried out to establish:

- a) the experimental data for the heat pipe exchanger to compare with those predicted by the simulation, and hence to validate the heat pipe exchanger computer program, and
- b) the experimental application of a heat pipe exchanger to a grain dryer and the investigation of the performance of the overall system.

In order to fulfill these objectives, the experiments were divided into two parts:

- a) those related to the heat pipe exchanger, and
- b) those related to the performance of a grain dryer and the heat exchanger.

4.2 Heat pipe exchanger

A commercial heat pipe exchanger (similar to Figure 3-1) was purchased from Isothermics, Inc., Augusta, New Jersey. The coil construction and performance characteristics of the heat exchanger as supplied by the manufacturer are shown in Table 4-1.

Table 4-1. Performance characteristics and the construction of the experimental heat pipe exchanger, ISO-FIN, as specified by the manufacturer.

Performance:

Nominal effectiveness	%	67 ± 3
Supply air volume	m ³ /min	2.83
Exhaust air volume	m ³ /min	4.25
Supply inlet temperature	°C	-1
Supply outlet temperature	°C	43.3
Exhaust inlet temperature	°C	65.5
Exhaust outlet temperature	°C	35.5
Supply pressure drop	mm	4.3
Exhaust pressure drop	mm	7.6
Energy recovery	kJ/hr	9115

Construction:

Number of rows	6
Pipe material	Aluminum
Fin pitch	4.3 fins/cm
Overall dimensions:	width 3 m, depth .3 m, length .46 m

Isothermics, Inc., Augusta, New Jersey.

During the test the heat exchanger was equipped with four transition ducts and a port at the bottom for the condensate to drip out. The assembly was connected to an Aminco unit which provides airflows of different temperature and humidity (Figure 4-1). The supply side of the heat exchanger preheated the cold ambient air before entering into the Aminco unit. The exhaust side of the heat exchanger received the conditioned air with a specific temperature and humidity from the Aminco. The outlet and inlet temperatures were measured by copper-constantan thermocouples. Two thermocouples connected to a multichannel temperature recorder were used in each location.

The humidity ratio of the air exhausted from the Aminco unit was adjusted using the controls provided on the unit. The humidity ratio of the supply side was measured using psychrometrics as follows: a thermocouple wrapped in a wick and soaked with water was installed in the air passage to measure the wet bulb temperature; using the dry bulb and the wet bulb temperatures, the humidity ratio was found from the psychrometric chart.

The airflow in each side was measured by a pitot tube. A variable speed fan was used on the Aminco unit to provide different airflows.

4.3 Grain dryer

Two series of experiments were performed with the grain dryer. The first experiments were carried out in the summer of 1976 when newly harvested soft wheat was dried in a laboratory concurrent-counterflow dryer. The second series of experiments was performed in the fall of the same year, drying shelled corn in a modified laboratory concurrent counterflow dryer.

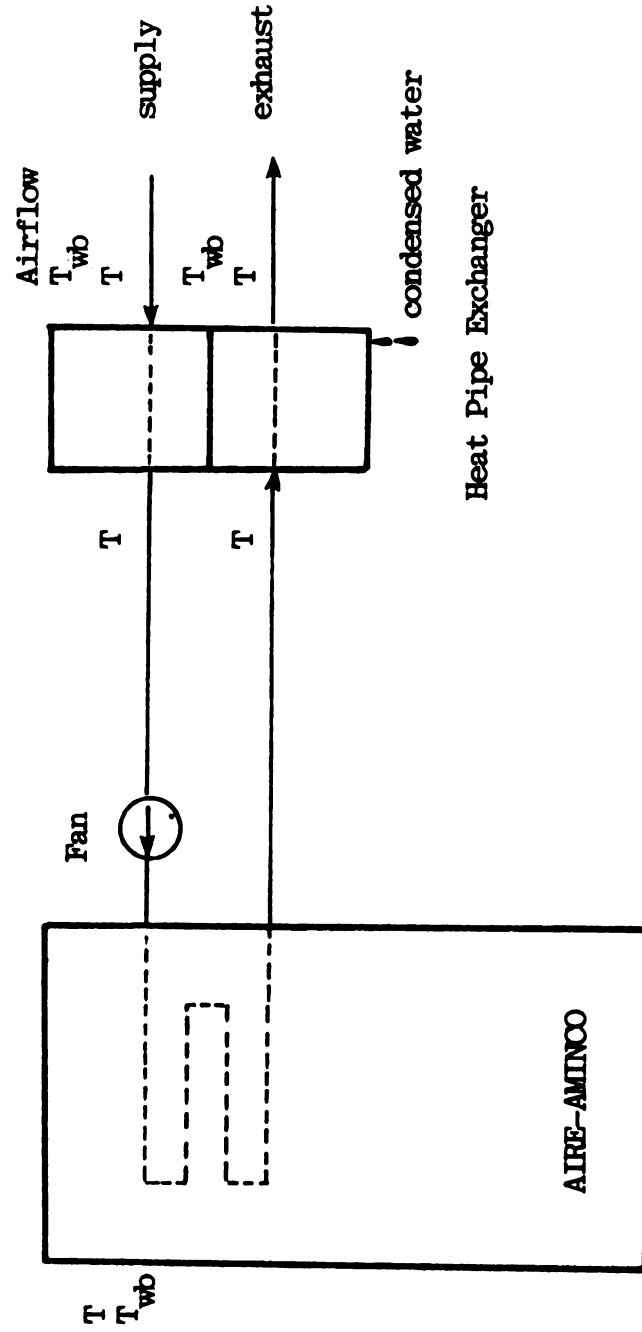


Fig. 4-1. Experimental set up for the performance tests of the heat pipe exchanger.

A sketch of the first dryer is shown in Figure 4-2. The dryer was equipped with two airlocks to separate and direct the air passing through the cooler and the dryer. The measurements for the heat exchanger were the same as the previous tests. Table 4-2 contains the dryer dimensions and the process settings for the wheat drying tests.

For the second experiment the design of the grain dryer was extensively modified in order to reduce the moving parts and consequently, to eliminate the air leakage (Kline, 1977). The air locks were replaced by columns of grain to prevent the air leakage (Figure 4-3). In addition the cooler was separated from the dryer so the cooler could be bypassed whenever cooling operation was not necessary. The method of heat exchanger application to the grain dryer in both tests was similar to the way it was used in Aminco tests. Table 4-3 lists the dryer settings used in the corn drying experiment.

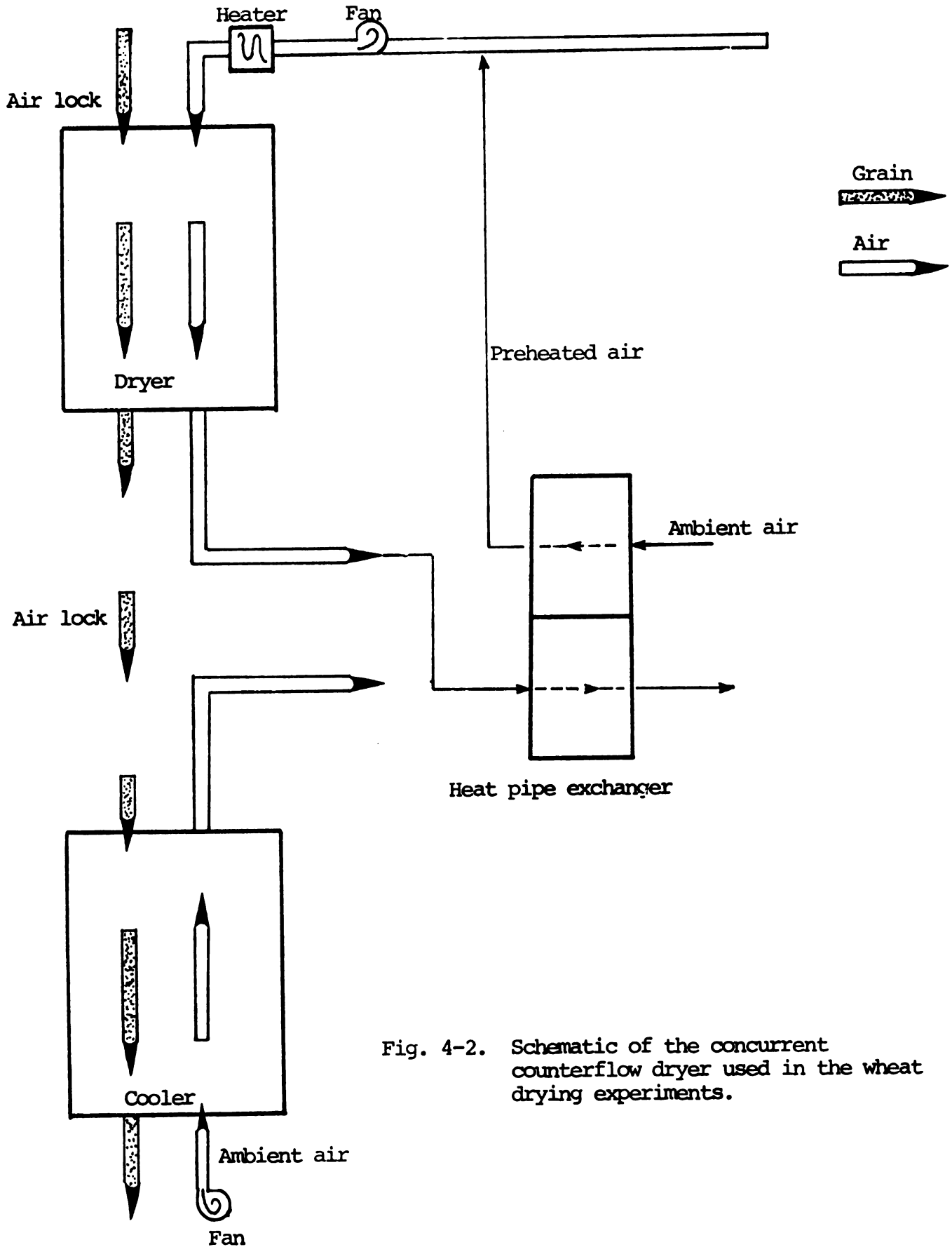


Fig. 4-2. Schematic of the concurrent counterflow dryer used in the wheat drying experiments.

Table 4-2. Settings for the concurrent-counterflow dryer utilized in the soft wheat drying experiment.

Inlet air temperature	120, 150, 177 & 205	°C
Inlet absolute humidity	.015	kg/kg
Airflow rates:		
— Dryer	18.3	m ³ /min-m ²
-- Cooler	6.1	m ³ /min-m ²
Ambient air	30	°C
Inlet grain temperature	30	°C
Inlet moisture content	18	% (WB)
Grain flow rate	.976	tonnes/hr-m ²
Length:		
— Dryer	.61	m
— Cooler	.30	m
Cross section area of the dryer and the cooler	.09	m ²

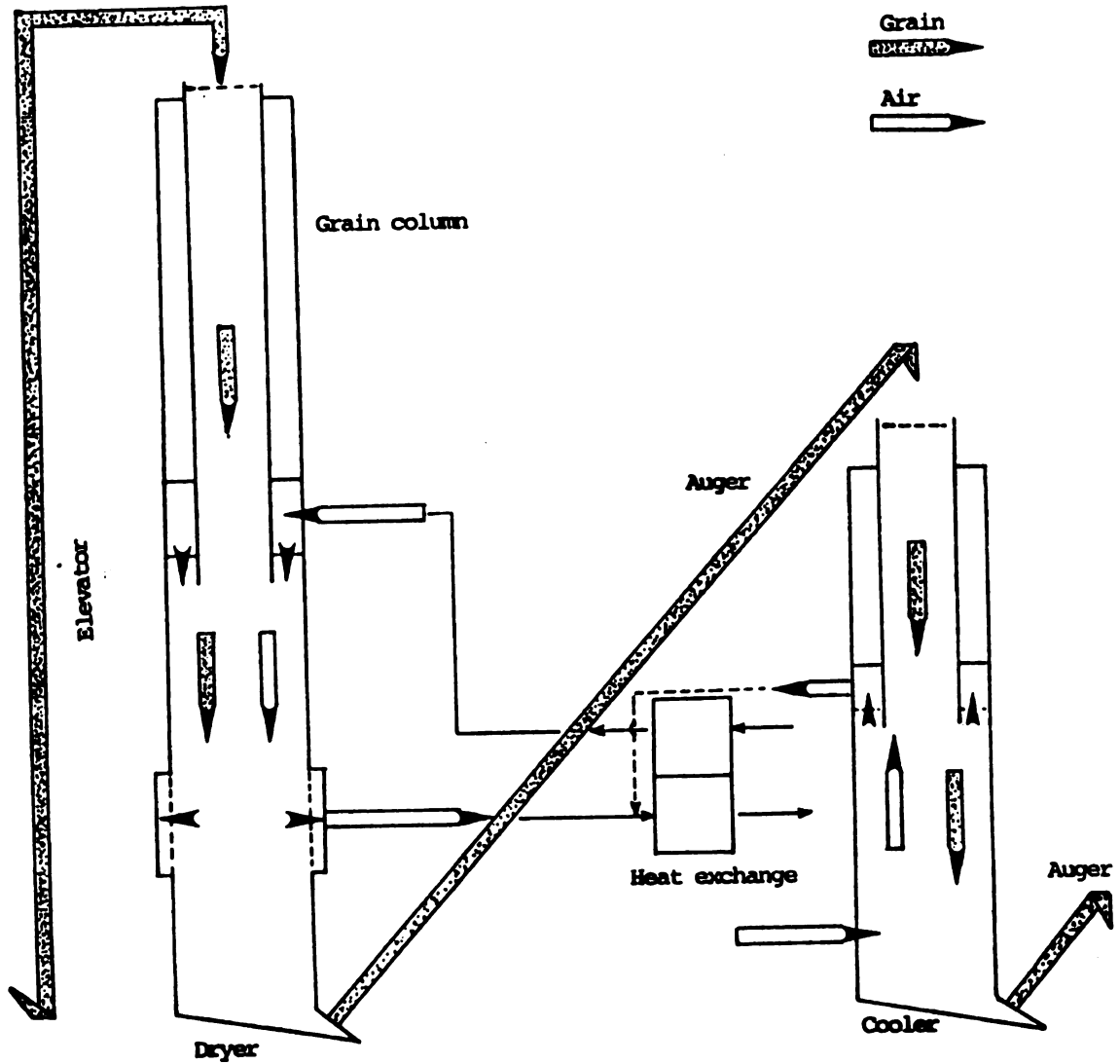


Figure 4-3. Schematic of the concurrent-counterflow dryer used in the corn drying experiment.

Table 4-3. Settings for the concurrent-counterflow dryer utilized in the corn drying experiment.

Inlet drying air temperature	205	°C
Inlet absolute humidity	.005	kg/kg
Airflow rates:		
-- Dryer	42.7	m ³ /min-m ²
-- Cooler	6.1	m ³ /min-m ²
Ambient air temperature	12 to 15	°C
Inlet grain temperature	22	°C
Inlet moisture content	20 to 22.5	% (WB)
Grain flow rate	1.5 to 2.5	tonnes/hr-m ²
Length:		
-- Dryer	1.0	m
-- Cooler	.6	m
Cross section of dryer and cooler	.09	m ²

5. HEAT PIPE EXCHANGER OPTIMIZATION

5.1 Introduction

The design of a heat pipe exchanger for a specified set of inputs including airflow, inlet air temperature, and humidity is discussed in this chapter.

Heat exchanger optimization is a complex procedure that requires the combination of experience and mathematical models. Kays and London (1964) stated that "the methodology of arriving at an optimum heat exchanger design is a complex one, not only because of the arithmetic involved, but more particularly because of the many qualitative judgments that must be introduced".

Exhaustive design requires optimization across at least 12 control variables. Multivariate search methods are typically employed for optimization. The product of the multivariate search method will be an optimal heat exchanger with detailed specified dimensions. However, for the purpose of cost estimates and overall planning a rough estimation of the size and performance is sufficient. For this case a cheaper and faster optimization scheme will be appropriate.

Two optimization methods are utilized in this investigation. One is a linear optimization that is based upon the heat exchanger's overall performance relationships. The other is a non-linear search method that utilizes the performance and dimensional characteristics of most of the control variables.

5.2 Linear optimization

The general form of a linear optimization problem (Hillier and Lieberman, 1967) can be written as follows:

$$\text{maximize: } Z = \sum_{j=1}^n C_j X_j \quad (5-1)$$

subject to:

$$\begin{aligned} \sum_{j=1}^n a_{ij} X_j &\leq b_i & (5-2) \\ X_j &> 0 \\ i &= 1, 2, \dots, m \\ j &= 1, 2, \dots, n \end{aligned}$$

Here equation (5-1) represents the net annual savings, and equation (5-2) specifies the constraints on the variables in the objective function.

For the heat pipe exchanger the net annual savings can be written as:

$$\text{NAS} = P_1 Q - P_2 \text{KWH} - P_3 A^{.6} \quad (5-3)$$

(Q) represents the annual fuel savings in million kj, and (P_1) the price of fuel in \$ per million kj. (KWH) represents the annual power expenditure in kilowatt-hours, and (P_2) is the price of electricity in \$ per kilowatt-hours. The expression ($P_3 A^{.6}$) represents the annual fixed cost of the heat exchanger. The first cost of the heat exchanger is calculated by:

$$\text{FC}_b = \text{FC}_a \left(\frac{A_b}{A_a} \right)^{.6} \quad (5-4)$$

Using the first cost (\$320) and the surface area (7.8 m²) of the purchased heat exchanger from Isothermies, Inc., Augusta, New Jersey; equation (5-4) can be written as :

$$FC_b = 320 \left(\frac{A_b}{7.8}\right)^{.6} \quad (5-5)$$

Assuming that the heat exchanger service life is 5 years, the annual fixed cost of the heat exchanger is:

$$FC_b = 64 \left(\frac{A_b}{7.8}\right)^{.6} \quad (5-6)$$

or

$$FC_b = 18.7 (A_b)^{.6} \quad (5-7)$$

Thus P_3 is equal to 18.7 in equation (5-3).

The constraints on the variables are obtained from the following relationships:

- a) to establish the constraints on the friction power expenditure, a simplified equation given by Kays and London (1964) is used:

$$KWH = 1.07 \times 10^{-14} \frac{G^3}{\rho^2} A \text{ Hr} \quad (5-8)$$

Equation (5-8) does not require estimates for various primary variables, whereas, the equations in Table 3-2 do.

Substituting .02 and .06 as lowest and highest values for the friction factor, and simplifying; equation (5-8) can be written:

$$KWH - 1.9 \text{ E-16} (G_{\min}^3 + G_{\max}^3) A \text{ Hr} \geq 0 \quad (5-9)$$

and

$$KWH - 5.7 E-16 (G_{\min}^3 + G_{\max}^3) A Hr \leq 0 \quad (5-10)$$

b) The maximum heat that can be transferred theoretically in a counterflow heat exchanger can be written as:

$$Q_{\max} = C_{\min} d_o \quad (5-11)$$

where $C_{\min} = (MC)_{\min}$

and $d_o = (T_{hi} - T_{ci})$

Multiplying equation (5-11) by a heat exchanger's effectiveness (ϵ), gives the actual heat that is transferred in a given heat exchanger:

$$Q = C_{\min} d_o \epsilon \quad (5-12)$$

Assuming that $C_{\min} = C_{\max}$, the effectiveness can be written for a counterflow problem as follows (Kays and London, 1964):

$$\epsilon = \frac{\frac{UA}{C_{\min}}}{1 - \frac{UA}{C_{\min}}} \quad (5-13)$$

Substituting equation (5-13) in equation (5-12) results in:

$$Q = \frac{UA}{1 - \frac{UA}{C_{\min}}} d_o \quad (5-14)$$

Equation (5-14) specifies a value for the surface area when the heat exchanger effectiveness is specified.

The exact value of (ϵ) depends on the design and performance of the heat exchanger. In order to introduce the variations of the effectiveness into the optimization scheme, equation (5-12) can be written as:

$$Z = C_{\min} d_o \epsilon^* \quad (5-15)$$

where (ϵ^*) is a specified value for (ϵ) with possible variations. The objective then will be to maximize the value of (ϵ^*) in order to maximize the net annual savings (equations 5-12 and 5-3). However, the maximum of Q cannot exceed Q_{\max} of equation (5-11). Actually Q may be equal to the product of maximum value of ϵ^* and Q_{\max} . A probability is associated with this objective, that can be stated as:

$$\text{Prob} \left(-\lambda \leq \frac{Z - E(Q)}{V(Q)} \leq \lambda \right) = \alpha \quad (5-16)$$

where (α) is a decimal representing the odds that (ϵ) falls somewhere between the maximum and the minimum of (ϵ^*) ; (Black and Fox, 1976).

A normally distributed random variable, (Q) can be converted into a standard normal distributed random variable, (λ) , as follows:

$$\frac{Z - E(Q)}{V(Q)} \quad (5-17)$$

where

$$\lambda \geq \frac{Q - E(Q)}{V(Q)} \geq -\lambda$$

$V(Q)$ and $E(Q)$ are the variance and the expected value of (Q) , respectively.

Replacing $E(Q)$ by Q and re-arranging, equation (5-17) yields:

$$Q - Z + \lambda V(Q) \geq 0 \quad (5-18)$$

$$Q - Z - \lambda V(Q) \leq 0 \quad (5-19)$$

Since (ϵ) is a random variable, using equation (5-12), the variance of Q is written:

$$V(Q) = V(C_{\min} d_o \epsilon) = C_{\min}^2 d_o^2 V(\epsilon) \quad (5-20)$$

and the standard deviation (s.d.) of (Q) is written:

$$\text{s.d.}(Q) = \sqrt{V(Q)} = C_{\min} d_o \text{s.d.}(\epsilon) \quad (5-21)$$

Substituting equations (5-15) and (5-20) in equation (5-18) yields:

$$Q - C_{\min} d_o \epsilon^* + \lambda C_{\min} d_o \text{s.d.}(\epsilon) \geq 0$$

or

$$Q - C_{\min} d_o [\epsilon^* - \lambda \text{s.d.}(\epsilon)] \geq 0 \quad (5-22)$$

and similarly

$$Q - C_{\min} d_o [\epsilon^* + \lambda \text{s.d.}(\epsilon)] \leq 0 \quad (5-23)$$

Equations (5-9), (5-10), (5-14), (5-22) and (5-23) are the constraints to the objective function (5-3). The optimization scheme can be summarized as follows:

$$\text{Maximize: } NAS = P_1 Q - P_2 \text{ KWH} - P_3 A^6 \quad (5-24)$$

subject to:

$$\text{KWH} - 1.9 \text{ E} - 16 (G_{\max}^3 + G_{\min}^3) A \text{ Hr} \geq 0 \quad (5-25)$$

$$\text{KWH} - 5.7 \text{ E} - 16 (G_{\max}^3 + G_{\min}^3) A \text{ Hr} < 0 \quad (5-26)$$

$$Q - \frac{UA}{1 - \frac{UA}{C_{\min}}} d_o = 0 \quad (5-27)$$

$$Q - C_{\min} d_o [\epsilon^* - \lambda \text{ s.d. } (\epsilon)] \geq 0 \quad (5-28)$$

$$Q - C_{\min} d_o [\epsilon^* + \lambda \text{ s.d. } (\epsilon)] \leq 0 \quad (5-29)$$

$$Q, A, \text{ KWH} \geq 0 \quad (5-30)$$

As can be seen, the objective function (5-24) and equation (5-27) are not linear in terms of A. In order to linearize these two equations, several points on the area domain will be assumed, and then, the points will be linearly interpolated to approximate the original equation. Assuming a three-point interpolation, the function containing the surface area can be written:

$$f(A) = W_1 f(A_1) + W_2 f(A_2) + W_3 f(A_3) \quad (5-31)$$

where W_1 , W_2 , and W_3 are the interpolating weights, such that:

$$\sum_1^3 W_i = 1 \quad (5-32)$$

For example the expression A^6 in equation (5-24) is written:

$$A^6 = W_1 A_1^6 + W_2 A_2^6 + W_3 A_3^6 \quad (5-33)$$

After linearizing, equations (5-24) through (5-30) and equation (5-32) will be all linear in terms of the variables; and can be solved by the Simplex algorithm (Hillier and Lieberman, 1967).

Example:

A heat pipe exchanger is to be optimized for the following data¹:

Airflow	3.5 m ³ /min (supply and exhaust side airflows are equal)
T _{hi}	65 °C
T _{ci}	5 °C
ε	65 percent
s.d. (ε)	15 percent
Hr	750 hrs/year
P ₁	3.3 \$/10 ⁶ kj
P ₂	.035 \$/kWhr
P ₃	\$ 18.7
U	40 W/m ² -°C
α	95 percent
ρ	1 kg/m ³
C	1.005 kj/kg-°C
Heat exchanger life	5 years

The calculated values:

$$d_o = T_{hi} - T_{ci} = 60 \text{ C}$$

$$C_{min} = C_{max} = mC$$

¹The data of this example are similar to the data specified for the ISO-FIN, the experimental unit.

$$= 210 \times 1.005$$

$$= 211 \text{ kj/hr-C}$$

$$G_{\max} = G_{\min} = 11175 \text{ kg/m}^2 \text{ - hr}$$

(based on .015 m² of free frontal area)

From a probability table for $\alpha = 95\%$ the value of λ is 1.96.

Substituting the specified and calculated values in equations (5-24)

through (5-29) yields:

$$\text{NAS} = 3.3 Q - .035 \text{ KWH} - 3.74 A^6 \quad (5-34)$$

$$\text{KWH} - .398 A \geq 0 \quad (5-35)$$

$$\text{KWH} - 1.193 A \leq 0 \quad (5-36)$$

$$Q - \frac{6.48 A}{1 - .68 A} = 0 \quad (5-37)$$

$$Q \geq 3.38 \quad (5-38)$$

$$Q \leq 9.02$$

$$Q, A, \text{ KWH} \geq 0 \quad (5-39)$$

Assuming 3 points for A, as follows: $A_1 = 1$, $A_2 = 10$, and $A_3 = 100$; equation (5-34) through (5-39) are tabulated in Table 5-1. A computer program developed by Harsh and Black (1975) was utilized. The program utilizes the Simplex algorithm. Table 5-2 contains the resulting output of the program for the given inputs of Table 5-1. Table 5-2 shows that the designed heat exchanger has an effectiveness of 80 percent. The designed surface area, 4.3 m² is smaller than that of the experimental unit; and the amount of savings is higher. In fact, the algorithm obtains the maximum value of Q, and then from equation (5-37) finds the value of A. The friction power is found after Q and A are specified,

Table 5-1. Tabulation of the sample linear programming problem.

Q	KWH	W ₁	W ₂	W ₃		
3.3	-.035	-18.7	-74.05	-294.8		
0	1	-.398	-3.98	-39.8	≥	0
0	1	-1.193	-11.93	-119.3	≤	0
1	0	-20.25	11.17	9.67	=	0
1	0	0	0	0	≥	3.38
1	0	0	0	0	≤	9.02
0	0	1	1	1	=	1

Table 5-2. The output of the linear programming optimization using the inputs of Table 5-1.

Objective function	-8.71	\$
Q	9.02 x 10 ⁶	kJ/year
	(12026	kJ/hr)
KWH	1.67	kWhr
A	4.3	m ²

because (KWH) has a small price in the objective function.

5.3 Nonlinear optimization

The exhaustive design of a heat pipe exchanger requires a two-step optimization scheme. First, the individual heat pipes are optimized based on the properties of working fluid, structural characteristics of the wick, and the geometry of the pipe. Second, the heat exchanger is optimized for the overall performance and the core specifications. This study is concerned with the second scheme which is similar to optimal design of a conventional finned pipe heat exchanger.

The objective function used in nonlinear optimization is the same as the one used in the linear optimization (see equation 5-3). Several methods can be utilized to arrive at an optimal heat exchanger. One method is the Lagrange multiplier technique by which the partial derivatives of the objective function with respect to each variable are set equal to zero. The resulting system of equations is solved for the optimum variables. The Lagrange method is simple and fast provided that the derivatives are defined and can be found.

A multivariate method reported by Kuester and Mize (1973) and written in FORTRAN Code is utilized in this study. The method is based on the complex procedure of Box. The procedure consists of maximizing the function:

$$F(X_1, X_2, \dots, X_N) \quad (5-40)$$

subject to:

$$G_k \leq X_k \leq H_k \quad k = 1, 2, \dots, M \quad (5-41)$$

The implicit variables X_{N+1}, \dots, X_M are dependent functions of the explicit variables X_1, X_2, \dots, X_N . The upper and lower constraints H_k and G_k are constants or functions of the independent variables. The procedure finds an optimum solution from the combination of the points scattered over the feasible region. The feasible points are generated by the following equation;

$$X_{i,j} = G_i + Y_{i,j} (H_i - G_i) \quad (5-42)$$

$$i = 1, 2, \dots, N$$

$$j = 1, 2, \dots, k - 1$$

k is the number of complex points chosen and is at least equal to $N + 1$.

$Y_{i,j}$ are random numbers between 0 and 1. The selected points must satisfy both explicit and implicit constraints.

As can be seen from the flow chart given in Figure 5-1, the convergence of the objective function to a small specified value after certain iterations provides the optimum design.

5.3.1 Application to heat pipe exchanger

The computer program consists of three parts:

- (1) The main program HPEXG that reads the inputs necessary for the optimization:
 - a) inlet process conditions such as airflows, humidity ratios and temperatures,
 - b) economic parameters such as fuel and electricity prices,
 - c) initial estimates for the following primary variables: fin

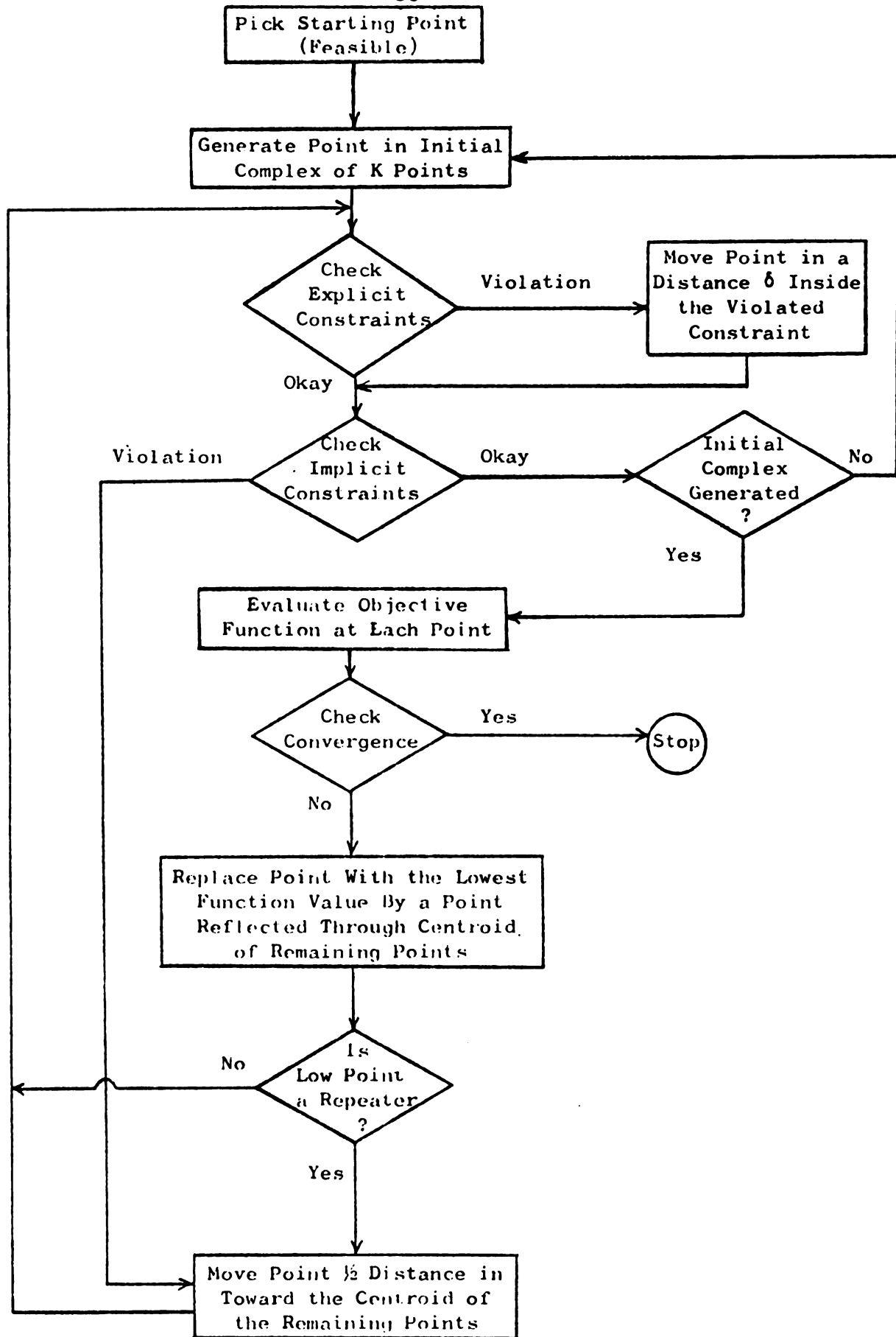


Fig. 5-1. Box (COMPLEX ALGORITHM) logic diagram

- diameter, pipe diameter, fin thickness, number of fins per unit length of the pipe, hot side pipe length, cold side pipe length, number of pipes in a row, number of rows, distance between two rows (center to center) and distance between two pipes in a row (center to center),
- d) maximum values for the overall heat exchanger dimensions, i.e., width, height, and depth,
- e) number of iterations and the convergence criteria.
- (2)Subroutines DETAILED, CONSX, CHECK, and CENTER published by Kuester and Mize. These subroutines carry out the optimization procedure until either a maximum function value is reached or the number of specified iterations is exceeded.¹
- (3) Additional subroutines are supplied to the main program as follows:
- CONST. . . . contains the constraints on the primary independent and dependent variables
- FU contains the objective function
- PROCESS. . . contains the performance relationships
- CALC contains the relationships to calculate the heat exchanger dimensions
- REPORTP. . . output of the performance results
- REPORTC. . . output of the dimensional and the core specifications

5.3.2 Results

A set of inputs similar to those specified for the experimental unit were supplied to the computer program. Table 5-3 shows a comparison between

¹The programs are listed in the Appendix -A.

Table 5-3. A comparison between an optimal design of heat pipe exchanger with ISO-FIN unit.¹

	Units	Optimal Design	ISO-FIN
Length	cm	37.0	46.0
Height	cm	21.0	17.0
Depth	cm	29.0	29.0
Fin diameter	cm	4.03	3.81
Fin thickness	cm	.03	.04
Pipe diameter	cm	1.80	1.91
Fins per cm		4.40	4.30
No. of rows		6	6
No. of pipes in a row		4	4
Surface area ²	m ²	7.42	7.80
Efficiency ³	Percent	57	67 ± 3
Energy saved	kJ/hr	6928	9115
Objective function ⁴	¢	.373	—

¹For the input conditions see Table 4-1.

²Total surface area including pipe and fins.

³Values for ISO-FIN is given by the manufacturer.

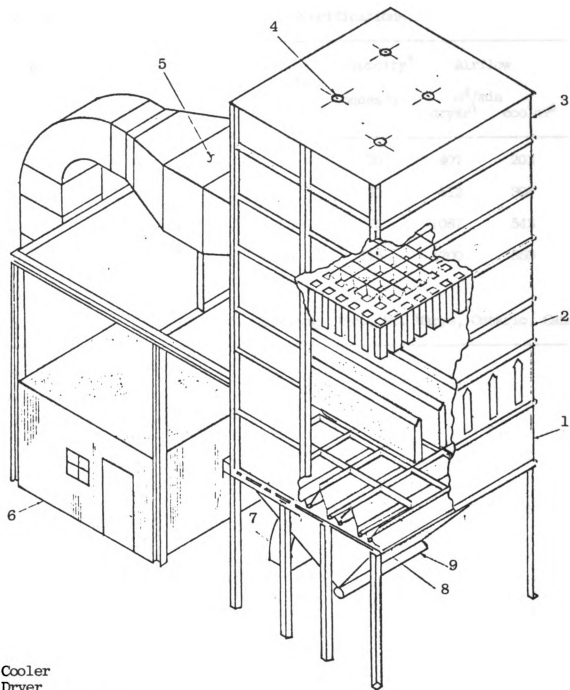
⁴Based on \$3.3 per million kJ; 3.5¢ per KWhr, and the heat exchanger cost from equation (5-7).

the optimal design of the heat exchanger and the experimental unit, ISO-FIN. As can be seen the optimal unit with a lower efficiency has almost the same surface area and dimensions of the ISO-FIN. The optimal unit has also a larger fin diameter and slightly more fins per cm than the ISO-FIN.

The 1975 models of the Westelaken grain dryers manufactured by the Westlake Agricultural Engineering, Inc., St. Marys, Ontario, Canada were used as examples of one-stage concurrent flow dryers. Figure 5-2 is schematic of the typical dryer. Table 5-4 contains the relevant dimensions and the capacity of the different dryer models.

Table 5-5 lists the input conditions that remained fixed for the analyses of the convergence criterion, the optimal design of the heat pipe exchanger for various models of the Westelaken grain dryers, and the effects of the fouling factor on the optimal design. Those values which are not fixed are specified for the specific analysis. The choice of the fixed values are arbitrary and generally are typical values in a grain drying operation.

Table 5-6 shows the effect of different values of the convergence criteria on the optimal designed dimensions for Model 810-A grain dryer, CPU time, and the computer cost (CDC-6500, Michigan State University). The number of iterations is also shown for each convergence value. As can be seen from the table, the objective function (equation 5-3) value increases significantly as a smaller convergence criteria is used. At the same time, the increase in the accuracy results in a larger number of iterations and hence a higher computer cost. For the purpose of this investigation, a convergence of 1.0 is chosen for further analysis.



1. Cooler
2. Dryer
3. Holding hopper
4. Grain inlet
5. Dryer duct
6. Control room
7. Cooler duct
8. Grain outlet
9. Air locks

Figure 5-2. Westelaken grain dryer.

Table 5-4. The Westelaken grain dryer specifications.

Model No.	Cross Section Area m ²	Dryer Length m	Cooler Length m	Capacity ³ tonnes/hr	Airflow m ³ /min dryer ¹ cooler ²	
810-A	8.90	2.0	1.0	20	407	203
1210-A	13.40	2.0	1.0	30	612	306
3010-A	23.80	2.0	1.0	75	1087	543
4510-A	37.20	2.0	1.0	115	1700	850

Source: Westlake Agricultural Engineering, Inc., St. Marys, Ontario, Canada

¹Based on 45.72 m³/min/m²

²Based on 22.86 m³/min/m²

³At 5 point moisture removal

Table 5-5. The inputs for optimal design of heat pipe exchangers for various models of Westelaken grain dryers.¹

Inlet air temperatures	
-- Exhaust ²	62.0 °C
-- Supply ³	15.5 °C
Inlet humidity ratios ⁴	
-- Exhaust	.05 kg/kg
-- Supply	.005 kg/kg
Fuel cost \$/million kj ⁵	3.31
Electricity cost \$/k W hr	.035

¹For the airflows and the dryers dimensions, see Table 5-4.

²Airflow to the exhaust side of the heat exchanger consists of the combined exhaust from cooler and dryer.

³Airflow to the supply side of the heat exchanger consists of the airflow to the dryer.

⁴The choice is representative of typical humidity ratios.

⁵Based on \$92/m³ No. 2 fuel oil with 3.86×10^7 kj/m³ heating value and about 70 percent combustion efficiency.

Table 5-6. Comparison of different values of the convergence criterion for the optimal designed heat pipe exchanger.

	Units	Convergence Criterion			
		0.01	0.1	1.0	2.0
Surface area	m ²	7.42	7.01	9.32	8.33
Objective function value ¹	¢	-.78	-1.13	-2.92	-14.25
Iterations	No.	716	360	124	34
CPU ²	Seconds	45.4	16.9	3.9	1.4
Cost ³	\$	4.19	1.77	.68	.47

¹Objective function value is based on annual net profit maximization.

²Central Processing Unit CDC-6500, Michigan State University.

³Program execution cost.

Table 5-7 shows the optimized dimensions of the designed heat pipe exchangers for the various models of Westelaken grain dryers. As the dryer size increases, the heat exchanger size increase is primarily in the number of pipes. A small increase in the number of fins per unit length is also evident. More savings are realized in larger heat exchangers than in the smaller ones.

Table 5-8 shows the effect of different values of thermal resistances due to the fouling on the optimal design of heat pipe exchanger. This shows that thermal fouling does not have a significant effect on the performance of the heat exchanger as far as heat transfer is concerned. In other words the relative values of (R_f) and $(\frac{1}{h_c \eta_c})$ or $(\frac{1}{h_h \eta_h})$ with respect to each other do not change significantly. The choice of .02 and .002 is based on the TEMA (Tubular Exchanger Manufacturers Association) recommendations for the fouling allowance (Perry, 1974).

Table 5-7. The optimal designed heat pipe exchangers for various models of Westelaken grain dryers.¹

	Units	Grain dryer models			
		810-A	1210-A	3010-A	4510-A
Length	cm	182.0	234.0	304.0	360.0
Height	cm	120.0	184.0	219.0	272.0
Depth	cm	64.0	73.0	62.0	65.0
Fin diameter	cm	4.54	4.61	4.87	4.88
Fin thickness	cm	.04	.04	.04	.04
Pipe diameter	cm	1.58	1.58	1.59	1.60
Fins per cm		5.27	5.17	5.24	5.51
No. of rows		7	8	7	8
No. of pipes in a row		28	43	48	48
Surface area	m ²	553	1264	1837	2610
Efficiency	Percent	63	72	63	60
Energy savings	kJ/hr	.78x10 ⁶	1.33x10 ⁶	2.1x10 ⁶	3.08x10 ⁶

¹Recycling of combined drying and cooling air through the heat exchanger.

Table 5-8. The effect of fouling resistance on the optimal designed heat pipe exchanger for the Westelaken grain dryer Model 810-A.¹

	Units	Fouling thermal resistance C/W		
		0.0	.002	.02
Length	cm	182.0	183.0	178.0
Height	cm	120.0	118.0	119.0
Depth	cm	64.0	34.0	39.0
Fin diameter	cm	4.54	4.52	4.87
Fin thickness	cm	.04	.04	.05
Pipe diameter	cm	1.58	1.58	1.59
Fins per cm		5.27	4.53	5.27
No. of rows		7	7	7
No. of pipes in a row		28	25	23
Surface area	m ²	553	421	510
Efficiency	Percent	63	54	54
Energy savings	kg/hr	.78x10 ⁶	.67x10 ⁶	.67x10 ⁶

¹Recycling of combined drying and cooling air through the heat exchanger.

6. RESULTS AND DISCUSSIONS

6.1 Introduction

The primary objective of this study was to evaluate the technical and economic aspects of heat pipe exchanger application to grain dryers. In this chapter the experimental and the simulated results will be compared. Heat recovery by recycling the dryer and cooler exhausts, either directly or through a heat pipe exchanger, will be investigated, using the simulation models. The economics of heat pipe exchanger application to different types of grain dryers and the effect of fouling on heat exchanger economics will be presented.

6.2 Laboratory test results

Table 6-1 is a list of the performance test results of the experimental heat pipe exchanger. Tests 1 to 4 are the results of using an Aminco-Aire unit. Tests 5 to 8 represent corn drying experiments and test number 9 is the result of a wheat drying experiment. The last column of Table 6-1 shows the heat pipe exchanger effectiveness obtained from the experimental data. The average effectiveness is about 73 percent which is higher than the reported 67 ± 3 percent by the heat exchanger supplier.

Table 6-1. Heat pipe exchanger performance test results.

Test Number	Exhaust side of heat exchanger				Supply side of heat exchanger				Effectiveness %				
	mass flow $\text{m}^3/\text{min-m}^2$	Temp °C In	Temp °C Out	Humidity In	Humidity Out	Ratio Out	mass flow $\text{m}^3/\text{min-m}^2$	Temp °C In		Temp °C Out	Humidity In	Humidity Out	Ratio Out
1	1.7	63	29	.035	.027	.027	1.7	9	48	.006	.006	.006	72
2	1.0	59	24	.030	.019	.019	1.0	5	47	.006	.006	.006	77
3	1.4	64	25	.027	.020	.020	1.4	4	50	.006	.006	.006	76
4	2.0	67	27	.026	.022	.022	2.0	5	51	.006	.006	.006	74
5	4.0	52	43	.077	.059	.059	2.7	16	42	.018	.018	.018	72
6	4.0	39	31	.042	.029	.029	4.0	16	31	.012	.012	.012	65
7	4.0	52	38	.079	.044	.044	4.0	12	38	.005	.005	.005	65
8	4.0	57	49	.085	.082	.082	2.5	14	49	.014	.014	.014	81
9	1.7	41	38	.055	.032	.032	1.7	29	38	.021	.021	.021	75

Note: 1-4 Aminco tests
5-9 Dryer tests

Figure 6-1 shows a comparison between deviations of the predicted effectivenesses from the experimentally obtained values. The horizontal line represents the experimental results. The black circles represent the use of equation (3-11) (Kays and London, 1964). The black squares represent the use of equations (3-39) and (3-40) (finite difference). The black triangles represent the use of equation (3-88) (finite element). Finite difference and finite element techniques are used to find outlet temperatures and humidities. Knowing the outlet conditions, equations (3-1) and (3-2) or (3-3) are used to find the heat exchanger effectiveness. Equation (3-88) predicts the temperature gradient along the pipe only. In order to use the finite element analysis a term representing the mass balance between the supply and exhaust side must be added to equation (3-41). The addition of the new term will complicate the finite element solution, because the new governing differential equation contains pipe and air temperature gradients along n and y , directions. Furthermore, the temperature gradient along the pipe is minimal due to the low resistance in the axial direction, and hence, the left hand side of equation (3-41) is almost zero. For these reasons finite element solution was abandoned for further analysis. Figure 6-1 shows that the accuracy of the predicted values largely depends on the absolute humidity of the exhaust air. For a balanced flow, i.e. equal supply and exhaust ($m C$), the predictions by equation (3-11) and by the finite element method and the experimental values are in good agreement up to a humidity ratio of .04 kg/kg. When the humidity ratio is higher than .04 kg/kg, the results of the finite difference are slightly superior to those predicted by equation (3-11).

Kays and London's equation (3-11) is utilized in this investigation for the economic analysis of a heat pipe exchanger in conjunction with a grain dryer.

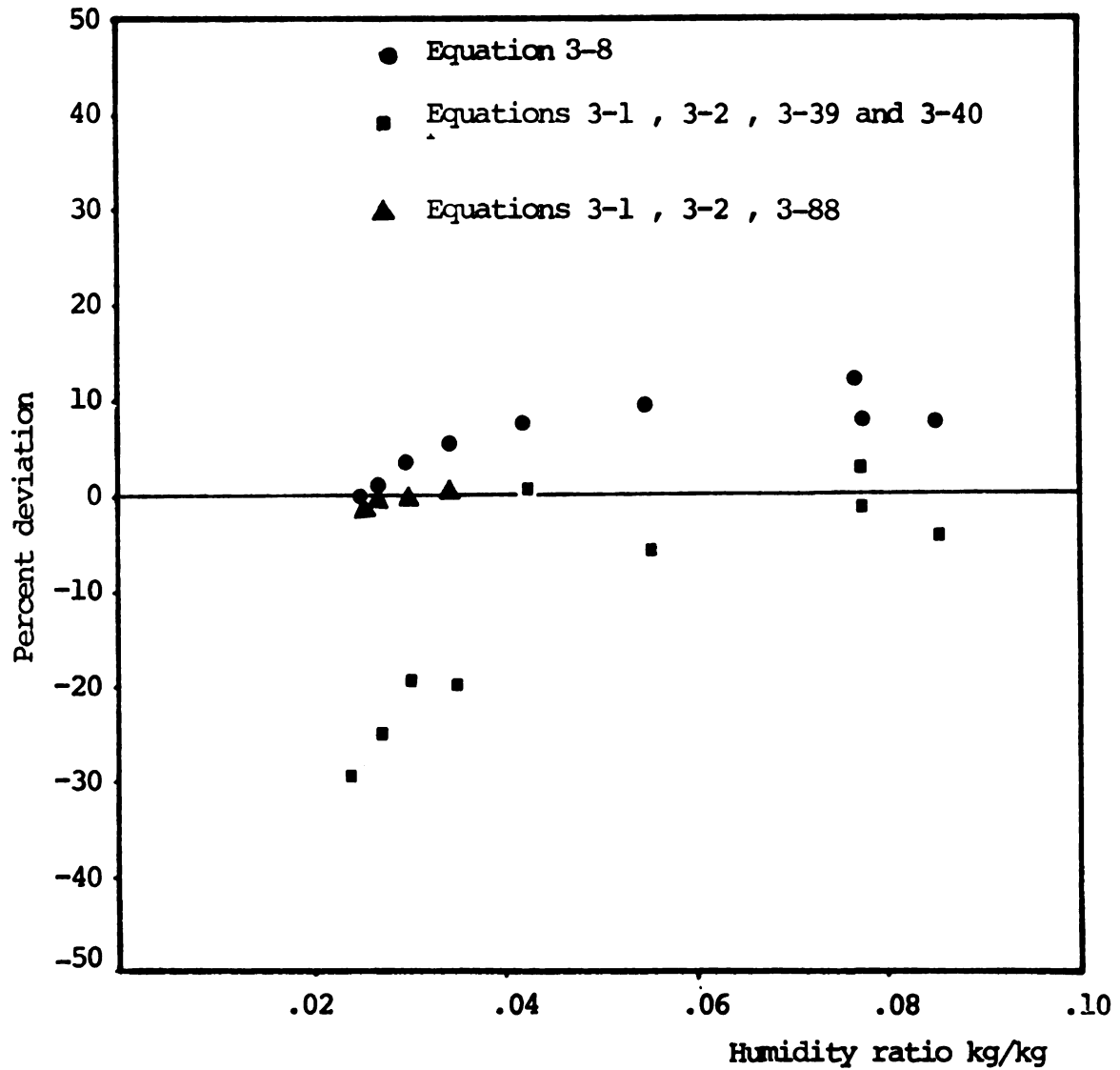


Fig. 6-1. Deviations of the predicted energy savings from the experimental values; (0 line).

Table 6-2 shows the results of the wheat drying experiments. The savings indicated in the table are the results of recycling the dryer exhaust air through the heat pipe exchanger to preheat the drying air. The low values of percent savings (5.5 to 7.5 percent) are mainly due to the high ambient temperature and low airflows. Table 6-2 also indicates that as the drying temperature increases the percentage savings slightly increase.

Table 6-3 shows the test results of corn drying in a modified concurrent-counterflow grain dryer. The main variables were the grainflow rate and the initial moisture content. The experimental and simulated energy requirements for removing one kg of water are in good agreement. Energy savings due to different forms of recycling are between 8 and 18 percent. The largest saving is obtained when the combined dryer and cooler exhausts are recycled through the heat exchanger.

6.3 Simulation results

A series of simulated tests were conducted using the drying programs developed by Bakker-Arkema et al. (1974). The one stage Westelaken concurrent-counterflow dryer model 810-A was used as an example. For each simulation a heat exchanger surface area was calculated, assuming an effectiveness of 60 percent and an overall heat transfer coefficient of $40 \text{ W/m}^2 - ^\circ\text{C}$. The chosen values are based on the optimized values which were between 55 to 72 percent for effectiveness and 20 to 60 $\text{W/m}^2 - ^\circ\text{C}$ for overall heat transfer coefficient.

Table 6-2. Test results of wheat drying in a concurrent-counterflow dryer equipped with heat pipe exchanger.¹

Drying Temperature °C	Dryer Outlet Temperature °C	Initial MC % WB	Final MC % WB	kJ/kg of H ₂ O Removed	Savings %
120	43	18.0	16.5	6298	6.1
150	45	17.7	15.6	5824	5.6
177	45	15.7	13.6	7349	6.1
205 ²	48	17.9	13.7	6007	7.4

¹A schematic view of the dryer is shown in Figure 4-2; dryer settings are listed in Table 4-2.

²Airflow in this experiment was 28.6 m³/min-m² for the dryer section.

Table 6-3. Test results of corn drying in a concurrent-counterflow dryer.¹

Ambient Air Temp. °C	Grainflow rate tonnes/hr-m ²	MC initial %	MC final %	Energy		Savings ³ (experimental) %	Recycling ²
				kJ/kg of H ₂ O removed Experiment.	Predicted		
12	1.56	22.4	15.7	3625	3542	13.4	a
15 ⁴	2.34	21.9	19.1	3855	3814	17.9	b
14	1.56	22.4	16.2	3911	3837	15.3	c
15	2.53	20.5	17.2	4340	4261	15.0	d
14	2.53	21.9	18.2	4688	4623	8.0	e

¹A schematic view of the dryer is shown in Figure 4-3; drying settings are listed in Table 4-3.

- ²a. 100% dryer exhaust to the exchanger. Drying air from exchanger 100%
 b. 100% dryer and cooler exhausts combined to the exchanger. 100% drying air from the exchanger.
 c. 100% dryer to the exchanger. Drying air from the exchanger supply 50% and from exchanger exhaust 50%.
 d. 100% dryer to the exchanger. Drying air from the exchanger 70% and from the cooler 30%.
 e. Drying air 30% from the cooler and 70% from the ambient.

³Savings are the percentage of total drying energy, obtained by preheating the drying air as a result of the performed recycling.

⁴Inlet drying air temperature in this experiment was 140°C.

Table 6-4 is a list of inputs to the program simulating a corn drying process. Tables 6-5 and 6-6 show a summary of the output. The recycling settings and the nomenclature are shown by a diagram on the left side of the table. The ratios indicated in the table are provided as inputs. The program will iterate until the final moisture content reaches within .05 percent.

Table 6-5 is a list of the simulated test results, using a heat pipe exchanger to recover heat in a concurrent-counterflow dryer (Westelaken Model 810-A). The program did not converge for a 75 percent direct recycling of the dryer exhaust, because in each iteration inlet air humidity was increased. The least amount of energy (2988 kg/kg) is used for the test in which the dryer exhaust is recycled into the heat exchanger, the cooler exhaust is directly recycled back to the dryer, and the make up is from the preheated ambient air. Table 6-6 shows the savings obtained as a result of direct recycling of the exhausts, and by-passing the heat pipe exchanger. The first test indicates conventional drying without using any heat recovery methods. As the table shows a 30 percent make up from the ambient air will result in a 3030 kJ per kg of water removed which is only about 1.5 percent more than the lowest value in Table 6-5.

Tables 6-5 and 6-6 show that not much difference can be found between a direct recycling and indirect recycling through a heat exchanger. Holding an optimum ratio of direct recycling is a difficult task and usually results in a varying inlet condition. When the exhausts are indirectly recycled through the heat exchanger the inlet conditions can be controlled more effectively. One more point must be mentioned that the specified heat exchanger effectiveness of 60 percent is a

Table 6.4 Settings for simulation of the concurrent-counterflow grain dryer. Model 810-A.

Inlet air temperature	230°C
Inlet absolute humidity	.004 kg/kg
Airflow rates	
...dryer	47.72 m ³ /min-m ²
...cooler	22.86 m ³ /min-m ²
Ambient air temperature	18°C
Inlet grain temperature	24°C
Grain	shelled corn
Grain moisture content	25% (WB)
Grainflow rate	2.184 tonnes/hr-m ²
Length	
...dryer	2 m
...cooler	1 m
Cross section area of the dryer and cooler	8.9 m ²

Table 6-5. Simulated test results, using a heat pipe exchanger in the concurrent-counterflow dryer, the Westelaken Model 810-A.

	Recycling ratios percent			Energy to remove one kg of water kJ			Moisture content percent (WB)		
	RDD	RDX	RAX	Dryer	Direct	Ht pipe	System	MC _i	MC _f
	0	100	100	3488	0	349	3138	25.00	18.71
	10	90	90	3519	71	322	3134	25.00	18.69
	30	70	70	3595	244	258	3102	25.00	18.56
	50	50	50	3791	511	197	3094	25.00	18.08
	75	25	25	did not converge					
	0 ¹	100	50	3419	347	179	2988	25.00	18.37
	0 ²	100	50	3419	319	222	2964	25.00	18.37
	0 ²	100	100	3488	0	466	3046	25.00	18.71

¹For this and the following tests, the cooler exhaust air was recycled to the dryer.

²A heat exchanger effectiveness of 75 percent was assumed for these two tests.

Table 6-6. Simulated tests results, using direct recycling, in the concurrent-counterflow dryer, the Westelaken Model 810-A.

	Recycling ratios percent			Energy to remove one kg of water kj			Moisture content percent (WB)	
	RDD	RCD	RAD	Dryer	Direct	Ht pipe system	MC _i	MC _f
	—	—	—	—	—	—	—	—
	0	0	100	3488	0	0	25.00	18.71
	00	100	50	3409	379	0	25.00	18.33
	10	100	40	3427	428	0	25.00	18.36
	30	100	20	3460	524	0	25.00	18.29
	50	60	20	3667	591	0	25.00	18.22
	50	0	50	3658	381	0	25.00	18.44
	75	0	25	did not converge				

conservative value (it might be as much as 75 percent). The last two tests of Table 6-5 are the repeat of the first and second tests, but with a heat pipe exchanger effectiveness of 75 percent. The resulting energy consumption is reduced by 2.8 percent.

Table 6-7 shows the effect of drying temperature on the energy savings resulted from simulating the use of a heat pipe exchanger in the concurrent counterflow model 810-A, Westelaken grain dryer. As the drying temperature increases, a heat pipe will save more energy and the required surface area decreases. However, the overall energy requirements increase.

6.4 Economics of heat pipe exchanger

Equation (3-119) is used to analyze the profitability of the heat pipe exchangers used in different sizes and types of grain dryers. For each grain dryer an optimal heat exchanger is designed and the following assumptions are made: (a) the purchase cost of the heat exchanger is obtained using equation (5-7). The ducting system is calculated based on the length, the number of bends and also cross section to match the airflow and the size of the heat exchanger frontal area. The cost of the duct system is calculated based on \$3.85 per kg (Goodfrey, 1977). The first cost (FC) is the sum of the heat pipe exchanger and the ducting purchase cost, (b) the annual operating cost is obtained from the power requirement to overcome the static pressure in the ducts and the heat exchanger. The power requirement is expressed in kilowatt hours per year and is calculated based on 750 operating hours per year. The price of electricity is taken as 3.5 cents per kWhr. A 5 percent of the first cost is added to the operating cost as maintenance cost (Perry, 1974), (c) the annual savings is obtained

Table 6-7. The effect of drying temperature on the savings, as a result of simulating the use of a heat pipe exchanger in the concurrent-counterflow dryer Model 810-A.¹

Drying Temp °C	MC _i	MC _f	Heat exchanger surface area m ²	Dryer	Energy kj/kg	
	Percent	Percent			Heat pipe	System
121	25	22	509	3237	310	2927
149	25	21	508	3305	324	2981
177	25	20	506	3349	334	3015
232	25	18	503	3413	338	3075
288	25	17	500	3488	359	3138

¹See Table 6-4 for the dryer settings. The combined dryer and cooler exhaust are recycled through the heat pipe exchanger.

based on the heat gain by the supply side of the heat exchanger expressed in million kj. Fuel oil number 2 is chosen as a typical fuel for the dryer. The price of fuel expressed in dollars per million kj, is calculated assuming a heating value of 3.86×10^7 kj per m^3 with a 70 percent (Isothermics, 1975) efficiency and a price of \$92 per m^3 .

6.4.1 Heat pipe exchanger and concurrentflow dryer

Table 6-8 is a list of costs and savings data for the profitability analyses of the heat pipe exchangers used in the Westelaken grain dryers. Table 6-9 is generated by using equation (3-125) and applying data of Table 6-8. A ten-year cashflow and a net present value analysis is utilized assuming typical values for interest, fuel escalation, inflation and tax rates. Table 6-9 shows that in 4 to 5 years the heat pipe exchanger will break even. The exhausts from the dryer and the cooler must be combined and recycled into the heat exchanger, unless the heat exchanger is designed for smaller airflows. In other words a heat pipe exchanger must be operated at its maximum potential, in order to give the desired economical results.

The net present value is analyzed as a function of the fuel escalation for three different ranges of tax rate, inflation rate and discounted cashflow rate of return. For each case two different service lives, 5 and 10 years, are considered. Figure 6-2 shows that, for a service life of 5 years, an annual fuel escalation rate of 10 percent will have a net present value of about \$2200 when no taxes are paid, while the same yields minus \$200 if a 50 percent tax rate is to be paid. The profitability of the heat exchanger will be altered to a large extent

Table 6-8. Present (first year) costs and savings data for use in the profitability analysis of heat pipe exchangers, used in different models of the Westelaken grain dryers.

Model	Surface area m ²	First cost \$	Heat exchanger kWhr/year	Operating ¹ cost \$	Savings kJ/hr	Savings \$/year
810-A	553	3711	8647	399	.78x10 ⁶	1941
1210-A	1264	6137	10252	471	1.33x10 ⁶	3319
3010-A	1837	7943	15712	692	2.1x10 ⁶	5230
4510-A	2610	9828	26280	1269	3.08x10 ⁶	7667

¹Five percent of the First Cost for maintenance is included.

Table 6-9. Cashflow and net present value analysis of different sizes of heat pipe exchangers, used in the Westelaken grain dryers.

810-A								
		<u>Interest Rate</u>	<u>Fuel Rate</u>	<u>Inflation Rate</u>	<u>Tax Rate</u>			
		.12	.15	.05	.50			
<u>Year</u>	<u>First Cost</u>	<u>Fuel Cost</u>	<u>Operating Cost</u>	<u>Cash Income</u>	<u>Dep- reci- ation</u>	<u>Net Cash Flow</u>	<u>Discount Cash Flow</u>	<u>Net Present Value</u>
0	3711	0	0	0	0	-3711	-3711	-3711
1	0	1941	399	1542	371	956	813	-2897
2	0	2232	418	1813	371	1092	789	-2107
3	0	2566	439	2127	371	1249	768	-1339
4	0	2952	461	2490	371	1430	747	-591
5	0	3394	484	2909	371	1640	729	137
6	0	3904	509	3394	371	1882	711	849
7	0	4489	534	3954	371	2163	695	1544
8	0	5163	561	4601	371	2486	679	2224
9	0	5937	589	5348	371	2859	664	2889
10	0	6828	618	6209	371	3290	650	3539

1210-A								
		<u>Interest Rate</u>	<u>Fuel Rate</u>	<u>Inflation Rate</u>	<u>Tax Rate</u>			
		.12	.15	.05	.50			
<u>Year</u>	<u>First Cost</u>	<u>Fuel Cost</u>	<u>Operating Cost</u>	<u>Cash Income</u>	<u>Dep- reci- ation</u>	<u>Net Cash Flow</u>	<u>Discount Cash Flow</u>	<u>Net Present Value</u>
0	6137	0	0	0	0	-6137	-6137	-6137
1	0	3319	471	2848	613	1730	1471	-4665
2	0	3816	494	3322	613	1968	1423	-3242
3	0	4389	519	3870	613	2241	1378	-1863
4	0	5047	545	4502	613	2558	1337	-526
5	0	5804	572	5232	613	2923	1299	773
6	0	6675	601	6074	613	3344	1264	2037
7	0	7677	631	7045	613	3829	1231	3268
8	0	8828	662	8165	613	4389	1200	4468
9	0	10152	695	9457	613	5035	1170	5639
10	0	11675	730	10945	613	5779	1142	6781

Table 6-9 (continued)

3010-A

		<u>Interest Rate</u>	<u>Fuel Rate</u>	<u>Inflation Rate</u>	<u>Tax Rate</u>			
		.12	.15	.05	.50			
0	7943	0	0	0	0	-7943	-7943	-7943
1	0	5230	692	4538	794	2666	2267	-5675
2	0	6014	726	5287	794	3041	2198	-3476
3	0	6916	762	6153	794	3474	2136	-1340
4	0	7954	801	7153	794	3973	2077	736
5	0	9147	841	8306	794	4550	2023	2759
6	0	10519	883	9636	794	5215	1971	4731
7	0	12097	927	11169	794	5982	1923	6654
8	0	13911	973	12938	794	6866	1876	8531
9	0	15998	1022	14976	794	7885	1832	10364
10	0	18398	1073	17324	794	9059	1790	12155

4510-A

		<u>Interest Rate</u>	<u>Fuel Rate</u>	<u>Inflation Rate</u>	<u>Tax Rate</u>			
		.12	.15	.05	.50			
0	9828	0	0	0	0	-9828	-9828	-9828
1	0	7667	1269	6398	982	3690	3138	-6689
2	0	8817	1332	7484	982	4233	3061	-3628
3	0	10139	1339	8740	982	4861	2989	-639
4	0	11660	1469	10191	982	5587	2921	2281
5	0	13409	1542	11867	982	6424	2856	5138
6	0	15421	1619	13801	982	7392	2794	7932
7	0	17734	1700	16033	982	8508	2735	10668
8	0	20394	1785	18608	982	9795	2677	13346
9	0	23453	1874	21578	982	11280	2622	15968
10	0	26971	1968	25002	982	12992	2568	18536

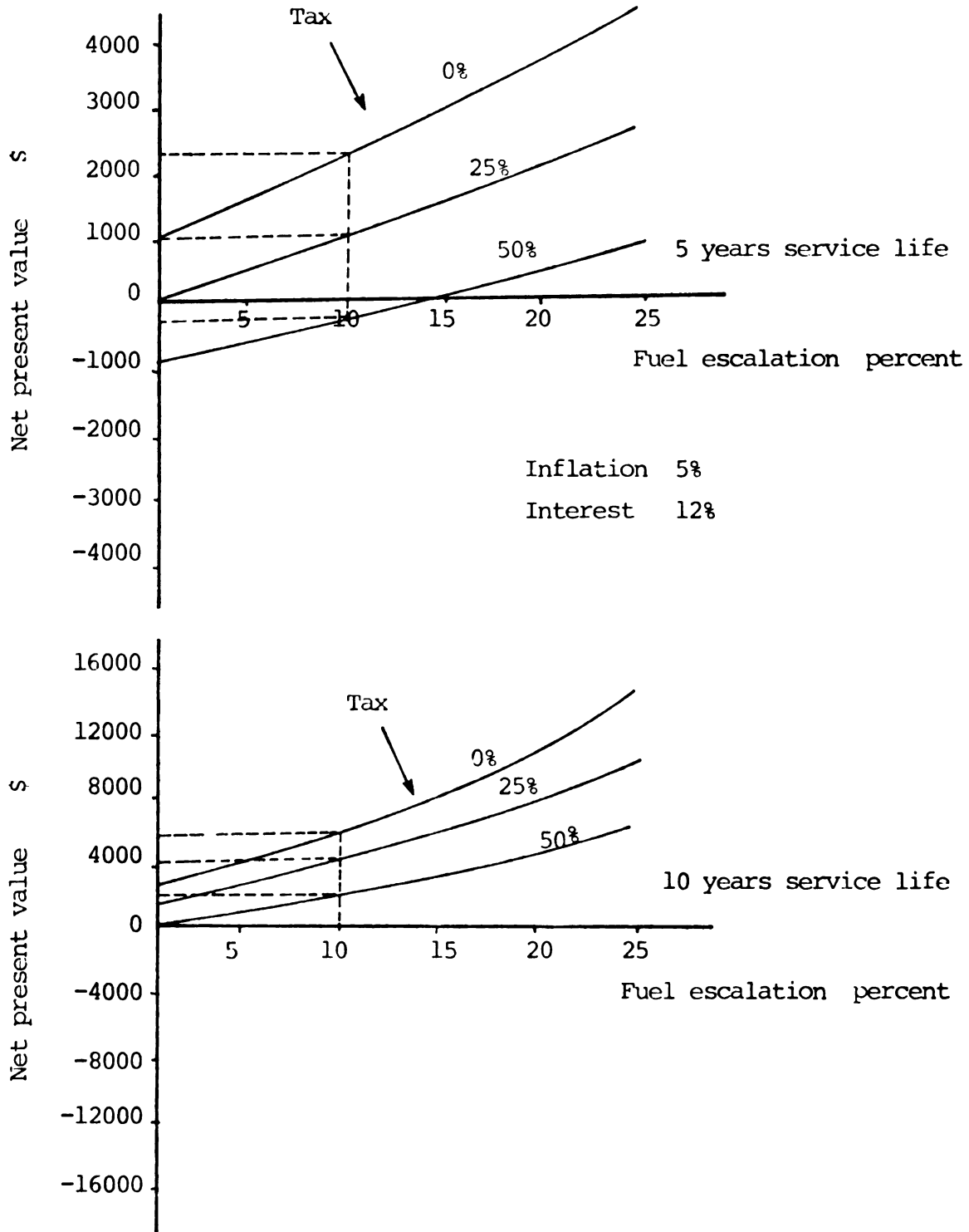


Fig. 6-2. Net present value as a function of fuel escalation and tax rate, for a heat pipe exchanger life of 5 and 10 years of service; and 750 hours of operation per year.

when a longer service life can be expected from the heat exchanger. Considering similar conditions the importance of the inflation rate on the profitability is shown in Figure 6-3. In this figure a 10 percent fuel escalation and a 5-year service life will not generate any net income unless the fuel price escalation reaches a value of more than 14 percent. Figure 6-4 shows that if a 20 percent discounted cashflow rate of return (DCFR) is the result of investment in the heat pipe exchanger, the life of the project must be at least 10 years.

In summary, Figures 6-2, 6-3 and 6-4 indicate that a careful study of such parameters as fuel escalation, interest rate, tax rate, and inflation rate is necessary in the profitability analysis of a heat pipe exchanger.

6.4.2 Heat pipe exchanger and commercial crossflow dryers

Figure 6-5 shows a schematic view of a recirculating crossflow dryer manufactured by Ferrel-Ross, Saginaw, Michigan. The exhaust air from the heat levels 3, 4 and 5, and the cool level 2 is recycled directly back to the burner after it is mixed with the ambient air. Typical dimensions and process conditions are listed in Table 6-10. For the purpose of a profitability analysis, it is assumed that the recycled exhaust is directed to a heat pipe exchanger to preheat the drying air. An optimal heat pipe exchanger is specified using the non-linear optimization program, developed in the previous chapter.

Table 6-11 lists the inputs for optimal design and some of the outputs specifying an optimal designed heat pipe exchanger for heat recovery in the Ferrel-Ross crossflow dryer. Table 6-12 contains the surface area, the savings and the profitability analysis of using

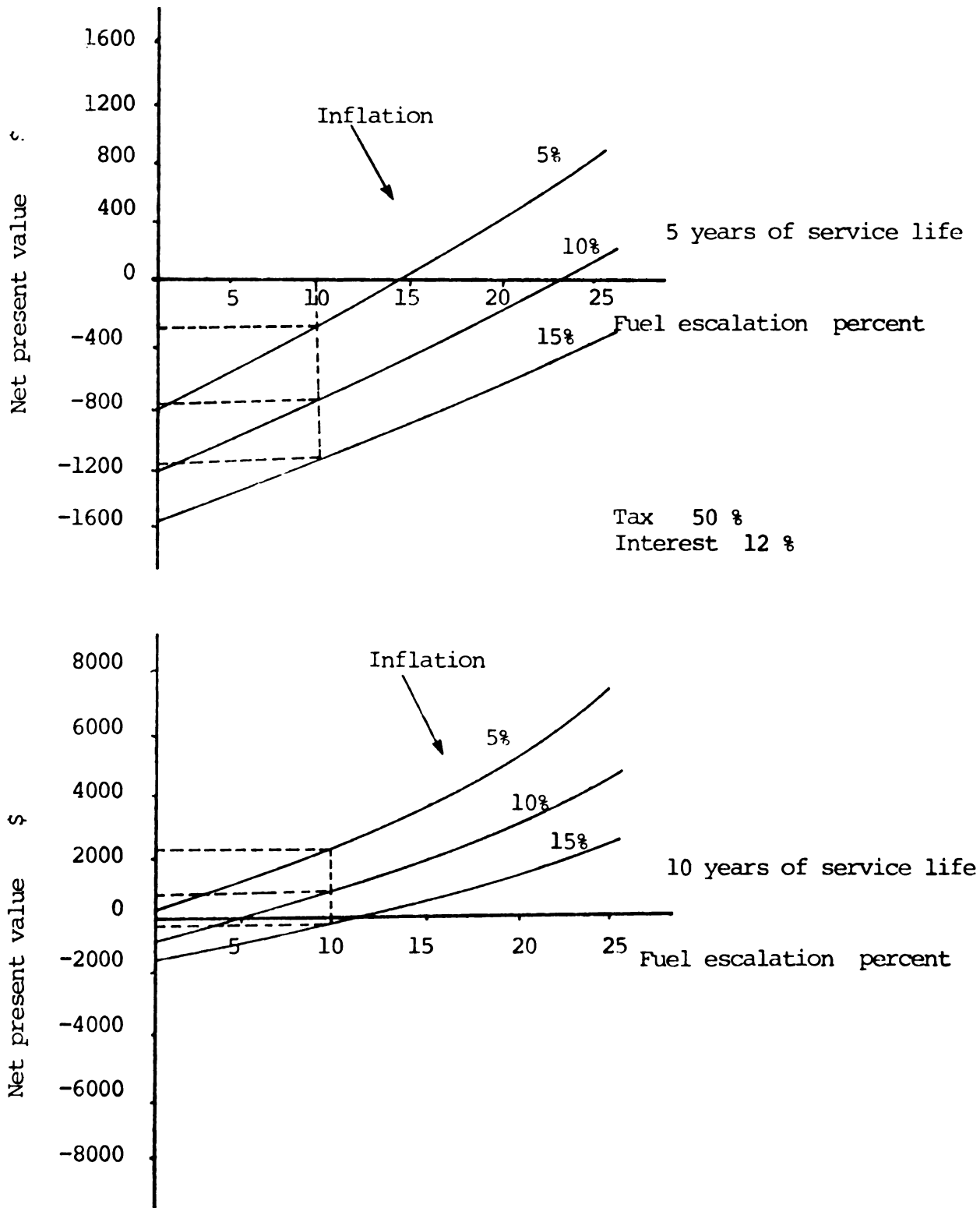


Fig. 6-3. Net present value as a function of fuel escalation and inflation rate for a heat pipe exchanger life of 5 and 10 years of service; and 750 hours of operation per year.

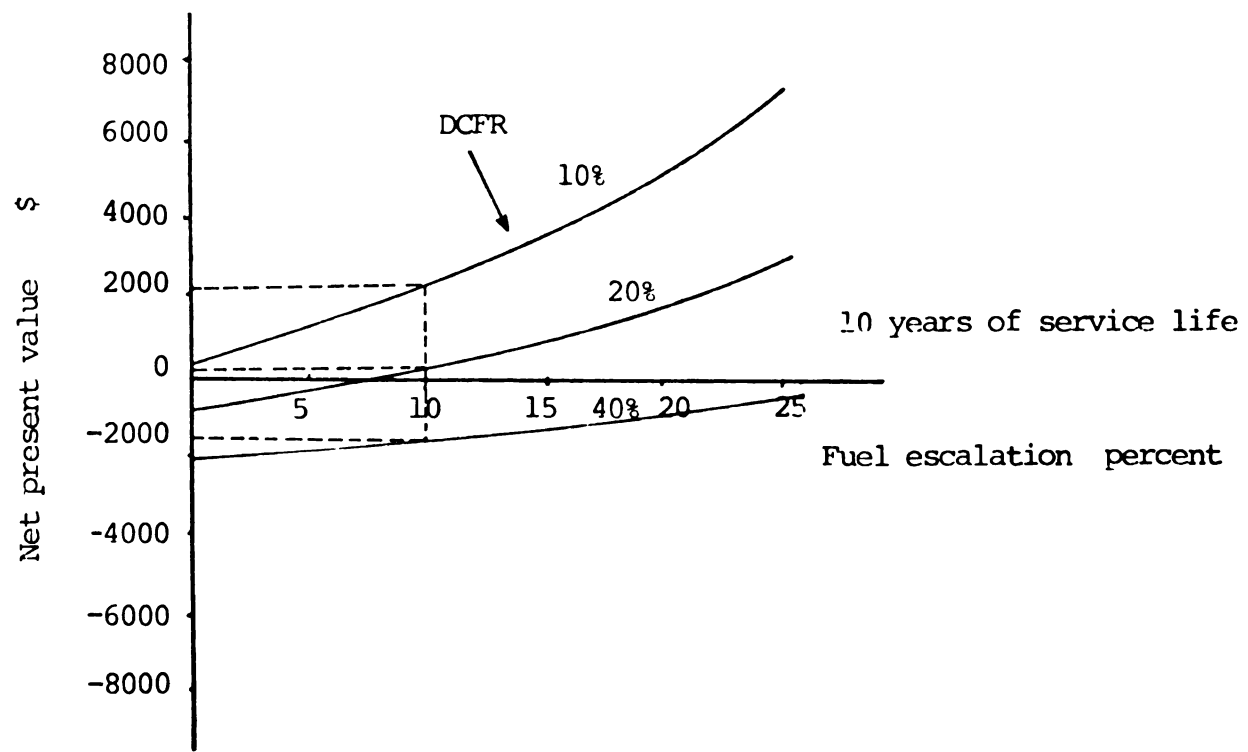
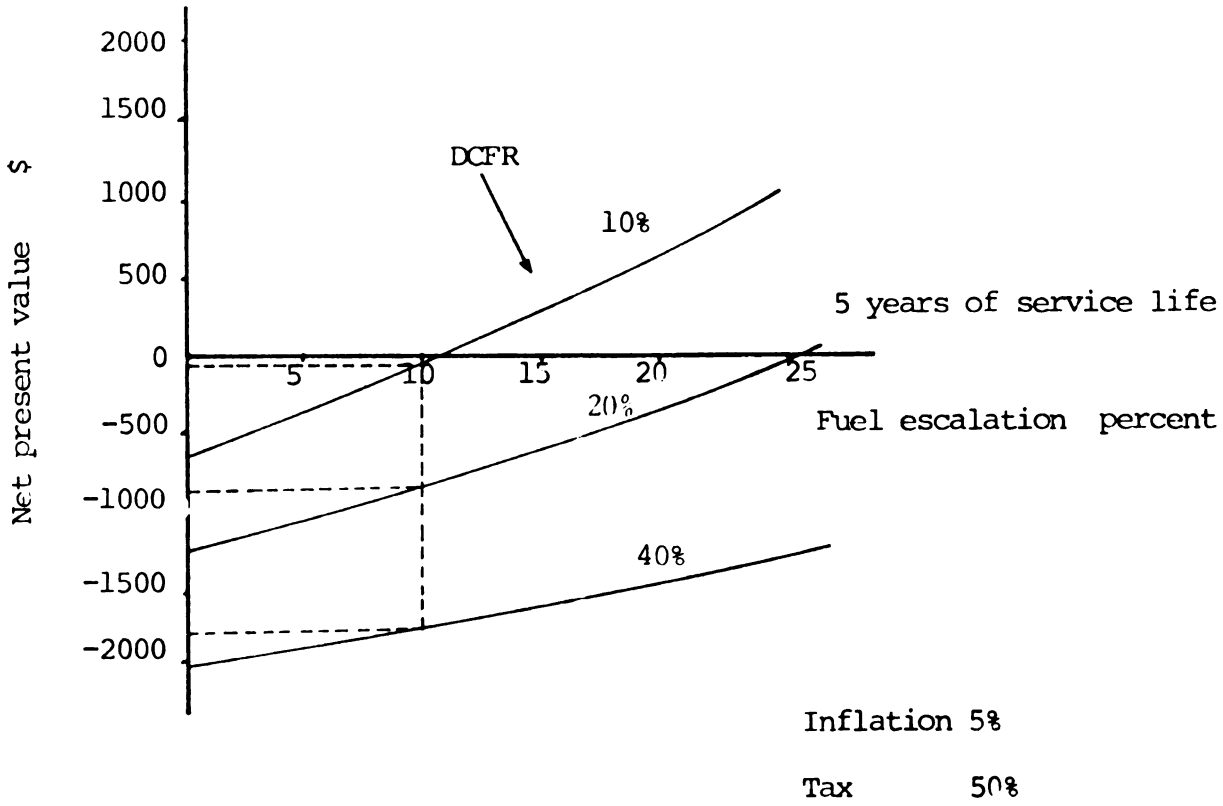


Fig. 6-4. Net present value as a function of fuel escalation and discounted cashflow rate of return (DCFR), for a heat pipe exchanger life of 5 and 10 years of service; and 750 hours of operation per year.

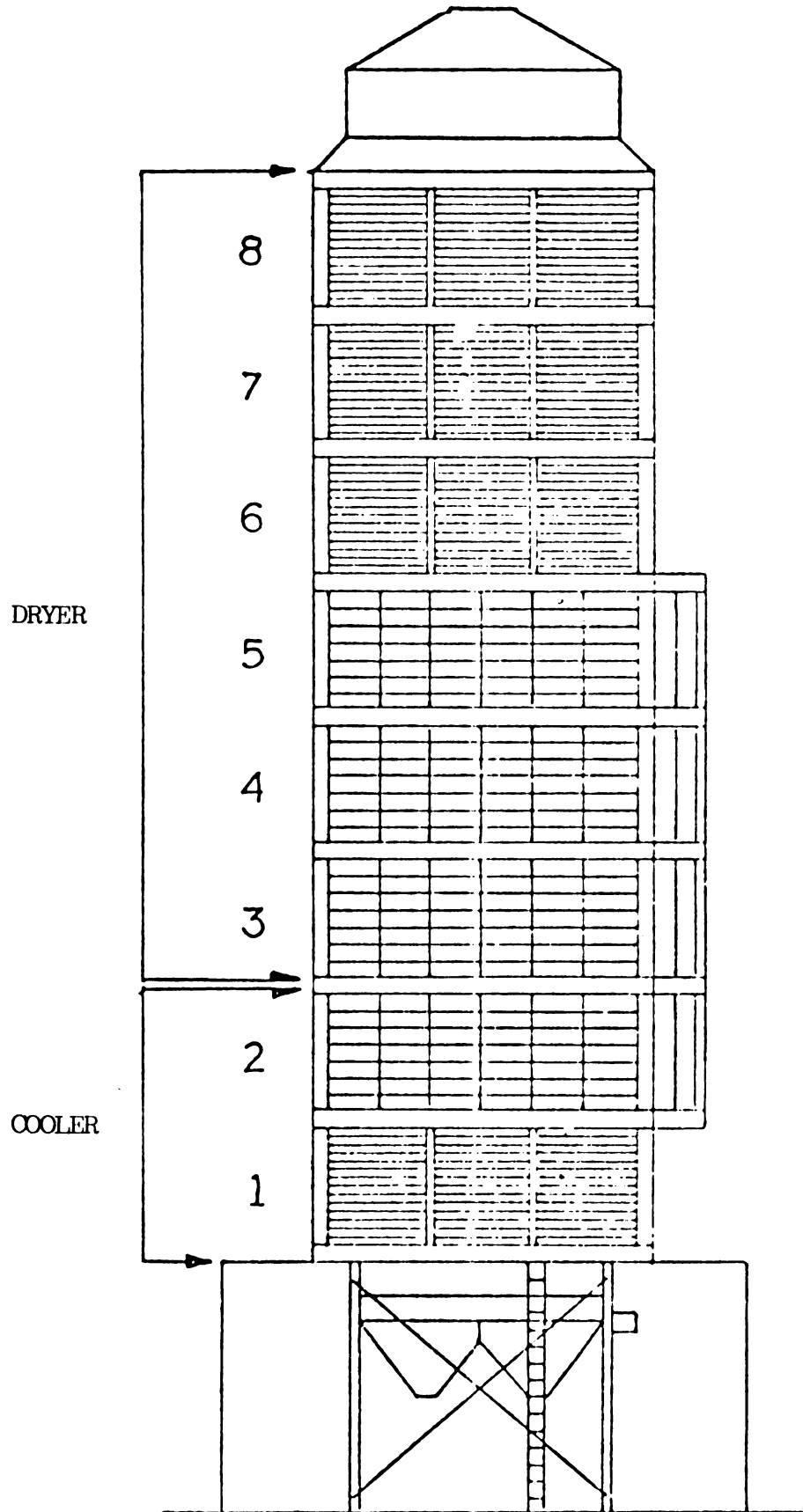


Figure 6-5. Ferrel-Ross recirculating crossflow dryer

Source: Bauer et al. (1977)

Table 6-10. Some typical dimensions and process values of a commercial crossflow dryer manufactured by Ferrel-Ross Co., Saginaw, Michigan.

Drying air temperature:	outlet air temperature:
level 8 102°C	33°C
level 5 106°C	70°C
level 2 23°C	52°C
Ambient air temperature	18°C
Ambient absolute humidity	.004 kg/kg
Grainflow rate	100 tonnes/hr
Airflow rate:	
...Dryer	40 m ³ /min-m ²
...Cooler	20 m ³ /min-m ²
Length:	
...Dryer	14.6 m
...Cooler	4.8 m
Drying and cooling columns	.3 x 2.4 x 3.1 m
Number of column in each level	6
Number of levels:	
Dryer	6
Cooler	2
Holding Capacity	81.5 tonnes (shelled corn)

Source: Bauer et al. (1977)

Table 6-11. Input for the optimal design and output specifying the optimal designed heat pipe exchanger for use in the Ferrel-Ross crossflow dryer.

Inputs:

		<u>Exhaust side</u>	<u>Supply side</u>
Airflow ¹	m ³ /min	4813	5776
Temperature ²	°C	60	18
Humidity ³	kg/kg	.01	.005
Fuel price	dollars/million kj	3.31	
Electricity	dollars/kWhr	.035	

Outputs:

Overall dimensions	m	5.8x2.8x.8
Fins	per cm	5.04
No. of rows		10
No. of pipes in a row		48
Surface area	m ²	4842
Effectiveness	percent	56
Savings	kj/hr	6.43x10 ⁶

¹Based on 94.5 m /min.-tonn of grain

²An average temperature

³A typical condition

Table 6-12. Annual cashflow and net present value analysis of the optimal heat pipe exchanger, used in the Ferrel-Ross crossflow dryer.

First cost	\$ 33246
Operating cost	\$ 4972
Savings	\$ 15962

	<u>Interest rate</u>	<u>Fuel escalation</u>	<u>Inflation rate</u>	<u>Tax rate</u>				
	.12	.15	.05	.50				
<u>Year</u>	<u>First cost</u>	<u>Fuel cost</u>	<u>Operating cost</u>	<u>Cash income</u>	<u>Depreciation</u>	<u>Net cash flow</u>	<u>Discount cashflow</u>	<u>Net present value</u>
0	33246	0	0	0	0	-33246	-33246	-33246
1	0	15962	4972	10990	3324	7157	6086	-27159
2	0	18356	5220	13135	3324	8230	5951	-21208
3	0	21109	5481	15628	3324	9476	5826	-15382
4	0	24276	5757	18520	3324	10922	5710	-9671
5	0	27917	6043	21874	3324	12599	5601	-4069
6	0	32105	6345	25759	3324	14542	5497	1427
7	0	36921	6662	30258	3324	16791	5398	6825
8	0	42459	6696	35463	3324	19393	5301	12127
9	0	48828	7345	41482	3324	22403	5207	17335
10	0	56152	7713	48439	3324	25881	5115	22451

the heat pipe exchanger in the crossflow dryer. Table 6-12 shows that savings in fuel will pay back the heat pipe exchanger costs after 5 years. The heat pipe exchanger in the crossflow dryer shows a lower level of profitability than the concurrentflow dryers. However, at the present, crossflow dryers are the major types being used and the heat pipe exchanger definitely results in net savings which otherwise will be lost.

6.4.3 Heat pipe exchanger and batch type dryers

Application of heat pipe exchangers to deep bed dryers largely depends on the price of fuel. The exhaust air from a well designed and operated deep bed dryer is saturated and its temperature is low. However, when the ambient air temperature is lower than the exhaust, sensible and latent heat available in the exhaust stream can be recovered by using a heat pipe exchanger. The effectiveness of the heat exchanger will increase as the drying proceeds in the bed and more heat becomes available to be recovered.

Use of heat pipe exchangers in layer drying operation is similar to the crossflow dryer. However, layer dryers operate at lower temperatures than the crossflow dryer, and thus, a lower net present value is expected.

Use of heat pipe exchangers in fluidized bed dryers is similar to concurrent flow dryers. In fluidized dryers, the total airflow is higher than in a concurrent flow dryer with the same dimensions. The absolute humidity of the exhaust air is also higher. The high airflow and available latent heat are the two characteristics that make the heat pipe exchangers economically attractive in fluidized bed dryers.

6.4.4 The effects of fouling on heat pipe exchanger economics

The effects of fouling on the economics of a heat pipe exchanger is shown in Figure 6-6 where the annual costs and the annual savings are plotted versus the thickness of fouling layer. The analysis is for a heat pipe exchanger specified for the Westelaken grain dryer model 810-A. However, the results will be similar for other units. Figure 6-6 shows that the savings and costs intersect at a fouling layer thickness that can be considered a critical value (.44 mm)¹. Beyond this point, the heat exchanger is not economical. Figure 6-6 also indicates that the changes in savings are small compared with the changes in costs. The reason is the relative value of resistances due to the heat transfer (h) and fouling (R_f). The fouling build up results in higher velocity air which eventually produces a high heat transfer coefficient. The relative increase in the heat transfer coefficient is the same or more than the relative increase in fouling. As a result, not much change is noted in the amount of heat transferred. However, high velocity air results in a higher pressure drop which is responsible for the operating cost increases.

To calculate the frequency of heat pipe exchanger cleaning in a year, Figure 6-7 has been plotted. Meiering and Hoefkes (1976) measured an average amount of 200 g/m²/hr dust in the exhaust air of several sizes of crossflow grain dryers, and gave various quantities and sizes of the grain dust particles (Table 6-13). Meiering and Hoefkes (1976) stated that

¹The thermal conductivity of fouling material is assumed to be the same as those of grains (about 1056 W/m-C).

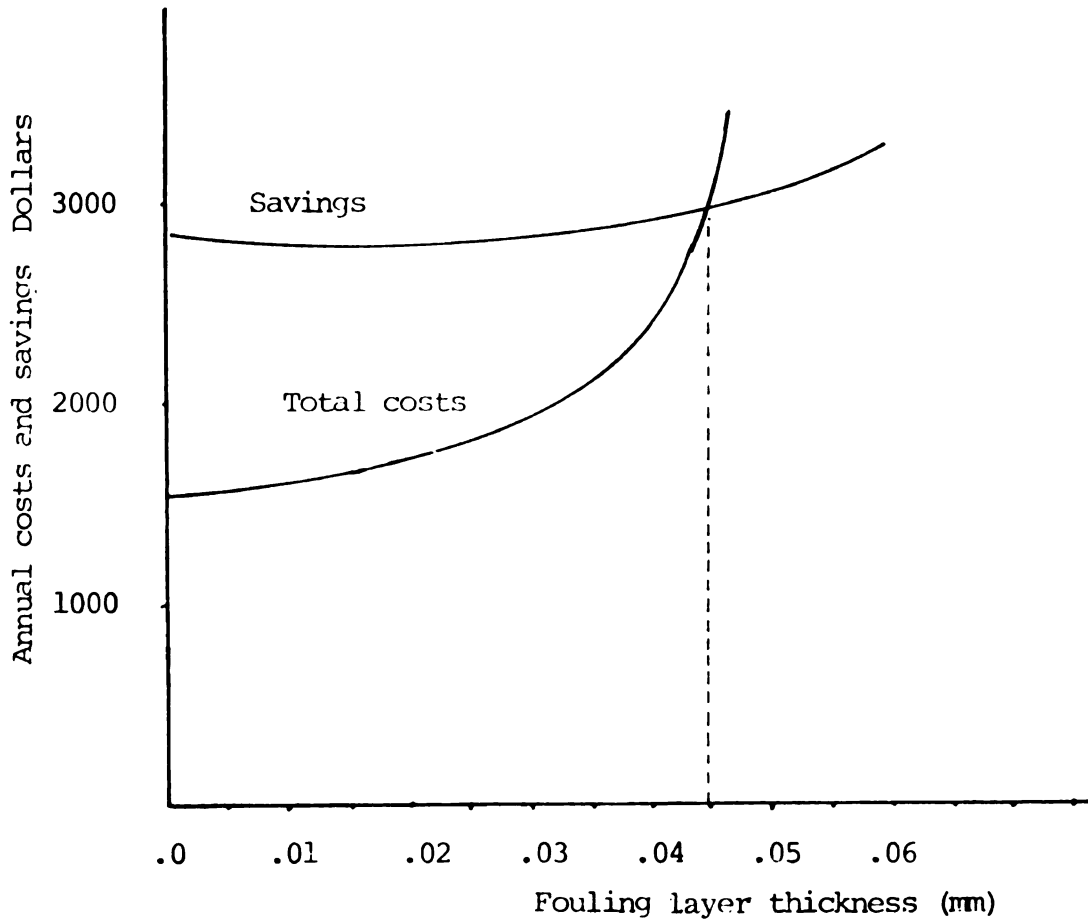


Fig. 6-6. The effect of fouling thickness on the total annual costs and savings of a heat pipe exchanger specified for the Westelaken grain dryer Model 810-A.

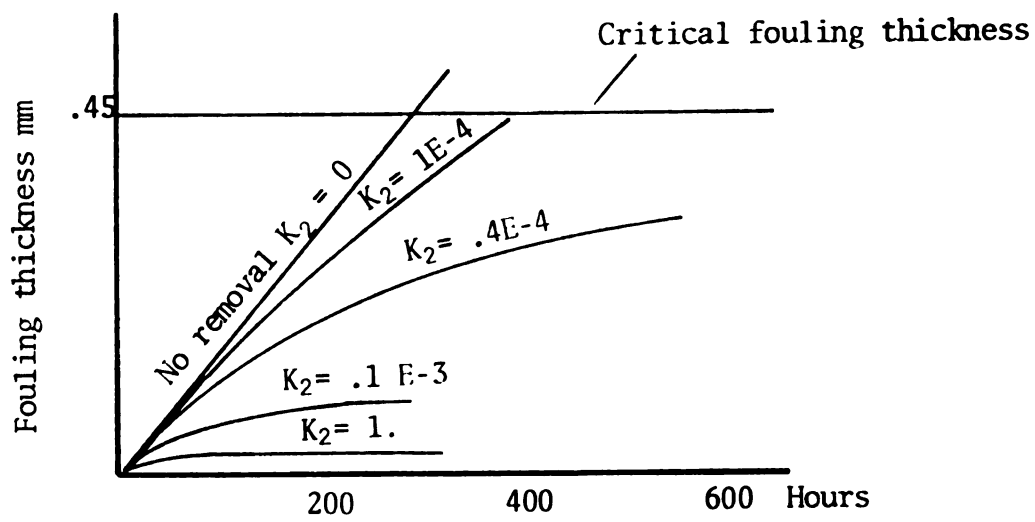


Fig. 6-7. Time required for the fouling thickness to reach to the critical thickness for various values of removal rate (K_2); see equation 3-114.

Table 6-13. Particle size and the weight percentage in a typical exhaust air from a crossflow dryer.

Category	Particle Size mm	Weight Percentage of Total
I	> 1.2	44
II	.6 - 1.2	19
III	.4 - .6	12
IV	.15 - .4	14
V	< .15	11

Source: Meiering & Hoefkes (1976)

"the particles below .6 mm can be assumed to have an amorphous, concentric shape with a density similar to that of many biological materials, about 1.2 g/cm^3 . The particles with diameters over .6 mm have a foliar shape".

It is assumed, in Figure 6-7, that the particles smaller than .6 mm stick to the heat transfer surface area and form the fouling crust. This amounts to 37 percent of the total emissions ($74 \text{ g/m}^2\text{-hr}$). The remaining 63 percent dust particles have to be removed in a settling chamber or a bag house. Otherwise, these particles will block the frontal area of the heat pipe exchanger. Figure 6-7 shows the time required to build up to .44 mm thickness with various removal rates (see equation 3-108). In about 300 hours of operation, fouling builds up to a critical value. Therefore, at least twice a year a cleaning operation is required if the heat exchanger is to be operated economically 750 hours a year.

The cost of filtering equipment has not been considered in the economic and fouling analysis, because most of the commercial dryers are equipped with some type of filtering device. The profitability of a heat pipe exchanger will be reduced considerably, if a collection device is to be used and the costs are charged to the heat exchanger.

7. CONCLUSIONS

Based on the analyses and experiments performed in this study, the following conclusions can be drawn:

1. Energy savings from 15 to 18 percent can be obtained in grain dryers as a result of heat pipe exchanger applications. These values were obtained both experimentally and by a simulation.
2. Simulation results showed a direct recirculation grain dryer yields savings in a concurrent-counterflow comparable to those obtained when recycling is performed through a heat pipe exchanger. A combination of direct recycling of the cooler exhaust and indirect recycling of the dryer exhaust through a heat pipe exchanger reduces the energy consumption to about 2964 kJ per kg of water removed as compared to 3488 kJ for a concurrentflow dryer without recirculation and use of a heat pipe exchanger.
3. The profitability of a heat pipe exchanger depends on the annual fuel escalation, inflation, interest and tax rate. Heat pipes used on a concurrentflow dryer showed a break even point after 5 years of operation, while on a crossflow showed a pay back after the fifth year of operation (750 hours of operation per year).
4. Particles larger than .6 mm must be removed from the exhaust air entering into the heat exchanger to prevent these particles

from blocking the air passages. It is recommended that heat pipe exchangers be used in the grain dryers already equipped with some type of emission control devices. Purchasing filtering devices solely for the sake of heat exchanger and charging the costs to the heat exchanger will alter the presented profitability analysis to a large extent, because the cost of filtering equipment is usually several times more than the cost of the heat pipe exchangers.

5. Fouling results in high pressure drop and increased operating costs. The rate of heat transfer and, as a result, the annual savings remain rather constant with increased fouling thickness. This is partly because the relative values of the convective resistance and fouling resistance do not change with the layer build up. Cleaning must be performed about 300 hours of operation before the operating costs exceed the savings.
6. The economics of heat pipe exchangers used in either a concurrent-counterflow dryer or in a crossflow dryer depends on the exhaust temperatures and the airflows. Concurrent-counterflow grain dryers have better design characteristics to use heat pipe exchangers more economically, than in crossflow and batch dryers. The high airflow in crossflow dryers will offset the large initial investments in the heat pipe exchanger equipment.
7. The analysis and the optimization methods developed in this investigation are valid for a wide range of size and process variables. Therefore, the computer programs can be used for future analysis and designs.

8. SUGGESTIONS FOR FUTURE WORK

Based on the analyses and conclusions of this study, the following recommendations are made for further investigations:

1. To investigate the characteristics and quantities of emissions from different types of dryers.
2. To install a heat pipe exchanger on commercial grain dryers to investigate:
 - a) fouling characteristics
 - b) heat exchanger performance
 - c) savings and costs under different operating conditions
3. To extend the application of heat pipe exchangers to other agricultural and food process industries.
4. To investigate the use of thermosyphons in grain drying and other processes.

REFERENCES

9. LIST OF REFERENCES

- Amode, J. O. and K. T. Feldman, 1975. Preliminary analysis of heat pipe exchangers for heat recovery. ASME Paper No. 75/WA/HT-36. The American Society of Mechanical Engineers, New York, NY.
- Anderson, R. J., 1972. Commercial concurrentflow heating, counterflow cooling grain dryer. The Anderson Model. ASAE Paper No. 72-846. Am. Soc. Agr. Eng., St. Joseph, MI.
- Anderson, R. J., 1976. Personal communications. The Andersons. Maumee, OH.
- Anon., 1977. Efficient grain dryers. Sales literature. Ferrel-Ross Co., Saginaw, MI.
- Aronson, R. B., 1976. The heat pipe: Hot new way to save energy. Machine Design 6:52-56.
- ASHRAE, 1974. ASHRAE Handbook of Fundamentals. American Society of Heating, Refrigerating, and Air Conditioning Engineers, Inc., New York, NY.
- Asselman, A. A. G. and D. B. Green, 1973. Heat pipes. Philips Tech Review 4:104-113 and 5:138-148.
- Avant, R. V., C. B. Parnel and J. W. Sorenson, Jr., 1976. Analysis of cyclone separator collection performance for grain sorghum dust. ASAE Paper No. 76-3543. Am. Soc. Agr. Eng., St. Joseph, MI.
- Bakker-Arkema, F. W., D. B. Brooker and C. W. Hall, 1972. Comparative evaluation of crossflow and concurrentflow grain dryers. ASAE Paper No. 72-849. Am. Soc. Agr. Eng., St. Joseph, MI.
- Bakker-Arkema, F. W., S. F. DeBoer, L. E. Lerew and M. G. Roth, 1973. Energy conservation in grain dryers: Performance evaluation. ASAE Paper No. 73-324. Am. Soc. Agr. Eng., St. Joseph, MI.
- Bakker-Arkema, F. W., L. E. Lerew, S. F. DeBoer and M. G. Roth, 1974. Grain dryer simulation. Research Report 224, Agricultural Experiment Station, Michigan State University, East Lansing, MI.
- Bakker-Arkema, F. W., S. Sokhansanj and M. G. Roth, 1974. Energy requirement for a two-stage recirculating counterflow grain dryer. ASAE Paper No. 74-3005. Am. Soc. Agr. Eng., St. Joseph, MI.

- Bakker-Arkema, F. W., S. Sokhansanj and D. M. Farmer, 1975. Heat pipes for saving energy in grain drying. ASAE Paper No. 75-3516. Am. Soc. Agr. Eng., St. Joseph, MI.
- Bauer, W., S. Fosdick, L. P. Walker and F. W. Bakker-Arkema, 1977. Testing of commercial sized conventional crossflow and modified crossflow grain dryers. ASAE Paper No. 77-3014. Am. Soc. Agr. Eng., St. Joseph, MI.
- Beal, S. K., 1970. Deposition of particles in turbulent flow on channel or pipe walls. Nuclear Science and Engineering. 40:1-11.
- Becker, H. A. and R. A. Isaacson, 1971. Wheat drying in well stirred batch and continuous moving bed dryers. Can. J. Chem. Eng. 48:560-567.
- Black, J. R. and D. G. Fox, 1976. Taking account of variation in nutrient values in least-cost ration formulation. Ag. Econ. Staff Paper No. 76-14. Michigan State University, East Lansing, MI.
- Brooker, D. B., F. W. Bakker-Arkema and C. W. Hall, 1975. Drying Cereal Grains. The AVI Pub. Co., Inc., Westport, CT.
- Carano, J. A., W. G. Bickert and F. W. Bakker-Arkema, 1971. Design and testing of a laboratory scale concurrent-counterflow high temperature corn dryer. ASAE Paper No. 71-320. Am. Soc. Agr. Eng., St. Joseph, MI.
- Chi, S. W., 1976. Heat Pipe Theory. McGraw-Hill Book Company, New York, NY.
- Clark, E. G. and W. J. Lamond, 1968. Drying wheat in two foot beds. 11 Energy Consumption., J. Agric. Eng. Res. 13:245-248.
- Converse, J. O., 1971. Clean air from the seed and grain handling industries. Speech given before Pacific Northwest Region. ASAE Meeting, Oct. 7, 1971, Portland, OR.
- Converse, J. O., 1972. A commercial crossflow-counterflow grain dryer: the H. C. ASAE Paper No. 72-828. Am. Soc. Agr. Eng., St. Joseph, MI.
- Dunn, P. and D. A. Reay, 1976. Heat Pipes. Pergamon Press. Oxford, England.
- Feldman, K. T. and G. H. Whiting, 1968. Application of the heat pipe. Mech. Eng. 90:18-68.
- Foster, G. H., 1976. Grain Drying - reflections and perspectives. ASAE Paper No. 76-3005. Am. Soc. Agr. Eng., St. Joseph, MI.
- Freidlander, S. K. and H. F. Johnson, 1957. Deposition of suspended particles from turbulent gas streams. Industrial and Engineering Chemistry 7:1151-1156.

- Goodfrey, R. S., 1977. Building Construction Cost Data. Robert Shaw Means Company, Inc., Duxbury, MA.
- Graham, D. L., 1967. Concurrentflow grain dryer design. ASAE Paper No. 67-859. Am. Soc. Agr. Eng., St. Joseph, MI.
- Grover, G. M., T. P. Cotter and G. E. Erickson, 1964. Structure of a very high thermal conductance. J. Applied Physics. 35:1990-1991.
- Guillory, J. L. and F. C. McQuiston, 1973. An experimental investigation of air dehumidification in a parallel plate exchanger. ASHRAE Trans. 2:146-151.
- Harsh, B. S. and J. R. Black, 1975. Agricultural economics linear package version 2. April 1975. A. E. Staff Paper No. 75-10. Michigan State University, East Lansing, MI.
- Hillier, S. D. and G. J. Lieberman, 1967. Operations Research. Holden-Day, Inc., San Francisco, CA.
- Holland, F. A. and F. A. Watson, 1977a. Putting inflation into profitability studies. Chemical Engineering 6:87-91.
- Holland, F. A. and F. A. Watson, 1977b. Project risk, inflation and profitability. Chemical Engineering 7:133-136.
- Holman, J. P., 1976. Heat Transfer. McGraw-Hill Book Company. New York, NY.
- Hughes, 1975. Evaluation of different types of air to air heat transfer recovery units. Application Note No. 1. Hughes Electron Dynamics Division. Torrance, CA.
- Isothermics, 1975. ISO-FIN THERMO-COIL. Effective energy recovery with heat pipes reduces operational costs for industry. Isothermics, Inc., Augusta, NJ.
- Jameson, S. L., 1945. Tube spacing in finned tube banks. Trans. ASME 67:633-643.
- Japikse, D., 1973. Advances in thermosyphon technology. In: Advances in Heat Transfer. 9. Academic Press, New York, NY.
- Johnson, C. E., 1976. Grain dust collector. ASAE Paper No. 76-3024. Am. Soc. Agr. Eng., St. Joseph, MI.
- Kays, W. M. and A. L. London, 1964. Compact Heat Exchangers. McGraw-Hill Book Company, New York, NY.
- Kern, D. Q. and R. E. Seaton. 1959. A theoretical analysis of thermal surface fouling. British Chemical Engineering 5:258-262.

- Kline, D. P., 1977. Design of a pilot scale concurrentflow grain dryer. Unpublished M. S. Thesis. Michigan State University, East Lansing, MI.
- Kuester, J. L. and J. H. Mize, 1973. Optimization Techniques with Fortran. McGraw-Hill Book Company, New York, NY.
- Lai, F. S. and G. H. Foster, 1975. Improvement in grain dryer fuel efficiency through heat recovery. ASAE Paper No. 75-3517. Am. Soc. Agr. Eng., St. Joseph, MI.
- Lehman, D. C., 1976. Evaluating energy savings measures: Impact of rising energy cost. ASHRAE Journal 18:46-47.
- Lerew, L. E., F. W. Bakker-Arkema and R. C. Brook, 1972. Simulation of a commercial crossflow dryer: The Hart-Carter Model. ASAE Paper No. 72-829. Am. Soc. Agr. Eng., St. Joseph, MI.
- Lukey, J. A., 1975. Index of computer programs available at Michigan State University. Computer Laboratory. Michigan State University, East Lansing, MI.
- McQuiston, C. F. and D. R. Tree, 1972. Optimum space envelopes of finned tube heat transfer surface. ASHRAE Trans. 2:144-152.
- McQuiston, F. C., 1975. Fin efficiency with combined heat and mass transfer. ASHRAE Trans. 2:350-355.
- Meiering, A. G. and H. E. Hoefkes, 1976. Particulate emission in corn drying. A Research Report. School of Engineering, University of Guelph. Ontario, Canada.
- Mirkovich, A., 1974. Heat transfer and flow resistance correlation for helically finned and staggered tube banks in crossflow. In: Heat Exchangers, Design and Theory Source Book. McGraw-Hill Book Company, New York, NY.
- Mizushima, T., 1974. Design of cooler condensers and evaporative coolers. In: Heat Exchangers, Design and Theory Source Book. McGraw-Hill Book Company, New York, NY.
- Morey, V. R. and W. E. Lueschen, 1974. Practices for efficient utilization of energy for drying corn. ASAE Paper No. 74-3541. Am. Soc. Agr. Eng., St. Joseph, MI.
- NASA, 1975. Heat Pipe. Contract Report CR-2508. Midwest Research Institute, Kansas City, MO.
- Noyes, R. T., 1977. SUPERB-'OPTIMUM' continuous crossflow commercial grain dryers. ASAE Paper No. 77-3015. Am. Soc. Agr. Eng., St. Joseph, MI.
- Perry, H. B. and C. H. Chilton, 1973. Chemical Engineers Handbook. McGraw-Hill Book Company, New York, NY.

- Q-DOT, 1976. Q-Pipes Thermal Recovery Units for HVAC Energy Conservation Systems. Bulletin No. QHV-76-1. Q-Dot Corp., Dallas, TX.
- Rich, D. G., 1973. The effect of fin spacing on the heat transfer and friction performance of multirow, smooth plate fin and tube heat exchangers. ASHRAE Trans. 2:137-145.
- Rich, D. G., 1975. The effect of the number of tube rows on heat transfer performance of smooth plate fin and tube heat exchangers. ASHRAE Trans. 1:307-317.
- Rohani, R. A. and C. C. Tien, 1974. Minimum heat transfer limit in simple and gas loaded heat pipes. AIAA J. 4:530-532.
- Rohsenow, W. M. and J. P. Hartnet, 1973. Handbook of Heat Transfer. McGraw-Hill Book Company, New York, NY.
- Roth, M. G., F. W. Bakker-Arkema, S. F. DeBoer and L. E. Lerew, 1973. Energy conservation in grain dryers: A two-stage recirculating counterflow dryer. Paper No. 73-138. Presented at the 1973 Canadian Society of Chemical Engineering Conference. Vancouver, B.C. Sept. 9-12, 1973.
- Roth, M. G. and S. F. DeBoer, 1973. Optimization of concurrent-counter-dryer with heat exchanger. A Special Report. Agricultural Engineering Department. Michigan State University, East Lansing, MI.
- Ruch, M. A., 1976. Heat pipe exchangers as energy recovery devices. ASHRAE Trans. 82:1008-1014.
- Sheperd, D. G., 1956. Performance of one row tube coils with thin-plate fins, low velocity forced convection. Heating, Piping and Air Conditioning 4:137-144.
- Schmidt, T. E., 1949. Heat transfer calculations for extended surfaces. Refrig. Eng. 4:351-357.
- Segerlind, L. G., 1976. Applied Finite Element Analysis. John Wiley and Sons, Inc., New York, NY.
- Sokhansanj, S., 1974. Heating the Grain by Hot Water, "Part of a Two Stage Recirculating Counterflow Dryer." Unpublished M. S. Thesis. Michigan State University, East Lansing, MI.
- Streltsov, A. I., 1975. Theoretical and experimental investigation of optimum filling for heat pipes. Heat Transfer, Soviet Research 1:23-27.
- Taborek, J., T. Aoki, R. B. Ritter and J. W. Palen, 1972a. Fouling: The major unresolved problem in heat transfer. Chemical Engineering Progress 2:59-67.

- Taborek, J., T. Aoki, R. B. Ritter and J. W. Palen, 1972b. Predictive methods for fouling behavior. *Chemical Engineering Progress* 7:69-78.
- Winters, E. R. F. and W. O. Barsch, 1971. The Heat Pipe. In: *Advances in Heat Transfer*. 7.
- Woodforde, J. and P. J. Lawton, 1965. Drying cereal grain in beds six inches deep. *J. Agric. Eng. Res.* 10:146-171.

APPENDIX A

Appendix A-1. A list of the heat pipe exchanger analysis programs.

```

PROGRAM ANALYS(INPUT,OUTPUT,TAPES ,TAPE60=INPUT,TAPE61=OUTPUT)
      ANALYSIS OF THE PERFORMANCE OF A HEAT PIPE EXCHANGER
      SUBROUTINES:
      CALC, PROCESS, FINITEL, FINITED, KAYS, AASMBLY, BOY
      DCOMPBD, SOLVBD, REPORT, REPORTP, REPORTC

COMMON/PRIME/EFF,NTU1,Q,WE,WEH,HEC,OPC,OPH,REC,REH,ETAC,ETAH,R,QC,
*QH,VSC,VSH,GH,GC,VH,VC,UOV,UOVC,UOVH,RH,RMCT,RMHT,QSC,QSH,EFC,EFH,
*NTUC,NTUH
COMMON/DIMEN/ACC,ACH,SP,HT,D,V,AREAC,AREAH,AREA,AF,Z1,Z2,Z3,Z4
COMMON/ECONCHY/AUC,FUC,EUC,PI,FI,EI,XNY
COMMON/PPRTY/SA,CA,CP,CV,CW,RHOP,HFG
COMMON/PRT/IC(CUNT,SB,FB,SC,ITPMAX,HA,CO1,IFLOW,COEF
COMMON/PRTY/XKP,XKF,RFO,PI
COMMON/INLET/TINC,TINH,HINC,HINH,WC,WH
COMMON/OUTLET/TOC,TOH,HOC,HOH,CONOS
COMMON/PRESS/PATH
DIMENSION X(1,14)
DATA SA,CA,CP,CV,CW,RHOP,HFG/241.,.24.,.26.,.46,1.,.42.,1088./
DATA XKP,XKF,PI/123.,120.,3.1416/
DATA RI,EI,XNY,HR,FUC,EUC/.12.,.05,5.,750.,3.5.,.035/
PATH=14.7

      READ THE INDEPENDENT VARIABLES OF THE HEAT EXCHANGER TO BE
      ANALYZED *FIN DIAMETER, PIPE DIAMETER, FIN THICKNESS, FIN
      PITCH,
      PIPE LENGTH IN COLD SIDE, NUMBER OF ROWS, NUMBER OF PIPES IN
      A ROW(MAX), LONGITUDINAL PITCH, TRANSVERSE PITCH, PIPE LENGTH
      IN HOT SIDE.....ALL IN FEET

      READ 101,(X(1,J),J=1,10)

      INPUT INLET AIR TEMP F HOT SIDE TINH, COLD SIDE TINC,
      ABSOLUTE HUMIDITY LB/LB HOT SIDE HINH, COLD SIDE HINC

      READ 101,TINH,TINC,HINH,HINC
      PRINT 102,TINH,TINC,HINH,HINC
      FORMAT(5(XE12.6))
      FORMAT(8F10.0)

      AIR FLOWS IN LB/HR, HOT SIDE WH, COLD SIDE WC

      READ 101,WH,WC
      PRINT 101,WH,WC
      CALL CALC(1,14,1,X,1)
      CALL PROCESS(1,14,1,X,1)
      END

```



```

REAL NTU,NTUC,NTUM
XL=X(I,5)+X(I,10)
W1=WC*(CA+CV*FINC)
W2=WH*(CA+CV*MINH)
CMAX=A*AX1(W1,W2)
CMIN=AMIN1(W1,W2)
R=CMIN/CMAX
DO 25 JJ=1,7
25 MF(JJ)=MINH
MPCHK=0.
ITFR=0
C EQUIVALENT FIN RADIUS
HX=X(I,1)-X(I,2)
C
C MASS VELOCITY
GH=WH/ACH
GC=WC/ACC
C MAXIMUM SURFACE VELOCITY
T=(TINC+TINH)/2.
RHOA=1./VSDBA(T+460.,MINH)
VH=GH/RHOA/3600.
VC=GC/RHOA/3600.
C APPROACHING SURFACE VEL FT/MIN
VSC=WC/RHOA/(X(I,5)+X(I,11))/60.
VSH=WH/RHOA/(X(I,10)+X(I,11))/60.
C
C AIR FLOW CFM
QC=WC/RHOA/60.
QH=WH/RHOA/60.
C
C HEAT TRANSFER COEFFICIENT
S1=SP/HX*S2=SP/X(I,3)
R1H=2.*X(I,2)*GH/.0459
R1C=2.*X(I,2)*GC/.0459
HH=.00188/2./X(I,2)*R1H*.681*S1*.2*S2*.113
HC=.00188/2./X(I,2)*R1C*.681*S1*.2*S2*.113
HH=HH*CC1
HC=HC*CC1
C SINGLE FIN EFFICIENCY
BC=SQRT((2.*HC)/XKF/X(I,3))
BH=SQRT((2.*HH)/XKF/X(I,3))
PHIC=TANH(BC*HX)/(BC*HX)
PHIH=TANH(BH*HX)/(BH*HX)
C
C FINNED TUBE BANK EFFICIENCY
ETAC=1.-Z3*(1.-PHIC)
ETAH=1.-Z3*(1.-PHIH)
C FINNED PIPE METAL RESISTANCE
PMHT=(1.-ETAH)/ETAH/WH
PMCT=(1.-ETAC)/ETAC/HC
RM=PMCT+PMHT
C OVERALL U*A
C ON THE COLO SIDE
UOVC=1./(1./HC/ETAC+PMCT)
UOVH=1./(1./H/ETAH+PMHT)
H=(UOVC/UOVH)
UOV=1./(1./UOVH+1./UOVC)
C
C THERE ARE THREE CHOICES TO CALCULATE THE OUTLET TEMP
C EITHER TO USE FINITE ELEMENT TECHNIQUE
C CALL FINTEL(M,N,X)
C OR USE FINITE DIFFERENCE
C CALL FINTED(M,N,X)
C OR TO USE KAYS AND LONDON OVERALL ANALYSIS METHOD(NTU)
C CALL KAYS(M,N,X)
C
C QSH=W2*(TINH-TOH)+WH*CONDS*HFG
C QSC=W1*(TOC-TINC)
C QMAX=CMIN*(TINH-TINC)
C EFC=QSC/QMAX
C EFH=QSH/QMAX
21 PPRINT 21,QSC,QSH,EFC,EFH,CONDS
FORMAT(*,QSC=*E12.6*,QSH=*E12.6*,EFC=*E12.6*,
*EFH=*E12.6*,CONDS=*E12.6*)
RETURN
END

```

```

SUBROUTINE FINITEL(M,N,X)
      GENERATION OF THE ELEMENTS, APPLICATION OF THE BOUNDARY
      CONDITIONS, CALCULATION OF THE CONSTANTS OF THE STIFFNESS
      MATRIX
      COMMON/PRIME/EFF,NTU,Q,WE,WEH,WEC,DPC,DPH,REC,REH,ETAC,ETAH,R,QC,
      *QH,VSC,VSH,GH,GC,VH,VC,UOV,UCVC,UOVH,RH,RMCT,RMHT,QSC,QSH,EFC,EFH
      *NTUC,NTUH
      COMMON/PRT/ICCOUNT,SR,RH,SC,ITMAXP,HA,CC1,IFLOW,COEF
      COMMON/INLET/TINC,TINH,HINC,HINH,WC,WH
      COMMON/OUTLET/TOC,TOH,HOC,HOH,CONDS
      COMMON/PRTY/XKP,XKF,PI
      DIMENSION B(100),PHC(100),HUM(100),BV(6),IBN(6),IBF(6),NE
      * (12),X(N,M),D(100),NEB(12)
      DIMENSION NS(4),ESM(4,4),EF(4),PHI(4),A(2000)
      DATA IN/60/,IC/61/,NCL/1/,IO1/0/,NNPE/4/,NOOF/1/,KL/4/
      DATA CC1,IFLOW/1.,0/
      HA=HINH
      ICCOUNT=0
      NN=0
      NP=X(1,6)
      NP=13*NP+6
      NF=6*NP
      NRH=2*NR+2
      IC=6
      JGF=NP+NP*NCL
      JGSM=JGF+NP*NCL
      JEND=JGSM+NF*NBW
      JL=JEND-JGF
      DO 13 I=1,JEND
      A(I)=0.0
      ASSIGNING THE BOUNDARY VALUES:CCOUNTERFLOW..IFLOW=0,
      CONCURRENT FLOW..IFLOW=1
      IF(IFLOW.EQ.0) GO TO 10
      DO 11 I=1,3
      IBN(I)=(2*I-1)*NR+I
      BV(I)=TINH
      YBF(I)=2*I*NR+I
      DO 12 I=4,6
      IBN(I)=2*I*NR+I
      BV(I)=TINC
      IBF(I)=(2*I-1)*NR+I
      GO TO 14
      10 CONTINUE
      DO 4 I=1,6
      IBN(I)=(2*I-1)*NR+I
      BV(I)=TINH
      IF(I.GE.4) BV(I)=TINC
      CONTINUE
      DO 5 I=1,6
      IBF(I)=2*I*NR+I
      CONTINUE
      14 CONTINUE
      DO 6 I=1,6
      NEB(I)=(I-1)*NR+1
      DO 9 I=7,12
      NEB(I)=(I-6)*NR
      C1=1./ (RMHT)
      PRM=2.*Y(1,2)*PI
      INITIALIZING THE STIFFNESS MATRIX
      C*****
      DO 26 I=1,4
      DO 26 J=1,4
      26 ESM(I,J)=0.
      INITIALIZATION OF VECTOR B FOR USE IN SUBROUTINE CONDENS
      DO 27 I=1,100
      27 B(I)=0.
      KK=0
      DO 7 J=1,6
      C1=1./ (RMHT)
      NS(1)=(J-1)*(2*NR+1)
      IF(J-4)1,2,2
      C2=PRM*UOVH/(6.*12.)
      GO TO 3

```

```

2   C2=PRM*UOVC/(6.*12.)
3   C1=1./ (RMCT)
CONTINUE
DO 7 I=1, NR
  KK=KK+1
  NS(1)=NS(1)+1
  NS(2)=NS(1)+NR
  NS(3)=NS(2)+NR+1
  NS(4)=NS(2)+1
  DN=C2
  FSH(1,1)=FSH(3,3)=C1+4.*P2
  FSH(2,2)=FSH(4,4)=6.*P2
  FSH(1,2)=FSH(2,1)=-3.*P2
  FSH(1,3)=FSH(3,1)=-C1+2.*P2
  FSH(1,4)=FSH(4,1)=-3.*P2
  FSH(2,3)=FSH(3,2)=-3.*P2
  FSH(3,4)=FSH(4,3)=-3.*P2
DO 3000 KLMN=1,4
C 3000 EF(KLMN)=0.
C INSERTION OF ELEMENT PROPERTIES INTO THE GLOBAL STIFFNESS MATRIX
C
7 CALL ASMBLY(ESH,EF,A(JGF+1),NS,JL,KL,NCL,NP)
8 CONTINUE
CALL BNY (A(JGSM+1),A(JGF+1),NP,NBW,NCL,IC,IBN,BV)
CALL DCMPBD(A(JGSM+1),NP,NBW)
CALL SLVBD(A(JGSM+1),A(JGF+1),A(NP+1),NP,NBW,NCL,IO1,NE,RMC
  ,NN,HUM,NP,NEB,IRF,IBN,IC)
IF(NN.EQ.3) RETURN
IF(NN.EQ.2) RETURN
CALL CONDENS(ESH,A(NP+1),A( 1 ),NP,JL,KL,NCL,NE,JEND,JGF,NEB,NP
  ,NB,B,RHC,CONDS,HUM,NR,NN,PRM)
IF(NN.EQ.2) RETURN
GO TO 8
C*****
END

```

```

C SURROUTINE BDI(GSM,GF,NP,NBW,NCL,IC,IBN,BV)
C DIMENSION GSM(NP,NBW),GF(NP,NCL),IBN(6),BV(6)
C
C MODIFICATION OF THE GLOBAL STIFFNESS MATRIX AND THE
C GLOBAL FORCE MATRIX USING THE METHOD OF DELETION
C OF ROWS AND COLOUMNS

```

```

DO 1 IK=1,IC
  I=IBN(IK)
  BC=BV(IK)
  K=I-1
  DO 211 J=2,NBW
    M=I+J-1
    IF(M.GT.NP) GOTO 210
    DO 218 JM=1,NCL
      218 GF(M,JM)=GF(M,JM)-GSM(I,J)*BC
      GSM(I,J)=0.0
    210 IF(K.LE.0) GOTO 211
    DO 219 JM=1,NCL
      219 GF(K,JM)=GF(K,JM)-GSM(K,J)*BC
      GSM(K,J)=0.0
    K=K-1
  211 CONTINUE
  212 IF(GSM(I,1).LT.0.05) GSM(I,1)=500000.
  DO 220 JM=1,NCL
    220 GF(I,JM)=GSM(I,1)*BC
  221 CONTINUE
  1 CONTINUE
  RETURN
END

```

```

C SURROUTINE CONDENS(ESH,D,A,NP,JL,KL,NCL,NE,JEND,JGF,NFB,NPH,NB,9,
C 1RHC,CONDS,HUM,NR,NN,PRM)

```

```

C CALCULATION OF THE CONDENSATION FROM THE PSYCHROMETRIC
C CHART AND RECONSTRUCTION OF THE STIFFNESS MATRIX

```

```

COMMON/PRIME/EFF,NTU,Q,WE,WEH,WEV,OPC,OPH,REC,REH,ETAC,ETAH,R,OC,
+OH,VSC,VSH,GH,GC,VH,VC,UOV,UOVC,UCVH,CM,PMCT,FMHT,QSC,QSH,EFC,EFH
+NTIC,NTUH
COMMON/PRT/ICCONT,SB,RH,SC,ITHXP,HA,CC1,IFLOW,COEF

```



```

COMMON/PRESS/PATH
COMMON/PORT/XP,KF,PI
COMMON/INLET/TINC,TINH,HINC,HTNH,WC,WH
COMMON /PPRTY/SA,CA,CP,CV,CW,RHOP,HFG
DIMENSION ESM(KL,KL),A(JEND),NS(4),EF(4),NPC(60),D(NP),NEB(12),B(
1NP),RHC(NE),HUM(NE),SLP(12)
HA=HINH
ICOUNT=ICOUNT+1
IF(ICOUNT,GE,ITMAXP) CALL REPORT(NN)
IF(INN,FO,2) RETURN
25 DO 25 I=1,NP
   R(I)=A(I,MP)
   DO 6 I=1,4
     6 EF(I)=0.
     DO 8 I=1,JEND
       8 A(I)=0.
       DO 26 I=1,4
         DO 26 J=1,4
           26 ESM(I,J)=0.
C
   KK=0
   DO 7 J=1,6
     NS(1)=(J-1)*(2*NR+1)
     SUMH=0.
     DO 7 I=1,NR
       KK=KK+1
       NS(1)=NS(1)+1
       NS(2)=NS(1)+NR
       NS(3)=NS(2)+NR+1
       NS(4)=NS(3)+1
       I1=NS(1)
       I2=NS(2)
       I3=NS(3)
       I4=NS(4)
       TF(J)=10,17,11
       10 C2=PRH*UOVH/(6.*I2.)
       C1=1./RMHT
       GO TO 16
       17 C2=PRH*UOVC/(6.*I2.)
       TF=I2*(2*NR+1)
       T1=(B(I5)+B(I5+1))/2.
       T2=(B(I6)+B(I6+1))/2.
       TAA=(B(I1)+B(I3))/2.+460.
       DT=T4-T2
       IF(DT.LE.0.) DT=1.
C
C     RESISTANCE OF THE HEAT PIPE AGAINST THE HEAT FLOW
C
RTOTAL=RH+CC1*DT**.25/TAA
C1=1./RTOTAL
GO TO 16
11 C2=PRH*UOVC/(6.*I2.)
C1=1./RMCT
1E CONTINUE
IF(J,GE,4) GO TO 5
BAVG=(B(I1)+B(I3))/2.
IF(KK,EO,NER(J)) HA=HINH
RH=RHOBHA(BAV+460.,HA)
RHC(KK)=RH
IF(RH,GE,1.) RHC(KK)=1.
HAI=HADP(9A WG+460.)
HUM(KK)=HAI
HUMD=HA-HAI
IF(HUMD) 13,12,12
13 HUMD=0.
HUM(KK)=HA
GO TO 14
12 HA=HAI
C
C     SLOPE OF THE CONDENSATION S
C
14 SL=HUMD/(B(I2)-BAVG)
XI=I
SUMH=SUMH+SL
SLP(I)=SL
C3=1.+HFG*SLP(I)/CA
P2=C2*C3
GO TO 15
5 CONTINUE
P2=C2
15 CONTINUE
ESH(1,1)=ESH(3,3)=C1+6.*P2
ESH(2,2)=ESH(4,4)=6.*P2
ESH(1,2)=ESH(3,1)=-1.*P2
ESH(1,3)=ESH(3,1)=-C1+2.*P2

```

```

ESH(1,4)=ESH(4,1)=-3.*P2
ESH(2,3)=ESH(3,2)=-3.*P2
ESH(3,4)=ESH(4,3)=-3.*P2
7 CALL ASMBLY(ESH,EF,A(JGF+1),NS,JL,KL,NCL,MP)
CONTINUE
RETURN
END

```

```

SUBROUTINE REPORT(NN)
COMMON/PPT/ICOUNT,SB,RH,SC,ITMAXP,HA,CC1,IFLOW,COEF
COMMON/OUTLET/TOC,TOH,HOC,HOM,CONDS
IF(ICOUNT.EQ.ITMAXP)GO TO 1
GO TO 3
1 PRINT 2,ICOUNT
2 FORMAT(' THE ITERATIONS ON THE EXCHANGER STOPPED AFTER *I2* TRI
+S*/)
NN=2
RETURN
3 IF(ABS(SB-CONDS).GT.0.001) GO TO 5
XB=ABS(SB-CONDS)
PPTNT 4,XB
4 FORMAT(' ITERATION ON THE EXCHANGER STOPPED HR DIFFERENCE = *F6.
+ */)
NN=2
RETURN
5 IF(PH.GT.1.) GO TO 7
PRINT 6,SC,RH
6 FORMAT(' NO CONDENSATION AT MIN TEMP IN THE EXCHANGER *F6.2*
+AX RH *F6.4)
NN=2
RETURN
7 CONTINUE
RETURN
END

```

```

SUBROUTINE SLVBD(GSM,GF,X,NP,NBW,NCL,ID,NE,RHC,NN,HUM,NR,NEB
+,IBF,IBN,IC)
CCCC
SOLUTION TO THE GLOBAL MATRIX USING THE GAUSSIAN ELIMINATION
AND BACKWARD SUBSTITUTION, AND OUTPUT THE RESULTING
TEMPERATURES
COMMON/PRT/ICOUNT,SB,RH,SC,ITMAXP,HA,CC1,IFLOW,COEF
COMMON/PRES/PATM
COMMON/INLET/TINC,TINH,HINC,HINH,WC,WH
COMMON/OUTLET/TOC,TOH,HOC,HOM,CONDS
DIMENSION GSM(NF,NBW),GF(NP,NCL),X(NP,NCL),RHC(NE),HUM(NE)
DIMENSION NEB(12),IBF(IC),IBN(IC)
IO=61
NP1=NP-1
DO265KK=1,NCL
JM=KK
CCCC
DECOMPOSITION OF THE COLUMN VECTOR GF( )
DO250I=1,NP1
MJ=I+NBW-1
IF(MJ.GT.NP) MJ=NP
NJ=I+1
L=1
DO250J=NJ,MJ
L=L+1
250 GF(J,KK)=GF(J,KK)-GSM(I,L)*GF(I,KK)/GSM(I,L)
CCCC
BACKWARD SUBSTITUTION FOR DETERMINATION OF X( )
X(NP,KK)=GF(NP,KK)/GSM(NP,1)
DO252K=1,NP1
I=NP-K
MJ=NBW
IF((I+NBW-1).GT.NP) MJ=NP-I+1
SUM=0.0
DO251J=2,MJ
N=I+J-1

```

```

251 SUM=SUM+GSM(I,J)*X(N, KK)
252 X(I, KK)=(GF(I, KK)-SUM)/GSM(I, 1)
C
C OUTPUT OF THE CALCULATED NODAL VALUES
C
265 CONTINUE
   KK=NCL
C   PPTNT 301, ICOUNT
301  FORMAT(1H1,5X, * ITERATION NUMBER * I2 * ON THE EXCHANGER*/)

C   WRITE(IO, 259)
259  FORMAT(1X70(1H*))
     M1=1
     L1=1
     DO 10 J=1,3
     MM1=M1+NR-1
     LL1=L1+NR-1
     IF(NN, EQ, 1) GO TO 2
     DO 1 I=L1, LL1
     HUM(I)=HA
     PHC(I)=PHDBHA(X(I, KK)+460., HA)
     IF(RHC(I).GT.1.) GO TO 5
     GO TO 6
5    PHD=RHC(I)
     PHC(I)=1.
     GO TO 1
6    RHD=0.
     CONTINUE
     CONTINUE
C   WRITE(IO, 261) (X(I, KK), I=M1, MM1)
C   WRITE(IO, 262) (RHC(I), I=L1, LL1)
     M1=MM1+1
     NN1=N1+NR
C   WRITE(IO, 263) (X(I, KK), I=N1, NN1)
C   WRITE(IO, 267) (HUM(I), I=L1, LL1)
     L1=LL1+1
     M1=NN1+1
10  CONTINUE
     MM1=M1+NR-1
C   WRITE(IO, 261) (X(I, KK), I=M1, MM1)
C   WRITE(IO, 260)
     DO 11 J=1,3
     N1=MM1+1
     NN1=N1+NR
C   WRITE(IO, 266) (X(I, KK), I=N1, NN1)
     M1=NN1+1
     MM1=M1+NR-1
C   WRITE(IO, 261) (X(I, KK), I=M1, MM1)
C   11 CONTINUE
C   WRITE(IO, 259)
261  FORMAT(4X5(5XF5.1) / )
262  FORMAT(4X5(5XF5.3))
263  FORMAT( 7(5XF5.1))
267  FORMAT(4X6(5XF5.3) / )
266  FORMAT( 7(5XF5.1) / )
260  FORMAT(X7)(1H-)/)
     I1=IBF(1)*I2=IBF(2)*I3=IBF(3)*I4=IBF(4)*I5=IBF(5)*I6=IBF(6)
     TOH=(X(I1,1)+X(I2,1)+X(I3,1))/3.
     TOC=(X(I4,1)+X(I5,1)+X(I6,1))/3.
     HOC=HINC
     I1=NEB(7)
     I2=NEB(8)
     I3=NEB(9)
     HOM=(HUM(I1)+HUM(I2)+HUM(I3))/3.
     CONDS=HINH-HOM
     IF(NN, EQ, 0) GO TO 15
     IF(ABS(SB-CONDS).LE.0.001) CALL REPORT(NN)
     IF(NN, EQ, 2) RETURN
     SB=CONDS
C   WRITE(IO, 270) CONDS
270  FORMAT(/5X, 18HTOTAL CONDENSATION
1    10XF10.4, 5X14HLB H2O/LB AIR //)
15  CONTINUE
     IF(PHD.GT.1.) NN=1
     RETURN
     END

```

```

SUBROUTINE ASMBLY(ESH,EF,A,NS,JL,KL,NCL,NP)
  ASSEMBLY OF THE GLOBAL MATRIX
  DIMENSION ESH(KL,KL),EF(KL),A(JL),NS(KL)
  JGSM=NP*NCL
  DO 1 I=1,KL
  DO 2 J=1,NCL
  J1=(J-1)*NP+NS(I)
  1 A(J1)=A(J1)+EF(I)
  DO 3 J=1,KL
  JJ=NS(J)-NS(I)+1
  IF(JJ)3,3,2
  2 J1=JGSM+(JJ-1)*NP+NS(I)
  A(J1)=A(J1)+ESH(I,J)
  3 CONTINUE
  4 CONTINUE
  RETURN
  END

```

```

SUBROUTINE DCMPBD(GSM,NP,NBW)
  DECOMPOSITION OF THE GLOBAL MATRIX TO A BAND MATRIX
  DIMENSION GSM(NP,NBW)
  IO=61
  NP1=NP-1
  DO 226 I=1,NP1
  MJ=I+NRW-1
  IF(MJ,GT,NP) PJ=NP
  NJ=I+1
  MK=NBW
  IF((NP-I+1).LT,NBW) MK=NP-I+1
  ND=0
  DO 225 J=NJ,MJ
  HK=MK-1
  ND=ND+1
  NL=ND+1
  DO 225 K=1,MK
  225 GSM(J,K)=GSM(J,K)-GSM(I,NL)*GSM(I,NK)/GSM(I,1)
  226 CONTINUE
  RETURN
  END

```

```

SUBROUTINE FINITED(M,N,X)
  USING FINITE DIFFERENCE TO SOLVE FOR TEMPERATURES
  IN THE HEAT EXCHANGER. THIS SUBROUTINE REQUIRES CALLING
  SIMO FROM THE HAL .
  COMMON/PRIME/EFF,NTU,η,WE,WEH,HEG,DPC,DPH,REC,REH,ETAC,ETAH,R,GC,
  +QH,VSC,VSH,GH,GC,VH,VC,UOV,UOVC,UOVH,RH,RHOT,PMHT,QSC,QSH,EFC,EFH,
  +NTUIC,NTUH
  COMMON/ECONCMI /AUC,FUC,EUC,RI,FI,EI,XNY
  COMMON/DIMEN/ACC,ACH,SP,HT,D,V,AREAC,AREAH,AREA,AF,Z1,Z2,Z3,Z4
  COMMON/PROPPY/SA,CA,CP,CV,CH,RHOP,HFG
  COMMON/PRT/ICOUNT,SB,PH,SC,ITPMAX,HA,CC1,IFLOW,COEF
  COMMON/INLET/TINC,TINH,HINC,HINH,WC,WH
  COMMON/OUTLET/TOC,TOH,HOC,HOH,CONOS
  COMMON/PRTY/XKF,XKF,φFO,PI
  DIMENSION X(K,M),RA(12),A(12,12),TH(7),TC(7),HR(7),TP(6)
  W1=WC*(CA+CV*HINC)
  W2=WH*(CA+CV*HINH)
  CON1=1./W2-1./W1
  PFLA=AREA/12.
  B=UOV*CON1*CELA/2.
  COND=W1/W2
  IF(COND.LT.1.) B=-B
  DO 10 II=1,12
  DO 11 JJ=1,12
  11 A(JJ,II)=0.
  RA(II)=0.
  DO 15 J=1,6
  JJ=2+J-1
  IF(JJ.NE.1) A(JJ,JJ-1)=1+B
  IF(JJ.NE.11) A(JJ,JJ+2)=1-B
  A(JJ,JJ)=-1-B
  A(JJ,JJ+1)=-1+B
  KK=2+J
  IF(KK.NE.2) A(KK,KK-2)=1.
  IF(KK.NE.12) A(KK,KK+1)=COND
  10
  15

```

```

15  A(KK, KK)=-1. $A(KK, KK-1)=-COND
    CONTINUE
    BA(1)=- (1+B) *TINH
    BA(2)=-TINH
    BA(11)=- (1-B) *TINC
    BA(12)=-COND*TINC
    CALL SIMQ(A, BA, 12, KS)
    TH(1)=TINH$TC(7)=TINC
24  CONTINUE
    ITER=ITER+1
    JJ=1
    DO 12 II=2, 12, 2
    JJ=JJ+1
    TH(JJ)=BA(II)
12  CONTINUE
    JJ=0
    DO 13 II=1, 11, 2
    JJ=JJ+1
    TC(JJ)=BA(II)
13  CONTINUE
    DO 18 II=1, 12
    DO 19 JJ=1, 12
19  A(II, JJ)=0.
18  BA(II)=0.
    DO 17 J=1, 6
    THA=(TH(J)+TH(J+1))/2.
    TCA=(TC(J)+TC(J+1))/2.
    TP(J)=(THA+H*TCA)/(H+1)
17  CONTINUE
    PRINT 20, (TH(JJ), JJ=1, 7)
    PRINT 20, (HR(JJ), JJ=1, 7)
    PRINT 20, (TP(JJ), JJ=1, 6)
    PRINT 20, (TC(JJ), JJ=1, 7)
20  FOPMAT(2X7 (X=19, 4))
    IF(HINH.LE.HADP(TINC+460.)) GO TO 26
    IF(ITER.GT.5) GO TO 26
    DO 14 J=1, 6
    HAP=HADP(TP(J)+460.)
    IF(HAP.GE.HR(J)) HAP=HR(J)
    S=(HR(J)-HAP)/(TH(J)-TP(J))
    IF(S.LE.0.) S=0.
    HF(J+1)=HR(J)-S*(TH(J)-TH(J+1))
    HRA=(HR(J+1)+HR(J))/2.
    W2=WH*(CA+CV*HRA)
    W2N=W2+WH*S*HFG
    CON1=1./W2N-1./W1
    COND=W1/W2N
    COF=.919*(14.7-PVHA(HRA))/(14.7-PSDB(TP(J)+460.))
    IF(HRA.LE.0.04) COF=1.
    HM=UOVH/(COF*(CA+CV*HRA))
    UOVHN=UOVH+HM*S*HFG
    H=UOVC/UOVHN
    UOV=1./(1./UOVHN+1./UOVC)
    R=UOV*CON1*DELA/2.
    IF(COND.LT.1.) B=-B
    JJ=2+J-1
    IF(JJ.EQ.1.OR.JJ.EQ.11) BA(JJ)=B
    IF(JJ.NE.1) A(JJ, JJ-1)=1+B
    IF(JJ.NE.11) A(JJ, JJ+2)=1-B
    A(JJ, JJ)=-1-B
    A(JJ, JJ+1)=-1+B
    KK=2+J
    IF(KK.NE.2) A(KK, KK-2)=1.
    IF(KK.NE.12) A(KK, KK+1)=COND
    A(KK, KK)=-1. $A(KK, KK-1)=-COND
14  CONTINUE
    BA(1)=- (1+BA(1)) *TINH
    BA(2)=-TINH
    RA(11)=- (1-BA(11)) *TINC
    BA(12)=-COND*TINC
    CALL SIMQ(A, BA, 12, KS)
    IF(ABS(HR(7)-HRCHK).LE.1.E-4) GO TO 26
    HRCHK=HR(7)
    HR(1)=HINH
    GO TO 24
26  CONTINUE
    CONDS=HINH-HR(7)
    HOH=HP(7)
C
    TOH=TH(7)
    TOC=TC(1)
    RETURN
    END

```

SURROUTINE KAYS (N,M,X)

THE SUBROUTINE USES THE OVERALL EFFECTIVENESS METHOD GIVEN
BY KAYS AND LONDON (1964)

C
C
C
C

```

COMMON/PRIME/EFF,NTU,Q,WE,WEH,WEC,DPC,DPH,REC,REH,ETAC,ETAH,R,QC,
+QH,VSC,VSH,GH,GC,VH,VC,UOV,UOVC,UOVH,RM,RMCT,RMHT,OSC,QSH,EFC,EFH,
+NTIC,NTUH
COMMON/DIMFN/ACC,ACH,SP,HT,D,V,AREAC,AREAH,AREA,AF,Z1,Z2,Z3,Z4,Z5
COMMON /PPRTY/SA,CA,CP,CV,CW,RHOP,HFG
COMMON/PRT/ICCNT,SB,PH,SC,ITFMAX,HA,CO1,IFLOW,COEF
COMMON/INLET/TINC,TINH,HINC,HINH,WC,WH
COMMON/OUTLET/TOC,TOH,HOC,HOH,CONDS
COMMON/PRTY/XKP,XKF,PI
COMMON/ENTHALF/FNHO
DIMENSION X(K,M),A(10,10),B(10),F1(12)
W1=WC*(CA+CV*HINC)
W2=WH*(CA+CV*HINH)
CMAX=AMAX1(W1,W2)
CMIN=AMIN1(W1,W2)
P=CMIN/CMAX
C      TOTAL BTU SAVED
QMAX=CMIN*(TINH-TINC)
EXE=EXP((-UOV/CMIN)*(1.-R))
EFF=(1.-EXE)/(1.-R*EXE)
QSC=QSH=QMAX*EFF
TOC=QSC/W1+TINC
TOH=TINH-QSH/W2
HOH=HADP(TOH+460.)
IF(HOH.GT.HINH)HOH=HINH
HANG=(HINH+HOH)/2.
CONDS=HINH-HOH
PRINT 6,TOH,TOC,EFF,CONDS,ETAH
6      FORMAT(2X7F10.3)
RETURN
END

```


SUBROUTINE DETAILD

```

C
C
C      MAIN LINE PROGRAM FOR COMPLEX ALGORITHM OF BOX
COMMON/RESULT/PIE,PANN,PEA,PFA,99
DIMENSION X(14,14),R(14,10),F(14),G(14),H(14),XC(10)
INTEGER GAMMA
DATA (X(I,J),J=1,10)/.06,.03,.03,11...75,6...4...175,.16,.75/
DATA N,M,K,IC,IPRINT/10,14,14,4,0/
DATA ALPHA,GAMMA/1.3,5/

C
NI=60
NO=61
PRINT *,# ITERATION          CONVERGENCE #
READ 1,ITMAX,BETA
FORMAT(13,F7.0)

1
C
DO 100 II=2,K
DO 99 JJ=1,N
R(II, JJ)=RANF(-1)
99 CONTINUE
100 CONTINUE

C
WRITE(NO,010)
010 FORMAT(1H1,/,/,18X,24HCOMPLEX PROCEDURE OF BOX)
WRITE(NO,011)
011 FORMAT(//,2X,10HPARAMETERS )
WRITE(NO,011) N, M, K, ITMAX, IC, ALPHA, BETA, GAMMA
011 FORMAT (//,2X,4HN = ,I2,3X,4HM = ,I2,3X,4HK = ,I2,2),6HITMAX = ,
1I4,2X,5HIC = ,I2,/,2X,6HALPHA = ,F5.2,5X,7HBETA = ,F10.5,3X,
2HGAMMA = ,I2,3X,8HDELTA = ,F6.5)
IF(IPRINT)40,50,40
40 WRITE(NO,012)

012 FORMAT(//,2X,14HRANDOM NUMBERS)
DO 200 J=2,K
WRITE(NO,013) (J, I, R(J,I), I=1,N)
013 FORMAT(//,5(2X,2HR(,I2,1H,,I2,4H) = ,F6.4,2X))
200 CONTINUE

C
50 CALL CONSX (N,M,K,ITMAX,ALPHA,BETA,GAMMA,X,R,F,IT,IEV2,NO,6,
1H,XC,IPRINT)

C
IF(IT-ITMAX) 20,20,30
20 WRITE (NO,014) F(IEV2),IT
014 FORMAT (///,2X,3HFINAL VALUE OF THE FUNCTION = ,E20.8,5X8HAFTER
+ I4,3X10HITERATION )
WRITE (NO,015)
015 FORMAT(//,2X,14HFINAL X VALUES)
DO 300 J=1,N
WRITE (NO,016) J, X(IEV2,J)
016 FORMAT (/,2X,2HX(,I2,4H) = ,E20.8)
300 CONTINUE
I=IEV2
IX2=INT(X(I,6)+.5)
X(I,6)=FLOAT(IX2)
IX3=INT(X(I,7)+.5)
X(I,7)=FLOAT(IX3)
CALL CALC(N,M,K,X,I)
CALL PROCESS(N,M,K,X,I)
CALL REPORTC(N,M,K,X,I,1)
CALL REPORTP
PRINT *,# FC          AFC          AOP          SV          F(I) #
PRINT 2,PIE,PANN,PEA,PFA,99
FORMAT(3XF10.2,4(2XF10.2))
GOTO 999

30 WRITE (NO,017)ITMAX
017 FORMAT (///,2X,3HTHE NUMBER OF ITERATIONS HAS EXCEEDED ,I4,10X,18
/HPROGRAM TERMINATED)
999 STOP
END

```


SUBROUTINE CONSX(N,M,K,ITMAX,ALPHA,BETA,GAMMA,X,R,F,IT,IEV2,
 1NO,G,H,XC,IPRINT)

COORDINATES SPECIAL PURPOSE SUBROUTINES

ARGUMENT LIST

IT = ITERATION INDEX.
 IEV1 = INDEX OF POINT WITH MINIMUM FUNCTION VALUE.
 IEV2 = INDEX OF POINT WITH MAXIMUM FUNCTION VALUE.
 I = POINT INDEX.
 KODE = CONTROL KEY USED TO DETERMINE IF IMPLICIT CONSTRAINTS
 ARE PROVIDED.
 K1 = DO LOOP LIMIT

ALL OTHER PREVIOUSLY DEFINED IN MAIN LINE.

DIMENSION X(K,M), R(K,M), F(K), G(M), H(M), XC(N)
 INTEGER GAMMA

IT=1
 KODE=0
 IF(M-N) 20,20,10
 10 KODE=1
 20 CONTINUE
 DO 40 II=2,K
 DO 30 J=1,N
 30 X(II,J)=0.0
 40 CONTINUE

CALCULATE COMPLEX POINTS AND CHECK AGAINST CONSTRAINTS

DO 65 II=2,K
 DO 50 J=1,N
 I=II
 CALL CONST(N,M,K,X,G,H,I,1)
 X(II,J)=G(J) + R(II,J)*H(J) -G(J)
 50 CONTINUE
 K1=II
 CALL CHECK(N,M,K,X,G,H,I,KODE,XC,K1)
 IF(II-2) 51,51,55
 51 IF(IPRINT) 52,65,52
 52 WRITE(NO,01A)
 010 FORMAT(/,2X,30HCOORDINATES OF INTIAL COMPLEX)
 IO=1
 WRITE(NO,019) (IO,J, X(IO,J),J=1,N)
 019 FORMAT(/,5(2X,2HX(,I2,1H,,I2,4H) = ,1PE13.6))
 55 IF(IPRINT) 56,65,56
 56 WRITE(NO,019) (II,J,X(II,J),J=1,N)
 65 CONTINUE
 K1=K
 DO 70 I=1,K
 CALL FUN(N,M,K,X,F,I)
 70 CONTINUE
 KOUNT = 1
 IA=0

FIND POINT WITH LOWEST FUNCTION VALUE

IF(IPRINT) 72,80,72
 72 WRITE(NO,021)
 021 FORMAT(/,2X,22HVALUES OF THE FUNCTION)
 WRITE(NO,022) (J, F(J), J=1,K)
 022 FORMAT(/,5(2X,2HF(,I2,4H) = ,1PE13.6))
 80 IEV1 = 1
 DO 100 ICM=2,K
 IF (F(IEV1)-F(ICM)) 100,100,90
 90 IEV1 = ICM
 100 CONTINUE

FIND PCINST WITH HIGHEST FUNCTION VALUE

IEV2=1
 DO 120 ICM=2,K
 IF (F(IEV2)-F(ICM)) 110,110,120
 110 IEV2 = ICM
 120 CONTINUE

CHECK CONVERGENCE CRITERIA

IF (F(IEV2)-(F(IEV1)+BETA)) 140,130,130
 130 KOUNT=1
 GO TO 150
 140 KOUNT=KOUNT+1
 IF (KOUNT-GAMMA) 150,240,240

```

CC      REPLACE POINT WITH LOWEST FUNCTION VALUE
150 CALL CENTR (N,M,K,IEV1,I,XC,X,K1)
    OO 160 JJ=1,N
160 X(IEV1,JJ)=(1.0+ALPHA)*(XC(JJ))-ALPHA*FX(IEV1,JJ)
    I = IEV1
    CALL CHECK (N,M,K,X,G,H,I,KODE,XC,K1)
    CALL FUN (N,M,K,X,F,I)
CGC     REPLACE NEW POINT IF IT REPEATS AS LOWEST FUNCTION VALUE
170 IEV2=1
    DO 190 ICM=2,K
    IF(F(IEV2)-F(ICM))190,190,180
180 IEV2 = ICM
190 CONTINUE
    IF(IEV2-IEV1)220,200,220
200 DO 210 JJ=1,N
    X(IEV1,JJ)=(X(IEV1,JJ)+X(JJ))/2.0
210 CONTINUE
    I=IEV1
    CALL CHECK (N,M,K,X,G,H,I,KODE,XC,K1)
    CALL FUN (N,M,K,X,F,I)
    GO TO 170
220 CONTINUE
    IF (IPPRINT) 230,220,230
230 WRITE (NO,023) I
023 FORMAT (//,2X,17HITERATION NUMBER ,I5)
    WRITE (NO,024)
024 FORMAT (/ ,2X,30HCOORDINATES OF CORRECTED POINT)
    WRITE (NO,021) (IEV1, JC, X(IEV1,JC), JC=1,N)
    WRITE (NO,022) (I, F(I), I=1,K)
    WRITE (NO,025)
025 FORMAT (/ ,2X,27HCOORDINATES OF THE CENTROID)
    WRITE (NO,026) (JC, XC(JC), JC=1,N)
026 FORMAT (/ ,3(2X,2HX( ,I2,6H,C) = ,1PE14.6,4X))
220 IT=IT+1
    IF(IT-ITMAX)80,80,240
240 RETURN
    END

```

```

C      SUBROUTINE CENTR (N,M,K,IEV1,I,XC,X,K1)
C      DIMENSION X(K,M), XC(N)
C      DO 20 J=1,N
C      XC(J)=0.0
C      DO 10 IL=1,K1
10     XC(J)=XC(J) + X(IL,J)
C      RK= K1
20     XC(J) = (XC(J)-X(IEV1,J))/(RK-1.0)
C      RETURN
C      END
C      SUBROUTINE CHECK (N,M,K,X,G,H,I,KCODE,X0,K1)
C      ARGUMENT LIST
C      ALL ARGUMENTS DEFINED IN MAIN LINE AND CONSX
C      DIMENSION X(K,M), G(M), H(M), XC(N)
10     KT=0
C      CALL CONST (N,M,K,X,G,H,I,1)
C      CHECK AGAINST EXPLICIT CONSTRAINTS
C      DO 50 J=1,N
C      IF (X(I,J)-G(J)) 20, 20, 30
20     X(I,J)=G(J)+DELTA(J)
C      GO TO 50
30     IF (H(J) -X(I,J)) 40, 40, 50
40     X(I,J)=H(J) -DELTA(J)
50     CONTINUE
C      IF(KODE) 110, 110, 60
C      CHECK AGAINST THE IMPLICIT CONSTRAINTS
60     NN=N + 1
C      DO 100 J=NN,M
C      CALL CONST (N,M,K,X,G,H,I,2)
C      IF(X(I,J)-G(J)) 80, 70, 70
70     IF (H(J) -X(I,J)) 80, 100, 100
80     IEV1 = I
C      KT=1
C      CALL CENTR (N,M,K,IEV1,I,XC,X,K1)
C      DO 90 JJ=1,N
C      X(I, JJ)=(X(I, JJ)+ XC(JJ))/2.0
90     CONTINUE
100    CONTINUE
C      IF(KT) 110, 110, 10
110   RETURN
C      END

C      SUBROUTINE CONST(N,M,K,X,G,H,I,IPP)
C      THE LOWER AND UPPER BOUNDS ON THE EXPLICIT AND IMPLICIT
C      VARIABLES OF THE HEAT EXCHANGER
C      COMMON/PRIME/EFF,NTU,Q,WE,MEH,WEC,DPC,DPH,REC,REH,ETAC,ETAH,R,QC,
C      *QH,VSC,VSH,GH,GC,VH,VC,UOV,UOVC,UOVH,RH,RNCT,RNHT,QSC,QSH,EFC,EFH,
C      *NTUC,NTUH
C      COMMON /SIZE/HTD,XLD,OPD
C      DIMENSION X(K,M),G(M),H(M)
C      HIGH AND LOW ON THE CONSTRAINTS AND VARIABLES
C      ON FIN RADIUS
C      G(1)=.065;H(1)=.08
C      ON PIPE RADIUS
C      G(2)=.026;H(2)=.04
C      ON THE FIN THICKNESS
C      G(3)=.0008;H(3)=.0015
C      ON THE NUMBER OF FINS PER INCH
C      G(4)=7.;H(4)=14.
C      ON THE TUBE LENGTH
C      G(5)=.5;H(5)=10.
C      ON THE NUMBER OF ROWS
C      G(6)=2.;H(6)=10.
C      ON THE NUMBER OF PIPES IN A ROW
C      G(7)=4.;H(7)=40.
C      ON THE TRANSVERSE PITCH

```

```

C      G(A)=2.*G(1)+.01.*H(A)=.2
C      ON THE LONGITUDINAL PITCH
C      G(9)=.034 $H(9)=.3
C      ON THE HOT SIDE TUBE LENGTH
C      G(10)=.5 $H(10)=10.
C      ON THE FRONTAL AREA
C      G(11)=0.*H(11)=HTD
C      G(12)=0.*H(12)=XLD
C      G(13)=0.*H(13)=DPO
C      IF(IPP.EQ.1) RETURN
C      G(14)=G(8) $H(14)=SQRT(H(9)**2.+H(8)**2./4.)
C      CALL CALC(N,M,K,X,I)
C      RETURN
C      FND

```

```

C      SUBROUTINE FUN(N,M,K,X,F,I)
C      THE OBJECTIVE FUNCTION
C      COMMON/ECONOMI /AUC,FUC,FUC,RI,FI,EI,XNY,WR
C      COMMON/PRIME/EFF,NTU,Q,WE,WEH,HEC,DPC,DPH,REC,REH,ETAC,ETAH,R,QC,
C      +QH,VSC,VSH,GH,GC,VH,VC,UOV,UOVC,UOVH,FM,FMCT,FMHT,QSC,QSH,EFC,EFH,
C      +NTUC,NTUH
C      COMMON/DIMEN/ACC,ACH,SP,HT,D,V,AREAC,AREAH,AREA,AF,Z1,Z2,Z3,Z4
C      COMMON/RESULT/PIE,PANN,PEA,PFA,8B
C      DIMENSION X(K,M),F(K)
C      CALL CALC(N,M,K,X,I)
C      CALL PROCESS(N,M,K,X,I)
C      PIE=17.81*AREA**0.61
C      PE=EUC*WE*HR
C      PF=FUC*Q*HR*1.E-6
C      F2=RI-EI
C      F3=FI-EI
C      F1=(1.+F3)/(1.+F2)-1.
C      C1=((1.+F1)**XNY-1.)/(F1*(1.+F1)**XNY)
C      C2=((1.+F1)**(XNY+1.)-1.)/F1-1.
C      C3=((1.+F2)**(XNY+1.)-1.)/F2-1.
C      PANN=PIE/C1
C      PEA=PE+C3/XNY
C      PFA=PF*C2/XNY
C      F(I)=-PANN-PEA+PFA
C      BB=F(I)
C      RETURN
C      FND

```

```

C      SUBROUTINE CALC(N,M,K,X,I)
C      CALCULATION OF THE CORE AND DIMENSIONS OF THE HEAT EXCHANGER
C      COMMON/PRIME/EFF,NTU,Q,WE,WEH,HEC,DPC,DPH,REC,REH,ETAC,ETAH,R,QC,
C      +QH,VSC,VSH,GH,GC,VH,VC,UOV,UOVC,UOVH,FM,FMCT,FMHT,QSC,QSH,EFC,EFH,
C      +NTUC,NTUH
C      COMMON/DIMEN/ACC,ACH,SP,HT,D,V,AREAC,AREAH,AREA,AF,Z1,Z2,Z3,Z4
C      COMMON/PRTY/XKP,XKF,RFO,PI
C      DIMENSION X(K,M)
C      RA=X(I,5)/X(I,10)
C      TOTAL NUMBER OF PIPES
C      TPIPES=X(I,6)/2.*(2.*X(I,7)-1.)
C      FPI*FIN THICKNESS
C      TSP=X(I,3)*X(I,4)
C      FIN SPACING
C      SP=(1./12.-TSP)/X(I,4)
C      HEAT TRANSFER SURFACE AREA
C      C1=2.*PI*(X(I,1)**2.-X(I,2)**2.+X(I,1)*X(I,3))*X(I,4)
C      ACFAC=(C1+2.*PI*X(I,2)*SP*X(I,4))*X(I,5)*TPIPES*12.
C      AFEAH=AREAC/RA
C      EXCHANGER LENGTH
C      X(I,13)=X(I,9)*X(I,6)
C      EXCHANGER HEIGHT
C      X(I,11)=X(I,7)*X(I,8)
C      EXCHANGER LENGTH
C      X(I,12)=X(I,5)+X(I,10)
C      THE DIAGONAL DISTANCE
C      X(I,14)=SQRT(X(I,9)**2.+X(I,8)**2./4.)
C      EXCHANGER VOLUME
C      V=X(I,11)*X(I,12)*K(I,13)

```

```

C      FLOW AREA NOT AVAILABLE FOR FLUID FLOW
ATC=2*(X(I,1)*X(I,3)+X(I,2)*SP)*X(I,4)*X(I,5)*X(I,7)*12.
ATH=ATC/RA
C
C      FREE FLOW AREA
ACC=X(I,5)*X(I,11)-ATC
ACH=X(I,10)*X(I,11)-ATH
C
C      FIN AREA
AF=C1*X(I,5)*TPIPES*12.
C
C      TOTAL SURFACE AREA
AREA=AREAC+AREAH
C
C      EXCHANGER DIMENSIONAL PARAMETERS
Z1=AREA/V
Z2=ACC/(X(I,5)*X(I,11))
Z3=AF/AREAC
Z4=4.*X(I,13)*ACC/AREAC
C
C      RETURN
FNN
C
C      SUBROUTINE FRCESS (N,M,K,X,I)
C
C      CALCULATION OF THE PERFORMANCE RELATIONSHIPS
C      BETWEEN THE EXPLICIT AND IMPLICIT VARIABLES
COMMON/PRIME/EFF,NTU1,0,HE,MEH,WEC,DPC,DPH,RFC,PEH,ETAC,ETAH,R,OC,
+OH,VSC,VSH,GH,GC,VH,VC,UOV,UOVC,UOVH,RH,PMCT,PMHT,QSC,QSH,EFC,EFH,
+NTUC,NTUH
COMMON/ECONOMY/AUC,FUC,EUC,RI,FI,EI,XNY,HR
COMMON/DIMEN/ACC,ACH,SP,HT,0,V,AREAC,AREAH,AREA,AF,Z1,Z2,Z3,Z4
COMMON/PROP/ICOUNT,SB,RH,SC,ITPMAX,HA,CO1,IFLOW,COEF
COMMON/INLET/TINC,TINH,HINC,HINH,WC,WH
COMMON/OUTLET/TOC,TOH,MOC,HOM,CONDS
COMMON/PRTY/XKP,XKF,PI
DIMENSION X(K,M)
REAL NTU,NTUC,NTUH
XL=X(I,5)+X(I,10)
M1=WC*(CA+CV+HINC)
M2=MH*(CA+CV+HINH)
CMAX=MAX(M1,M2)
CHIN=AMINI(M1,M2)
R=CHIN/CMAX
C
C      EQUIVALENT FIN RADIUS
HX=X(I,1)-X(I,2)
C
C      MASS VELOCITY
GH=WH/ACH
GC=WC/ACC
C
C      MAXIMUM SURFACE VELOCITY
T=(TINC+TINH)/2.
PHOA=1./VSD*PHA(T+40.,HINH)
VH=GH/PHOA/3600.
VC=GC/PHOA/3600.
C
C      APPROACHING SURFACE VEL FT/MIN
VSC=WC/RHOA/(X(I,5)*X(I,11))/60.
VSH=WH/RHOA/(X(I,10)*X(I,11))/60.
C
C      AIR FLOW CFM
QC=WC/RHOA/60.
QH=WH/PHOA/60.
C
C      HEAT TRANSFER COEFFICIENT
S1=SP/HX*S2=SP/X(I,3)
P1H=2.*X(I,2)*GH/1459
RIC=2.*X(I,2)*GC/1459
MH=.00184/2./X(I,2)*P1H**-.681*S1**-.2*S2**-.113
MC=.00184/2./X(I,2)*RIC**-.681*S1**-.2*S2**-.113
C
C      SINGLE FIN EFFICIENCY
BC=SQRT(1.+MC)/XKF/X(I,3)
BH=SQRT(1.+MH)/XKF/X(I,3)
PHIC=TANH(BC*HX)/(BC*HX)
PHIH=TANH(BH*HX)/(BH*HX)
C
C      FINNED TUBE BANK EFFICIENCY
ETAC=1.-73*(1.-PHIC)
ETAH=1.-73*(1.-PHIH)
C
C      FINNED PIPE METAL RESISTANCE
PMHT=(1.-ETAH)/ETAH/MH

```

```

RMCT=(1.-ETAC)/ETAC/HC
RM=RMCT+RMHT
OVERALL U*A
ON THE COLD SIDE
UOVC=1./(1./HC/ETAC+RMCT+RFO)
ON THE HOT SIDE
UOVH=1./(1./HM/ETAH+RMHT+RFO)
UOV=1./(1./UOVC/AFEAC+1./UOVH/AREAH)

NTUC=UOVC*AREAC/W1
NTUH=UOVH*AREAH/W2
NTU=UOV/CMIN
REYNOLDS NUMBER
REH=GH*74/.0459
REC=GC*74/.0459
FRICTION FACTOR
S3=X(I,8)/2./X(I,2)
S4=X(I,8)/X(I,9)
FEC=18.93*R1H**(-.316)*S3**(-.927)*S4**.515
FEH=19.93*R1C**(-.316)*S3**(-.927)*S4**.515
DPC=FEC*X(I,6)*GC*GC/(RHOA*4.18E8)*12./62.4
DPH=FEH*X(I,6)*GH*GH/(RHOA*4.18E8)*12./62.4

HORSE POWER
HPC=DPC*QC/6350.
HPH=DPH*QH/6350.

IN KWHR
WEC=HPC/1.34
WEH=HPH/1.34
WE=WEC+WEH

EXCHANGER OVERALL EFFICIENCY
FROM KAY AND LONDON(1966)
EXE=EXP(-NTU*(1.-R))
EFF=(1.-EXE)/(1.-R*EXE)
QMAX=CMIN*(TINH-TINC)
Q=QSC=QSH=QMAX*EFF
EFC=1.-EXP(-NTUC)
EFH=1.-EXP(-NTUH)
TOC=TINC+Q/W1
TOH=TINH-Q/W2
HOH=HINH
CONDNS=0.

RETURN
END

SUBROUTINE REPORTC(N,M,K,X,I,JJ)
REPORTING THE CORE AND DIMENSIONS OF THE HEAT EXCHANGER
COMMON/DIMEN/ACC,ACH,SP,HT,D,V,AREAC,AREAH,AREA,AF,Z1,Z2,Z3,Z4
DIMENSION X(K,M)
NI=60
NO=61
WRITE(NO,020)
020 FORMAT(1H1,5X26HEAT PIPE EXCHANGER DESIGN /17X6HAE-MSU //)
IF(JJ.EQ.1) WRITE(NO,010)
010 FORMAT(1H,10X33CALCULATIONS AFTER ROUNDING OFFS ///)
WRITE(NO,015)
015 FORMAT(1X34HEXCHANGER OVERALL DIMENSIONS IN FT //
+1X6HLENGTH3X6HLENGTH3X6HHEIGHT3X6HDEPTH 3X6HTOTAL3X6HVOLUME/1X5H
+COLD 5X3HHOT //)
WRITE(NO,019)X(I,5),X(I,10),X(I,11),X(I,13),AREA,V
019 FORMAT(F6.3,5(2XF7.2)///)
X(I,1)=X(I,1)*24.
X(I,2)=X(I,2)*24.
X(I,3)=X(I,3)*12.
X(I,5)=X(I,5)*12.
X(I,10)=X(I,10)*12.
SNT=X(I,8)*12.
SPT=X(I,9)*12.
WRITE(NO,021)
021 FORMAT(1X,29HCORE SPECIFICATIONS IN INCHES /
+1X3HFIN5X4HPIFE5X3HFIN5X3HFPI/1X4HDIAM4X4HDIAM5X3HTHK5X3HDTY//)
WRITE(NO,022)X(I,J),J=1,4)
022 FORMAT(2(2XF5.3),4XF4.3,4XF5.2//)
WRITE(NO,025)
025 FORMAT(1X3HROW5X5HPIPES5X4HPIPE5X3HROW/

```

```

+1X7HQT4XAHIN A POW 3X9HSPACING 1X7HSPACING/)
026 WFLTE (NO,026)(X(I,6),X(I,7),SNI,SPI)
    FOPMAT(1XF4.1,4XF4.1,2(6XF5.3)/)
    WFLTE(NO,23)
023 FOPMAT(2X22HDIMENSIONAL PARAMETERS ///
+3X10HATOTAL/VOL2X12HAFLOW/AFRONT2X11HAFIN/ATOTAL2X8HHYD.DIAM/)
024 WFLTE(NO,024)Z1,Z2,Z3,Z4
    FOPMAT(4(2XF10.5)/)
    X(T,1)=X(I,1)/24.
    X(T,2)=X(I,2)/24.
    X(T,3)=X(I,3)/12.
    X(T,5)=X(I,5)/12.
    X(T,10)=X(I,10)/12.
    RETURN
    FND

```

SUBROUTINE REPORTP

C
C
C

REPORTING THE PERFORMANCE OF THE HEAT EXCHANGER

```

COMMON/PRIME/EFF,NTU,0,WE,WEH,WEC,DPC,DPH,REC,REH,ETAC,ETAH,R,OC,
+QH,VSC,VSH,GH,GC,VH,VC,UOV,UOVC,UOVH,PM,RMCT,RMHT,QSC,QSH,EFC,EFH,
+NTUC,NTUH
COMMON/DIMEN/ACC,ACH,SP,HT,D,V,AREAC,AREAH,AREA,AF,Z1,Z2,Z3,Z4
COMMON/ECONOMI/ALC,FUC,FUC,RI,FI,FI,XNY,HR
COMMON/INLET/TINC,TINH,HINC,HINH,WC,WH
COMMON/OUTLET/TOC,TOH,MOC,MOH,CONDS
PFAL NTU,NTUC,NTUH
PFINT 100
PRINT 120,TINC,TOC,TINH,TOM
PRINT 110,WC,WH
PRINT 200,QC,QH
PRINT 210,VSC,VSH
PRINT 220,GC,GH
PRINT 230,REC,REH
PRINT 130,DPC,DPH
PRINT 135,WEC,WEH
PRINT 140,UOVC,UOVH
PRINT 150,QSC,QSH
PRINT 240,EFC,EFH
PRINT 250,NTUC,NTUH
PRINT 260
UOV=UOV/((AREAC+AREAH)/2.)
PFINT 180,NTU,R,EFF
PRINT 190,UOV,PM,CONDS
100 FOPMAT(//1H1,20X16HPROCESS ANALYSIS ///34X6HSUPPLY 23X7HEXHAUST
+//34X6(1H-),23X7(1H-)/31X2HIN7X3HOUT18X2HIN7X3HOUT//)
110 FOPMAT(1H,15HAIR FLOW LB/HR 15XE12.6,18XE12.6/)
120 FOPMAT(1H,15HTEMPERATURE OF14XF5.1,4XF5.1,16XF5.1,5XF5.1/)
135 FOPMAT(1H,21HPRESSURE DROP IN H2O 9XF12.6,18XE12.6/)
140 FOPMAT(1H,23HPUMPING ENERGY KWH/YR 7XE12.6,18XE12.6/)
140 FOPMAT(1H,16HEAT TRANSF COEF 14XE12.6,18XE12.6
+//1H,2X13HBTU/HR/FT2/CF/)
150 FOPMAT(1H,20HENERGY SAVED BTU/HR 10XE12.6,18XE12.6/)
200 FOPMAT(1H,14HAIR FLOW CFM 16XE12.6,18XE12.6/)
210 FOPMAT(1H,21HFACE VELOCITY FT/MIN 9XE12.6,18XE12.6/)
220 FOPMAT(1H,24HMASS VELOCITY LB/HR/FT2 6XE12.6,18XE12.6/)
230 FOPMAT(1H,15HREYNOLDS NUMBER 15XE12.6,18XE12.6/)
240 FOPMAT(1H,10HEFFICIENCY 20XE12.6,15XE12.6/)
250 FOPMAT(1H,27HNO. OF TRANSFER UNITS (NTU) 3XE12.6,18XE12.6//)
260 FOPMAT(1H,16HVEPALL ANALYSIS //)
180 FOPMAT(4X3HNTL16X9HCMIN/CMAX 12X11HOVERALL EFF //4XF4.2,18XF4.2,
1 16XF4.3//)
190 FOPMAT(4X9HU-OVERALL1JX11HPIPE RESIST 10X12HCONDENSATION //
1 2XE10.4,11XE12.6,15XF4.3//)
    RETURN
    FND

```

FUNCTION DELTA(J)

C
C
C

THE INCREMENTS FOR THE EXPLICIT VARIABLES

```

GO TO (1,1,2,3,4,3,3,1,1,4) J
1 DELTA=.01
  RETURN
2 DELTA=.0001
  RETURN
3 DELTA=.5
  RETURN
4 DELTA=.05
  RETURN
END

```



```

CCC      INPUT TO THE COOLER: TEMP, AIRFLOW LB/HR-FT2, HUMIDITY
          LENGTH, CROSS SECTIONAL AREA (ALL IN ENGLISH UNITS)
C----- READ 300,TAMB,C,GAC,HINC,XLC,FT2
          INPUT CONCITIONS OF DRYER TO BE SIMULATED
          PFINT 301,ISAME,IPROD
          PFAD 331,ISO
          PPINT 341
          RFAD 300,TIN
          PRINT 302
          PFAD 300,HIN
          PRINT 303
          PFAD 300,CFM
          PPINT 315
          RFAD 300,TAMB
          PFINT 304
          READ 300,THIN
          PRINT 305
          RFAD 300,XMO
          PPINT 306
          READ 300,BPH
          PPINT 307
          READ 300,XLENG
          PPINT 308
          READ 300,DBTPR
          PRINT 342
342      FCPHAT(* CROSS SECTIONAL AREA OF THE DRYER *)
          PFINT 343
          (*OLFR*)
          READ 401,TAMB,C,GAC,HINC,XLC,FT2
401      FORMAT(5F10.3)
          INPUT TO THE EXCHANGER
          C-----
          501  READ 501,(X(I),I),I=1,10)
          FOPMAT(8F10.0)
          PPINT *,*FRACTION OF THE COOLER TO THE EXCHANGER#
          READ 300,PCX
          PPINT 300,PCX
          PRINT *,*FRACTION OF THE HEATER TO THE EXCHANGER#
          READ 300,RCX
          PFINT 300,RCX
          PPINT *,*FRACTION OF THE DRYER INPUT FROM #
          PRINT *,* DRYER#
          READ 300,RDD
          PPINT 300,RDD
          PPINT *,* COOLER#
          PFAD 300,PCD
          PPINT 300,PCD
          PRINT *,* EXCHANGER EXHAUST#
          RFAD 300,PXD
          PFINT 300,PXD
          PPINT *,* EXCHANGER SUPPLY#
          READ 300,RAX
          PPINT 300,RAX
          PPINT *,* AMBIENT AIR#
          READ 300,PA0
          PPINT 300,PA0
          PCA=1.-(PCX+PCD)*CDA=1.-(PDX+PCD)*RXA=1.-RXD
          GAOLD=60.*CFM/VSDBHA(F(TAMB),HIN)
          IF((RC0*GAOLD).GT.GAC)GAC=RC0*GAOLD
          WDOLD=GAOLD
          TAMB0=TAMB
          XMO0=XMO
          HINO=HIN
          CFM0=CFM
          IF (ISO.EQ.0) GO TO 131
          PRINT 209,TIN,HIN,CFM,TAMB,THIN,XMO,BPH,XLENG,DBTPR
          PPINT 309,C,A,CV,CP,CW,SA,RHOP,HFG,PATM
          TIN=CTF(TIN)
          TAMB=CTF(TAMB)
          THIN=CTF(THIN)
          XLENG=XLENG*.3.2908
          BPH=BPH/4.557
          CFM=CFM*.3.2808
          CA=CA/4.1869
          CV=CV/4.1868
          CP=CP/4.1868
          CW=CW/4.1869
          SA=SA*.3048
          RHOP=RHOP/16.019
          HFG=HFG/2.32458
          PATM=PATM/.068949
          GO TO 1010
101 CONTINUE

```

```

C      PRINT 209, TIN, HIN, CF4, TAMB, THIN, XMO, BPH, XLENG, DBTPR
C      PRINT 309, FT1, GAC, HINC, XLC, FT2
349   FORMAT(* CROSS SECTION OF THE COVER *F5.1/
      * INPUT CONDITIONS TO THE COOLER */
      * AIR FLOW LB/HR/FT2 *F10.2/* ABSOLUTE HUMIDITY *F5.4/
      * LENGTH OF THE DRYER*F5.2/* CROSS SECTION AREA*F5.1//)
C      PRINT 309, CA, CV, CP, CW, SA, RHOP, MFG, PATM
1010  CONTINUE
      DO 2020 I=1,202
2020  Y(I)=0.
      PPL=0.,PHC=.9999,EXIT=0
      XMO=XMO/(100.-XMO)
      XMEND=.01
C***** COMPUTE INLET RH AND INITIALIZE Y ARRAY
601   CONTINUE
      RHIN=RHD9HA(F(TIN),HIN)
      Y(1)=TIN
      Y(2)=XMO
      Y(3)=HIN
      Y(4)=THIN
      Y(5)=0.0
      Y(11)=0.0
      RH=RHIN
      SP=0.0
C***** CONVERT AIRFLOW TO LB/HR AND COMPUTE CONVECTIVE HEAT TRANS-
C***** FER COEFFICIENT AND EQUILIBRIUM MOISTURE CONTENT
      GA=GAOLD
      CFMHOT=GA*VSD9HA(F(TIN),HIN)/60.
      IF(GA-500.) 2,1,1
1     HC=.363*GA**.59
      GO TO 3
2     HC=.69*GA**.49
3     CONTINUE
      XME=EMC(RHIN,TIN)
C***** CONVERT GRAIN FLOW TO FT/HR AND LB/HR AND COMPUTE AIR-GRAIN
C***** RATIO
      GVFL=BPH*1.244
      GP=GVEL*RHOP
      AFGF=GA/GP
C***** PRINT HEADER PAGE OF CONDITIONS AND PROPERTIES
      XMEW=XME/(XME+1.)*100.
      IF(ISO.EQ.0) GO TO 102
      GAS=GA*4.976
      CFMHOTS=CFMHOT*.3048
      HCS=5.678*HC
      GVELS=GVEL*.3048
      GPS=GP*4.976
      PRINT 315,RH,GAS,CFMHOTS,HCS,XMEW,XME,XMO,GVELS,GPS
      PRINT 317
      GO TO 103
C 102  CONTINUE
      PRINT 310,PH,GA,CFMHOT,HC,XMEW,XME,XMO,GVEL,GP
      PRINT 311
C 103  CONTINUE
C***** COMPUTE CONSTANTS USED BY EQUATIONS IN SUBROUTINE DERFUN
      CON1=GA*CA
      CON2=GA*CV
      CON3=HC*SA
      CON4=GP*CP
      CON5=GP*CW
      CON6=1./AFGF
C***** CALL START TO INITIALIZE SOLUTION BY TAKING PUNGE-KUTTA STEPS
      CALL START(4,3,1,1,-6,1.E-6,1.E-8,.05,1.E-6,.5)
C***** BEGINNING OF LOOP
C***** CHECK MOISTURE CONTENT...IF .LT. .17 COMPUTE NEW MFG
4     IF(Y(2).LT..17) MFG=(1194.-.57*Y(4))*11.+.349*EXP(-23.25*Y(2))
C***** CHECK ABSORPTION AND CONDENSATION FLAG...IF SET EXIT
      IF(Y(11).GT.0.0) GO TO 10
C***** CALL PKAMSUB TO TAKE NEXT STEP
5     CALL PKAMSUB
C***** COMPUTE RH
      RH=RHD9HA(F(Y(1)),Y(3))
      CFMT=GA*VSD9HA(F(Y(1)),Y(3))/60.
      SP=(CFMT/58.)*.1.524*Y(6)
C***** CHECK IF LONG ENOUGH, MOISTURE CONTENT LOW ENOUGH OR TIME TO
C***** PRINT...IF NONE OF THESE GO TO BEGINNING OF LOOP
6     IF(Y(5)-XLENG) 6,6,8
7     IF(Y(2)-XMEND) 8,8,7
8     IF(Y(5)-PPL) 4,9,9
C***** SET FLAG IF EXIT CONDITION MET
8     EXIT=1
9     PPL=PPL+DBTPR

```

```

C***** MAKE FINAL CALCULATIONS AND PRINT
FTIME=Y(5)/CVEL
WATER=(XM0-Y(2))*RHOP*1.244
WB=Y(3)/(Y(2)+1.)*100.
IF(ISO.FQ.0) GO TO 104
DEPTH=Y(5)*.3048
ATEMP=FTC(Y(1))
GTEMP=FTC(Y(4))
PFRNT 312,DEPTH,ETIME,ATEMP,Y(3),PH,GTEMP,WB,Y(2)
GO TO 105
104 CONTINUE
PFRNT 312,Y(5),ETIME,Y(1),Y(3),PH,Y(4),WB,Y(2)
105 CONTINUE
C***** CHECK IF EXIT CONDITION HAS BEEN MET...IF NOT RETURN TO BEGIN
C***** NING OF LOOP
IF(IFEXIT-1) 4,11,4
C***** EXIT HERE FOR ABSORPTION OR CONDENSATION
10 CONTINUE
IF(ISO.FQ.0) GO TO 106
DEPTH=Y(11)*.3048
PRINT 313,Y(12),DEPTH
GO TO 107
106 CONTINUE
PFRNT 213,Y(12),Y(11)
107 CONTINUE
11 CONTINUE
FAIR=GA*(CA+CV*HIN)*(TIN-TAMBC)/BPH
HP=CFM*SP/6350.
FFAN=.766*HP*3413./(.5*BPH)
FAUG=0.0
FENERGY=FAIR+EFAN+FAUG
BTUH20=FENERGY/WATER
IF(ISO.FQ.0) GO TO 108
HPS=7245.8*HP
SPS=SP*.008164
FFANS=FFAN*.04159
FAIRS=FAIR*.04159
FAUGS=FAUG*.04159
FENERGYS=EFANS+EAIRS+EAUGS
WATERS=WATER*.4536
BTUH20S=BTUH20*2.32498
PFRNT 319,SPS,HPS,EFANS,EAIRS,EAUGS,ENERGYS,WATERS,BTUH20S
GO TO 109
108 CONTINUE
PFRNT 314,SP,HP,EFAN,EAIR,EAUG,ENERGY,WATER,BTUH20
C 109 CONTINUE
CALL COOLER(GAC,GP,TAMBC, Y(4),Y(2),HINC,TOUTC,THOUTC,XMOUTC,HOUTC
+
+XLC)
HAVG=(HOUTC+HINC)/2.
TAVG=(TAMBC+TOUTC)/2.
C
C ENERGY CALCULATIONS OF THE COOLER
C
CCFM=GAC*VSDRHA(TAVG+460.,HAVG)/60.
CSP=(CCFM/54.)**1.528*XLC
CWATER=(Y(2)-XMOUTC)*RHOP*1.244
CHP=CCFM*CSP/6350.
CEFAN=.766*CHP*3413./(.5*BPH)
CEAUG=0.
CENERGY=CEAUG+CEFAN
CEAIR=0.
XMOUTC=XMOUTC/(1.+XMOUTC)
PFRNT 331,THOUTC,XMOUTC,TOUTC,THOUTC
701 FORMAT (// 'COOLER OUTPUT : '//
+* GRAIN TEMP *F6.1/
+* GRAIN MC(WB) *F6.4/
+* AIR TEMP *F6.1/
+* AIR HUM *F6.4)
WD=GA
WAC=GAC
C
C CHECK FOR THE CONVERGENCE
C
IF(ABS(XMOUTC-XMOUT0).LE..0005) GO TO 1020
XMOUT0=XMOUTC
IF(RAX.LE.0.) GO TO 1030
C
C CALCULATE THE MIXTURE TEMP AND HUMIDITY OF THE AIR TO THE
C EXHAUST SIDE OF THE HEAT EXCHANGER
C
CALL INPUTM(TINH,HINH,WB,Y(1),Y(3),WD,ROX,TOUTC,HOUTC,WAC,RCX,
+0.,0.,0.,0.,0.,0.,0.,0.,0.,0.)
PRINT *, 'INPUTS TO THE EXHAUST SIDE OF THE EXCHANGER'
WHH=WH*FT1
PRINT *, 'TEMP OF HR AIR RLOW'
PRINT 299,TINH,HINH,WHH
C

```



```

PRINT 705,ENERGY,CENERGY,EENERGY,TENERGY
705 FORMAT(6H TOTAL 3X4(4XF6.1))
PRINT 706,WATER,CHATER,EWATER,TWATER
706 FORMAT(14H WATER REMOVED /7H LB/BU 2X4(6XF6.3))
PRINT 707,SP,CSP,ESP,TSP
707 FORMAT(16H STATIC PRESSURE /14H INCH OF WATER 4(4XF6.2))
PRINT 708,BTUH2O,CBTUH2O,EBTUH2O,EBTUH2O
PRINT 709,ABTUH2O
709 FORMAT(* BTU/H2O DIRECT RECYCLING * F6.1)
IF(RAX,LE.0.) STOP
C
C FORMATS
C
709 FORMAT(11H RTU/L9 H2O 4(5XF6.1))
300 FORMAT(5F10.3)
301 FORMAT(* CONCURRENT GRAIN DRYER SIMULATION*/
** USING THE *A10* THINLAYER EQUATION FOR*A10//
** PLEASE BE CONSISTENT WITH EITHER ENGLISH OR SI UNITS **//
** TYPE 0 FOR ENGLISH UNITS OR 1 FOR SI UNITS **//
341 FORMAT(* INPUT CONDITIONS:*/5X*INLET AIR TEMP, F OR C *)
302 FORMAT(5X*INLET ABS HUM RATIO *)
303 FORMAT(5X*AIR FLOW RATE (AT AMBIENT CONDITIONS) CFM/SQ FT OR M3
*/MTN/M2 *)
304 FORMAT(5X*INLET GRAIN TEMP, F OR C *)
305 FORMAT(5X*INLET MOISTURE CONTENT, WET BASIS PERCENT *)
306 FORMAT(5X*GRAIN FLOW RATE, BU/HR/SQ FT OR KG/HR/M2 *)
307 FORMAT(5X*DRYER LENGTH, FT OR M *)
308 FORMAT(5X*OUTPUT INTERVAL, FT OR M *)
309 FORMAT(//* ADDITIONAL INPUT FROM BLOCKDATA**//
** HEAT CAPACITIES, BTU/LB/F**//
** DRY AIR*F6.3* WATER VAPOR*F6.3* DRY GRAIN*F6.3
** LIQUID WATER*F6.3*/* SPECIFIC SURFACE AREA, SQ FT/CU FT*F6.0/
** BULK DRY MATTER DENSITY, LB/CU FT*F6.2/
** HEAT OF VAPORIZATION (MC.GT.14.5 PERCENT WB)*F6.0/
** ATMOSPHERIC PRESSURE, PSI*F6.2)
3090 FORMAT(//* ADDITIONAL INPUT FROM BLOCKDATA**//
** HEAT CAPACITIES, KJ/KG/C **//
** DRY AIR*F6.3* WATER VAPOR*F6.3* DRY GRAIN*F6.3
** LIQUID WATER*F6.3*/* SPECIFIC SURFACE AREA, M2/M3 * F6.0/
** BULK DRY MATTER DENSITY, KG/M3 * F6.2/
** HEAT OF VAPORIZATION (MC.GT.14.5 PERCENT WB) KJ/KG H2O *F6.0/
** ATMOSPHERIC PRESSURE, BAR*F6.2)
310 FORMAT(//* PRELIMINARY CALCULATED VALUES**// *REL HUM, DECIMAL*
*F6.4* AIRFLOW RATE, LB DRY AIR/HR/SQ FT*F6.1* CFM AT TIN*F6.1/
** HEAT TRANSFER COEF, BTU/HR/SQ FT/F*F6.3/
** EQUIL MC, WB PERCENT*F6.2* DRY BASIS, DECIMAL*F6.4/
** INLET MC, DRY BASIS DECIMAL*F6.4/
** GRAIN VELOCITY, FT/HR*F6.2* LB DRY MATTER/HR/SQ FT*F6.2)
311 FORMAT(//3X5HDEPT*4X4TIME5X3HAI*5X3HARS5X3HREL3X5HGRAIN6X2HMC
+6X2HMC/2X4HTEMP5X3HHUM5X3HHUM4X4HTEMP6X2HWR6X2HDB/
+6X2HFT6X2HHR7X1HF3X5HLB/L38H DECIMAL7X1HF PERCENT DECIMAL)
312 FORMAT(2F6.2,FA.1,2FA.4,FA.1,FA.2,F*.4)
213 FORMAT(//46HSITUATION ENCOUNTERED WHICH CAN NOT BE MODELED//A10,2
12H FLAG SET AT LENGTH OF F6.3,3H FT)
314 FORMAT(//31H STATIC PRESSURE, INCHES OF H2O*F6.2/17H HORSEPOWER/SQ
+FT*F6.2//22H ENERGY INPUTS, BTU/9U/10X12HFAN (.5 EFF)F7.0/10X8HHEAT
+AIR4XF7.0/10X10HMOVE GRAIN2XF7.0/10X5HTOTAL7XF7.0//21H WATER REMO
+VED, LB/3UF7.2//11H BTU/LB H2O*F9.2)
315 FORMAT(5X*AMBIENT TEMP, F OR C *)
331 FORMAT(I1)
209 FORMAT(23H INLET AIR TEMP OF F10.2/
1 19H HUMIDITY RATIO F10.5/
2 22H AIR FLOW CFM/FT2 F10.2/
3 19H AMBIENT TEMP OF F10.2/
4 23H GRAIN INLET TEMP OF F6.1/
5 21H GRAIN INLET MC(OB) F10.3/
6 30H GRAIN FLOW RATE LB/HR/FT2 F5.1/
7 18H DRYER LENGTH FT F10.2/
8 23H DIST. BET. PRINTS FT F5.3/ )
2090 FORMAT(23H INLET AIR TEMP OC F10.2/
1 19H HUMIDITY RATIO F10.5/
2 22H AIR FLOW M3/MIN/M2 F10.2/
3 19H AMBIENT TEMP OC F10.2/
4 23H GRAIN INLET TEMP OC F6.1/
5 21H GRAIN INLET MC(OB) F10.3/
6 30H GRAIN FLOW RATE KG/HR/M2 F5.1/
7 18H DRYER LENGTH M F10.2/
8 23H DIST. BET. PRINTS M F5.3/ )
316 FORMAT(//1H 20X,29HPRELIMINARY CALCULATED VALUES//
1 15X16HREL HUM DECIMAL F6.4/15X24HAIR FLOW RATE KG/HR/M2 F6.1/
2 15X22HAIR FLOW RATE AT TIN M3/MIN F6.1/15X27HHEAT TRANSFER COEF
3 W/OC/M2 FA.3/15X23HEQUIL MC (WB) PERCENT F6.2,5X2GHDRY BASIS DE
4CIMAL F6.4/15X29HINLET MC DRY BASIS DECIMAL F6.4/
5 15X 21HGRAIN VELOCITY M/HR F6.2,5X20HKG DRY MATTER/HR/M2 F6.2
7 /)

```



```

C***** DT/DX EQUATION
Y(7)=-CON3/(CON1+CON2*Y(3))*TMTM
C***** CALL SUBROUTINE CONTAINING DIFFERENTIAL FORM OF THINLAYER
C***** EQUATION
C***** CALL DIFEQ
C***** DM/DX EQUATION
Y(9)=-CON6*Y(8)
C***** DTHETA/DX EQUATION
Y(10)=(CON3*TMTM-(HFG+CV*TMTM)*GA*Y(9))/(CON4+CON5*Y(2))
RETURN
END
SUBROUTINE DIFEQ
C***** SUBROUTINE CONTAINING THINLAYER EQUATION BY T.L. THOMPSON
C***** IN DIFFERENTIAL FORM
C***** USED WITH CONCURRENT AND COUNTER FLOW GRAIN DRYER MODELS
C***** TO CALCULATE DM/DX
COMMON /MAIN/XMO,CFM,GVEL
COMMON /NAME/INAME,IPROD
COMMON /PKAM/Y(202)
DATA INAME,IPROD/10HTHOMPSON ,10H CORN
A=-1.86173+.1048143*Y(4)
B=427.364*EXP(-.33301*Y(4))
C***** CHECK HUMIDITY RATIO...IF OK CONTINUE AND COMPUTE RH
IF(Y(3).LT..1E-15) GO TO 3
RH=PHDBHA(Y(4)+459.69,Y(3))
C***** CHECK RH...IF OK CONTINUE AND COMPUTE EQUILIBRIUM MOISTURE
C***** CONTENT AND MOISTURE RATIO
IF(PH.GE.1.0) GO TO 4
IF(PHDBHA(Y(1)+459.69,Y(3)).GE.1.0) GO TO 4
XME=EMC(PH,Y(4))
XMP=(Y(2)-XME)/(XMO-XME)
C***** CHECK MOISTURE RATIO (ABSORPTION)...IF OK CONTINUE
IF(XMP) 2,2,1
1 ALMR=ALOG(XMR)
C***** COMPUTE EQUIVALENT TIME
TI=ALMR*(A+B*ALMR)
RAD=SQRT(A*A+4.*B*TI)
C***** DM/DX EQUATION
Y(8)=-(XMO-XME)/GVEL*EXP((-A-RAD)/(B+9))/RAD
RETURN
2 CONTINUE
C***** SET MOISTURE RATIO FLAG, FORCE POSITIVE AND CONTINUE COMPUTA-
C***** TIONS
Y(11)=Y(5)
Y(12)=10HMOIS RATIO
XMP=XMP*(-1.0)
GO TO 1
3 CONTINUE
C***** SET HUMIDITY FLAG, FORCE HUMIDITY RATIO UP AND CONTINUE COMPU-
C***** TATIONS
Y(11)=Y(5)
Y(12)=10H ABS HUM
Y(3)=.1E-15
XMP=Y(2)/XMO
XME=0.0
GO TO 1
4 CONTINUE
C***** SET RH FLAG, FORCE RH DOWN AND CONTINUE COMPUTATIONS
Y(11)=Y(5)
Y(12)=10H REL HUM
PH=.9999999999
XME=Y(2)
XMP=.1E-6
GO TO 1
END

```

APPENDIX B

Appendix B-1. A sample of finite element analysis.

```

*****
130.2 108.7 89.5 77.2 75.3 71.6
      .271 .492 .873 1.000 1.000 1.000
148.0 119.4 99.1 77.8 76.6 74.4 71.6
      .027 .027 .027 .020 .019 .017
130.2 108.7 89.5 77.2 75.3 71.6
      .271 .492 .873 1.000 1.000 1.000
148.0 119.4 99.1 77.8 76.6 74.4 71.6
      .027 .027 .027 .020 .019 .017
130.2 108.7 89.5 77.2 75.3 71.6
      .271 .492 .873 1.000 1.000 1.000
148.0 119.4 99.1 77.8 76.6 74.4 71.6
      .027 .027 .027 .020 .019 .017
130.2 108.7 89.5 77.2 75.3 71.6
*****
-----
125.1 116.5 99.2 84.3 75.6 68.2 40.0
120.0 107.3 91.3 79.1 70.9 55.1
120.0 113.6 99.3 85.2 75.0 63.0 40.0
120.0 107.3 91.3 79.1 70.9 55.1
120.0 113.6 99.3 85.2 75.0 63.0 40.0
120.0 107.3 91.3 79.1 70.9 55.1

```

Appendix B-2. A sample of the performance analysis of a designed heat pipe exchanger.

PROCESS ANALYSIS

	SUPPLY		EXHAUST	
	IN	OUT	IN	OUT
TEMPERATURE OF	50.0	62.7	130.0	117.4
AIR FLOW LB/HR	.400000E+03		.600000E+03	
AIR FLOW CFM	.976123E+02		.146419E+03	
FACE VELOCITY FT/MIN	.252228E+03		.378342E+03	
MASS VELOCITY LB/HR/FT ²	.272205E+04		.408307E+04	
REYNOLDS NUMBER	.226755E+03		.340132E+03	
PRESSURE DROP IN H ₂ O	.526520E+00		.109239E+01	
PUMPING ENERGY KWH/YR	.120801E+02		.375947E+02	
HEAT TRANSF COEF BTU/HR/FT ² /OF	.114100E+02		.142774E+02	
ENERGY SAVED BTU/HR	.123933E+04		.193537E+04	
EFFICIENCY	.158935E+00		.248196E+00	

Appendix B-3. A sample of the dimensions of a designed heat pipe exchanger.

HEAT PIPE EXCHANGER DESIGN
AE-MSU

CALCULATIONS AFTER ROUNDING OFFS

EXCHANGER OVERALL DIMENSIONS IN FT

LENGTH COLD	LENGTH HOT	HEIGHT	DEPTH	ATOTAL	VOLUME
2.695	3.30	4.00	2.02	5531.57	48.44

CORE SPECIFICATIONS IN INCHES

FIN DIAM	PIPE DIAM	FIN THK	FPI QTY
1.814	.624	.017	13.54
ROW QTY	PIPES IN A ROW	PIPE SPACING	ROW SPACING
7.0	25.0	1.920	3.462

DIMENSIONAL PARAMETERS

ATOTAL/VOL	AFLOW/AFRONT	AFIN/ATOTAL	HYD.DIAM
114.19100	.53275	.97659	.01866

Appendix B-4. A concurrentflow dryer analysis using a heat pipe exchanger

FRACTION OF THE COOLER TO THE EXCHANGER

1.000
FRACTION OF THE HEATER TO THE EXCHANGER

.400
FRACTION OF THE DRYER INPUT FROM :

DRYER
.600
COOLER
0.000
EXCHANGER EXHAUST
0.000
EXCHANGER SUPPLY
.400
AMBIENT AIR
0.000

DEPTH	TIME	AIR TEMP	ABS HUM	REL HUM	GRAIN TEMP	MC WB	MC DB
FT	HR	F	LB/LB	DECIMAL	F	PERCENT	DECIMAL
.01	.00	401.4	.1982	.0142	117.0	25.00	.3333
6.06	.59	163.9	.2576	.0278	163.7	19.40	.2407

COOLER OUTPUT :

GRAIN TEMP 73.5
GRAIN MC(WB) .1741
AIR TEMP 157.3
AIR HUM .0473
INPUTS TO THE EXHAUST SIDE OF THE EXCHANGER
TEMP OF HR AIR RLOW
.1610E+03 .1470E+00 .5477E+05
INPUT TO THE SUPPLY SIDE OF THE EXCHANGER
TEMP OF HR AIR RLOW
.6500E+02 .4000E-02 .2597E+05
EXCHANGER OUTPUT
TOC HOC
122.576 .004
TOH HOH
139.362 .147
AREA HE
1914.270 .010
NEW INPUT TO THE DRYER
TEMP OF HR AIR RLOW
157.559 .204 676.240

DEPTH	TIME	AIR TEMP	ABS HUM	REL HUM	GRAIN TEMP	MC WB	MC DB
FT	HR	F	LB/LB	DECIMAL	F	PERCENT	DECIMAL
.01	.00	401.0	.2042	.0144	117.0	25.00	.3333
6.04	.59	164.6	.2639	.0288	164.4	19.37	.2403

COOLER OUTPUT :

GRAIN TEMP 73.5
GRAIN MC(WB) .1737
AIR TEMP 158.0
AIR HUM .0475

		ENERGY BILL	COOLER	HEATPIPE	SYSTEM
		DRYER			
FAN	738.23	32.97	4.15	775.35	
MOVE GRAIN	0.00	0.00	0.00	0.00	
HEAT AIR	10473.2	0.0	-457.5	10015.0	
TOTAL	11211.5	33.0	-453.3	8726.5	
WATER REMOVED					
LB/BU	4.063	1.573	0.000	6.436	
STATIC PRESSURE					
INCH OF WATER	50.94	4.44	0.00	55.38	
BTU/LB H2O	1742.0	5.1	-70.4	1355.9	
BTU/H2O DIRECT RECYCLING		320.1			